

Unexpected Roles of Perivascular Cells in Angiogenesis and Cancer

Daniel L. Hess

B.S. Biology, University of Georgia, 2012

A Dissertation Presented to the Graduate Faculty of the University of Virginia in Candidacy for
the Degree of Doctor of Philosophy

Department of Biochemistry and Molecular Genetics

University of Virginia

December 2018

Gary K. Owens, PhD

Brian H. Annex, MD

Patrick A. Grant, PhD

Michael J. McConnell, PhD

Shayn M. Peirce, PhD

David Wotton, PhD

ABSTRACT

Angiogenesis, or the growth of new blood vessels, is critical during homeostasis, adaptation to injury, and disease. Proper functioning of the vasculature, including angiogenesis, requires coordinated action of both endothelial cells (EC) and perivascular cells, including smooth muscle cells and pericytes (SMC-P). SMC-P display remarkable phenotypic plasticity, which allows them to contribute to angiogenesis, tissue repair and disease pathogenesis. However, mechanisms by which perivascular cells directly contribute to angiogenesis following tissue injury, and to diseases such as cancer, remain largely unexplored.

Herein, we investigate the role of perivascular cells in angiogenesis and cancer pathogenesis using several different mouse models. Through combined SMC-P lineage tracing and genetic knockout of single genes exclusively in SMC-P, we demonstrate that SMC-P knockout of the stem cell pluripotency gene Oct4 leads to significantly impaired angiogenesis following corneal burn or hindlimb ischemia. We also demonstrate that SMC-P knockout of the interleukin 1-receptor (IL-1R) has no significant effect on primary tumor growth or metastasis. However, knockout of IL-1R specifically in EC results in significantly impaired primary tumor growth.

My work demonstrates that loss of a single gene in SMC-P can have profound effects on angiogenesis, thus adding to a growing body of literature demonstrating the essential role of SMC-P to effective angiogenesis. Additionally, these studies demonstrate that a functional role for Oct4 in SMC-P is not limited to the setting of atherosclerosis but instead likely evolved because it conferred survival and reproductive success by enhancing angiogenesis. The finding that IL-1R in EC, but not SMC-P, promotes primary tumor growth builds on the idea that, while both EC and SMC-P play essential roles in angiogenesis, tissue repair and disease pathogenesis, they utilize

unique, cell-specific mechanisms in the process. These studies add to the notion that future therapeutic approaches to modulate angiogenesis should target both EC and SMC-P function.

ACKNOWLEDGEMENTS

There are a number of individuals to thank, without whom successful completion of this journey would not have been as manageable or enjoyable. Each of you have enriched my life and for that, I am forever grateful.

To Mom and Dad, you both have always given me everything I need to succeed in life. Thank you for always stressing the value of hard work and success in school. Dad, I am grateful to you for encouraging me to read as a kid, even when I would have rather goofed off all day. You are a huge reason why I chose to go in to science and medicine. Mom, you have always put each of your children before yourself, and you have helped me through countless problems. Thank you for always supporting me, through all of the ups and the downs.

To my siblings, Lisa, Matthew, and Sara, I am grateful to have each of you in my life. Lisa, you have always been a great big sister and have always gone out of your way to make me feel included. Sara, I am glad Mom and Dad wanted a fourth child. I have always been amazed by your emotional maturity and am happy you are following your passion in life. Matt, I am grateful to have a brother who is also a best friend. I have always admired your drive, and I know you are, and will continue to be, an incredible doctor. I wish I could spend more time with all of you. When I doubt myself, I often think of how talented and loving each of you are, which always cheers me up. Doing so reminds me that, if you are all so wonderful, I am certainly capable of overcoming the next hurdle.

To each of the Owens Lab members, past and present, all of you have provided me with valuable advice, both scientific and other. You all have positively impacted my life and for that I

am thankful. Thank you to Missy Bevard, Mary McCanna, Coral Kasden, and Angie Washington for help with histology, and thank you to Rupa Tripathi for help with cell culture. I want to thank Dr. Olga Cherepanova for mentoring me, especially in the early years of this journey. Thank you for listening to more than one of my rants and for encouraging me through my failures. I would also like to thank Dr. Meera Murgai and Dr. Rosie Kaplan for all of their help with the studies in Chapter 4.

To my lab friends Ricky and Molly, I am very glad you two ended up together. Ricky, your positive energy and enthusiasm are an inspiration to me. Thank you for being a sounding board for my ideas and a plug for my cynicism. Molly, I am grateful we ended up being able to work so closely together. Your intelligence and enthusiasm are missed in Charlottesville, but I know they are greatly appreciated at Columbia.

To my friends outside of lab, both in Charlottesville and away, thank you for your support and friendship throughout the years. To Rishabh and Zach, both of you are like brothers to me. Thank you for listening to me and joining me in incredible adventures throughout the years.

To my dog, Goliath, you will never read this, but you already know that you saved my life. From that day on, you have always been right by my side, making sure I am ok, and always ready for the next game of fetch. You understand my emotions better than any human ever could.

To Emily and Mahima, the undergraduate students I have had the opportunity to mentor, thank you for your hard work and dedication. I have no doubt that you will be incredibly successful in whatever you decide to pursue scientifically.

To my PhD advisor, Dr. Gary Owens, thank you for supporting me throughout the years and for molding me into a better scientist. Your scientific rigor, leadership, enthusiasm, and analytical skills have been a constant source of inspiration to me. I hope to be at least half the scientist you are some day.

To my PhD co-mentor, Dr. Brian Annex, thank you for your support throughout the years and for your demonstration of what it means to be a successful physician scientist.

To my PhD committee, Dr. Patrick Grant, Dr. Mike McConnell, Dr. Shayn Peirce, and Dr. David Wotton, thank you for your ideas and improvements on my research and for helping me become a better scientist.

This journey has had its highs and lows. It was both the darkest and brightest time of my life. I am forever in debt to all those who helped me through it.

TABLE OF CONTENTS

Abstract.....	i
Acknowledgements.....	ii
Summary of Figures	viii
Summary of Tables.....	ix
1 Introduction	1
1.1 Perivascular cells	1
1.1.1 Smooth Muscle Cells.....	1
1.1.2 Pericytes.....	3
1.2 SMC-P phenotypic switching	4
1.2.1 SMC phenotypic switching in atherosclerosis.....	5
1.2.2 SMC-P phenotypic switching in injury and disease	6
1.3 Vascular growth and remodeling.....	7
1.3.1 Angiogenesis	7
1.3.2 Mechanisms of angiogenesis	8
1.4 Angiogenesis in disease.....	9
1.4.1 Angiogenesis in PAD	9
1.4.2 Angiogenesis in CNV	11
1.4.3 Angiogenesis in tumor growth and metastasis	12
1.4.4 Summary-Angiogenesis in disease.....	13
1.5 SMC-P phenotypic switching in angiogenesis	13
1.6 The stem cell pluripotency gene Oct4	14
1.6.1 Structure of Oct4.....	14
1.6.2 Role of Oct4 in stem cells.....	14
1.6.3 Regulation of Oct4.....	14
1.6.4 Isoforms and pseudogenes of Oct4.....	15
1.6.5 Dogma: Oct4 expression is limited to pluripotent stem cells and germline cells... 16	
1.6.6 Detection of Oct4 in mouse and human atherosclerotic lesions	17
1.7 Role for Oct4 in SMC in atherosclerosis.....	19
1.7.1 Oct4 in SMC is atheroprotective	19
1.7.2 Oct4 promotes SMC migration.....	20
1.7.3 Oct4 is reactivated in SMC through hydroxymethylation.....	20
1.7.4 Is Oct4 function in SMC unique to the setting of advanced atherosclerosis?	21
1.8 SMC-P phenotypic switching in cancer	22
1.9 IL-1 signaling in cancer	23
1.9.1 IL-1 signaling in BMDCs	24
1.9.2 IL-1 signaling in EC	24
1.9.3 IL-1 signaling in SMC-P	25
1.10 Overall Summary.....	25
2 Chapter 2: Materials and Methods.....	26
2.1 Mice	26
2.2 Whole mount retina imaging	28
2.3 eYFP+ cell sorting	28
2.4 Blood pressure telemetry	28

2.5	Corneal alkali burn	29
2.6	Intravital confocal microscopy and quantification	29
2.7	Bright field imaging and quantification of hemorrhaging	30
2.8	Rhodamine dextran injections	31
2.9	Whole mount cornea immunostaining.....	31
2.10	Harvesting, immunostaining, and analysis of tissue.....	32
2.11	Hindlimb ischemia model.....	33
2.12	RNA-Seq analysis.....	34
2.13	Cell Culture.....	34
2.14	RNA isolation, cDNA preparation, and qRT-PCR.....	35
2.15	Scratch wound assay	35
2.16	Orthotopic tumor models.....	36
2.17	Bioluminescence imaging and analysis	36
2.18	Statistical Analysis	37
3	Chapter 3: Perivascular cell-specific knockout of the stem cell pluripotency gene Oct4 inhibits angiogenesis.....	37
3.1	Abstract.....	38
3.2	Introduction	39
3.3	Results	42
3.3.1	Myh11-CreER ^{T2} eYFP efficiently labeled SMC and a large subset of pericytes in multiple tissues	42
3.3.2	SMC-P knockout of Oct4 in young, healthy mice had no discernable effect on microvascular phenotype	43
3.3.3	SMC-P knockout of the stem cell pluripotency gene Oct4 resulted in impaired angiogenesis following corneal burn, including reduced migration and increased cell death of SMC-P	44
3.3.4	SMC-P knockout of the stem cell pluripotency gene Oct4 resulted in increased vascular leakage from angiogenic vessels	46
3.3.5	SMC-P knockout of the stem cell pluripotency gene Oct4 resulted in delayed EC migration, but did not affect EC sprouting, apoptosis, or proliferation.....	47
3.3.6	SMC-P <i>Oct4</i> knockout resulted in impaired angiogenesis and decreased perfusion recovery following hindlimb ischemia	48
3.3.7	SMC-P <i>Oct4</i> knockout was associated with decreased expression of the guidance gene Slit3 both <i>in vivo</i> and <i>in vitro</i>	49
3.4	Discussion.....	72
4	Chapter 4: Interleukin 1-receptor signaling in endothelial cells, but not perivascular cells, promotes primary tumor growth.....	77
4.1	Abstract.....	77
4.2	Introduction	78
4.3	Results	79
4.3.1	IL-1R signaling in EC, but not SMC-P, promotes primary tumor growth of B16 F10 melanoma	79
4.3.2	IL-1R signaling in EC promotes primary tumor growth, but not metastasis, of M3-9M rhabdomyosarcoma	81
4.3.3	IL-1R signaling in SMC-P does not significantly affect primary tumor growth or metastasis of M3-9M rhabdomyosarcoma.....	82
4.4	Discussion.....	84
5	Chapter 5: Summary, Discussion and Future Directions.....	87
5.1	Summary of Chapters 3 and 4	87
5.2	How far does a functional role for Oct4 and IL-1R in the vasculature extend?.....	88
5.2.1	Evolutionary function of SMC-P.....	88

5.2.2	Why did Oct4 evolve a function in SMC-P?	88
5.2.3	Potential role of Oct4 in developmental or postnatal angiogenesis.....	89
5.2.4	Why did IL-1R evolve a function in SMC-P?	90
5.2.5	Potential role of Oct4 in tumor growth and metastasis.....	91
5.3	What are the changes resulting from loss of Oct4 in the vasculature?	92
5.3.1	Oct4-dependent regulation of Slit-Robo signaling	92
5.3.2	Proposed model of Slit-Robo signaling in the vasculature.....	93
5.3.3	Potential Slit3 loss-of-function approaches	94
5.3.4	Potential Slit3 gain-of-function approaches	96
5.3.5	Summary: Slit3 loss and gain-of-function approaches	98
5.3.6	Potential mechanisms of increased apoptosis following loss of Oct4	98
5.3.7	Identification of additional Oct4-dependent genes.....	99
5.3.8	Potential role of Oct4 in EC.....	100
5.4	What are the changes resulting from loss of IL-1R in the vasculature?	100
5.4.1	IL-1R signaling in perivascular cells	100
5.4.2	Design of mouse models to better mimic CANTOS study design	101
5.4.3	Use of better models to test IL-1R signaling in EC and SMC-P.....	103
5.4.4	IL-1R signaling in EC.....	104
5.5	How studies might inform future therapeutic strategies	106
5.5.1	Angiogenic therapies beyond VEGF	106
5.5.2	Vascular normalization.....	107
5.5.3	Therapeutic angiogenesis to target both EC and SMC-P	108
5.5.4	Summary and integration to inform future therapies.....	110
5.5.5	Final Outlook	111
6	References.....	112

SUMMARY OF FIGURES

Figure 1-1	2
Figure 1-2	18
Figure 3-1	51
Figure 3-2	53
Figure 3-3	55
Figure 3-4	57
Figure 3-5	58
Figure 3-6	59
Figure 3-7	61
Figure 3-8	64
Figure 3-9	65
Figure 3-10	66
Figure 3-11	67
Figure 3-12	68
Figure 3-13	70
Figure 3-14	71

Figure 4-180
Figure 4-281
Figure 4-383

SUMMARY OF TABLES

Table 163

1 INTRODUCTION

1.1 PERIVASCULAR CELLS

Blood vessels are responsible for circulation of blood and nutrients throughout the body. Healthy blood vessels consist of an inner layer of endothelial cells (EC), which line the lumen. EC act as a selectively permeable barrier between the blood and the rest of the body. They play critical roles in regulating vessel permeability, thrombosis, immune cell flux during inflammation, and blood vessel remodeling during angiogenesis. EC are invested by perivascular cells, which consist of both smooth muscle cells (SMC) and pericytes.

1.1.1 Smooth Muscle Cells

Differentiated SMC express a number of unique contractile proteins which aid in their principal homeostatic functions of regulating blood pressure, vessel diameter, and flow.¹ These proteins include but are not limited to SM22a (TAGLN), α -SMA (ACTA2), and SM-MHC (MYH11). Alpha smooth muscle actin (α -SMA) was the first known marker of SMC, and makes up 70% of the total actin in SMC and up to 40% of the total protein content in differentiated SMC.² α -SMA, despite its name, is not SMC specific and can be expressed in a number of different cell types including pericytes and myofibroblasts.^{3,4} SM1 and SM2, two smooth muscle myosin heavy chain isoforms of the SM-MHC gene, are more SMC specific. In fact, SM-MHC is the most specific SMC marker known to date.¹ SMC concentrically wrap around EC of arteries, arterioles, veins, and venules with diameters $>10 \mu\text{m}$ (**Figure 1-1**).

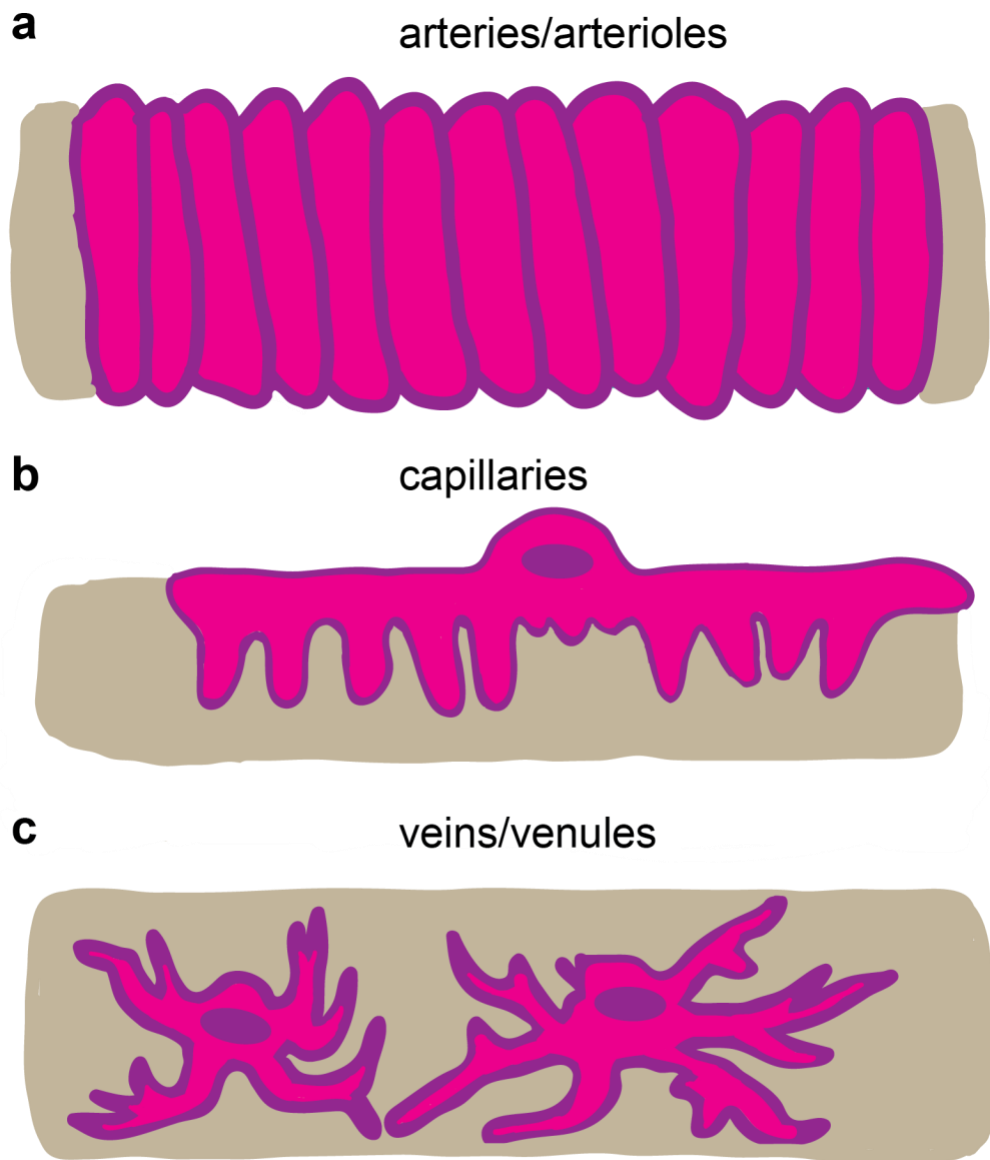


Figure 1-1

SMC invest large diameter vessels, while pericytes invest capillary size vessels <10 μm in diameter. a, SMC concentrically wrap around arteries and arterioles, with continuous coverage of the endothelial abluminal surface. b, Pericytes longitudinally invest capillary-size vessels. They have distinct cell bodies with multiple projections that typically span across multiple EC. c,

SMC with a more flattened, cobble-stone morphology invest veins and venules but in these lower pressure systems, coverage is often discontinuous.

1.1.2 Pericytes

In contrast, pericytes longitudinally invest capillary-size vessels $\leq 10\mu\text{m}$ in diameter. Pericytes can simplistically be thought of as SMC of the microvasculature and, indeed, these cell types express many of the same proteins and perform similar functions in promoting vessel stability and tone. Of note though, there are conflicting reports as to whether pericytes, at least in the CNS, actively contract and dilate, and therefore regulate blood pressure.^{5,6} The technical definition of a pericyte is a perivascular cell that is embedded in the basement membrane of an endothelial cell. However, this definition requires the use of electron microscopy and is therefore not applicable during active vascular remodeling or other non-homeostatic states. As such, classification of a cell as a pericyte typically involves assessment of morphology, location, and protein expression.³

Morphologically, pericytes have a well-defined cell body with projections that extend longitudinally along the abluminal surface of EC, so that one pericyte typically spans multiple EC. These longitudinal processes then extend perpendicular projections which encircle the vessel. Pericyte coverage of the abluminal side of EC is typically discontinuous. Estimates of pericyte to EC ratio vary between 1:1 and 1:10, depending on the type of tissue, with the CNS typically having the highest ratio of pericytes to EC.³ Pericytes express a wide variety of proteins dependent on developmental origin, vascular bed, pathological state, and *in vitro* culture conditions. These include ACTA2, PDGFR-B, NG2, Desmin, and many others. Of note, a major limitation of the field is that there is no specific marker for all pericytes. Additionally, there is no single marker that can be used to distinguish SMC from pericytes. Because of this, and because smooth muscle cells and pericytes share many anatomical and functional characteristics, we often refer to these cells together as smooth muscle cells and pericytes (SMC-P), or perivascular cells.

1.2 SMC-P PHENOTYPIC SWITCHING

While differentiated SMC-P express unique contractile proteins and signaling molecules critical for their contractile function, SMC-P are non-terminally differentiated cells and can undergo profound and reversible changes in phenotype, including in the setting of vascular injury.^{1,2} Although fully differentiated SMC exhibit a very low proliferation rate (<1%), a seminal study by Clowes and Schwartz (1985) showed that 40-50% of medial SMC proliferate following rat carotid artery injury.⁷ Further evidence for extensive SMC-P proliferation in the setting of injury/disease was provided by Bentzon et al. in the setting of atherosclerosis.⁸ Studies by our lab and others have shown that treatment of cultured SMC-P with various stimuli including PDGF-BB,⁹ oxidized phospholipids,¹⁰ or IL-1 β ¹¹ results in marked downregulation of conventional SMC genes, indicative of an altered phenotypic state. The process whereby SMC-P downregulate canonical proteins, concomitant with altered rates of proliferation, migration, and/or extracellular matrix production, has been termed SMC-P phenotypic switching. Indeed, this process of phenotypic switching was likely subject to high selection pressure throughout evolution. Mutations that conferred an increased ability of SMC-P to phenotypically modulate and contribute to vascular repair following injury would have increased overall fitness and thus been selected for over time.

Indeed, evidence for the evolved role of SMC-P phenotypic switching can be found by examining CArG-SRF regulation of SMC differentiation. CArG elements are DNA sequences containing the CC(A/T)₆GG motif, and they are found in the promoter and/or intronic regions of most SMC marker genes. CArG elements are binding sites for the ubiquitously expressed transcription factor, serum response factor (SRF), which binds as a homodimer. Of major interest, these CArG elements are degenerate, or imperfect, in that they often differ by a single nucleotide in the central A/T rich core, which dramatically reduces the binding affinity of SRF. This degeneracy is highly conserved across species. For example, α -SMA CArG boxes are 100% conserved between chicken and humans. Remarkably, gain-of-function mutations which increase

SRF binding to CArG boxes do not affect SMC marker gene expression, including α -SMA, during normal development. However, these same mutations cause SMC marker genes to fail to be suppressed following vascular injury. Therefore, it appears that degenerate CArG boxes evolved to enhance SMC-P phenotypic switching, allowing SMC contractile genes to quickly turn off in the setting of injury.^{1,12}

Although SMC-P phenotypic switching is critical for injury and wound repair, an unintended consequence of this remarkable degree of SMC-P plasticity is that it predisposes them to also contribute to pathologic states. Indeed, work from our lab has shown that SMC undergo extensive phenotypic switching *in vivo* in the setting of atherosclerosis.¹³ However, SMC-P phenotypic switching is difficult to study *in vivo* since a hallmark of this process is the downregulation of canonical SMC-P marker genes, making marker expression insufficient and unreliable in determining cell of origin. As such, studies of SMC-P phenotypic switching *in vivo* require rigorous SMC-P lineage tracing models to reliably track the fate of SMC-P following their phenotypic modulation. A number of SMC lineage tracing mouse models have been developed, including a Myh11-CreERT2 ROSA26 STOP-floxed eYFP line generated and validated in the Owens Lab.¹⁴

1.2.1 SMC phenotypic switching in atherosclerosis

Using these Myh11-CreERT2 ROSA26 STOP-floxed eYFP mice in an ApoE^{-/-} mouse model of atherosclerosis, Shankman et al. showed that over 80% of eYFP⁺ cells, indicating cells of SMC origin, were ACTA2⁻ following 18 weeks of Western Diet feeding. eYFP⁺ cells comprised over 30% of total cells within lesions and many expressed non-canonical markers such as LGALS3 and SCA1. SMC-specific knockout of the stem cell pluripotency gene *Klf4* resulted in significant reductions in eYFP⁺LGALS3⁺ cells as well as features consistent with increased lesion stability.¹⁵ Using these same Myh11-CreER^{T2} eYFP mice, Cherepanova et al. demonstrated that knockout of another stem cell pluripotency gene, *Oct4*, also resulted in profound changes in atherosclerotic

lesions. However, in complete contrast to *Klf4* knockout, loss of *Oct4* specifically in SMC led to decreased investment of eYFP⁺ cells into lesions and other changes consistent with decreased lesion stability.¹⁵ Together, these studies demonstrated that SMC can have drastically different effects on lesion composition and stability, depending on the nature of their phenotypic transitions. Other studies involving SMC-specific knockout of genes such as *Collagen 15a1* and *interleukin 1-receptor (IL-1R)* have further corroborated the idea that SMC phenotypic switching plays a critical role in the pathogenesis of atherosclerosis.^{16,17}

1.2.2 SMC-P phenotypic switching in injury and disease

While many of the early studies demonstrating SMC-P phenotypic switching were performed in cultured SMC and large vessels where SMC predominate, there is also extensive evidence that pericytes possess remarkable phenotypic plasticity in the setting of injury and disease. Indeed, pericytes have been suggested as a possible source of mesenchymal stem cells (MSCs). Pericytes isolated from multiple tissues on the basis of marker expression, including CD146, NG2, and PDGFR-B, have been shown to behave as mesenchymal stem cells when cultured *in vitro*. This includes differentiation to osteoblasts, chondrocytes, and adipocytes.¹⁸ However, there is no direct evidence that pericytes represent a source of MSCs *in vivo*. In fact, a recent study using Tbx18 to lineage tag a population of pericytes concluded that Tbx18 expressing pericytes behave as MSCs *in vitro* but not *in vivo*.¹⁹ This may be due in part to the inherent plasticity of SMC-P, which rapidly modulate upon *in vitro* culture. It also reflects the fact that there are numerous SMC-P populations throughout the body, each with dynamic marker expression as a function of their inherent plasticity. As a result, each SMC-P lineage tracing system is limited by what marker or markers is used to define the SMC-P population. Indeed, using other *in vivo* lineage tracing systems including Nestin,²⁰ NG2²¹ and/or PDGFRB,²² SMC-P have been shown to undergo phenotypic modulation and contribute to injury and disease in multiple settings including skeletal muscle repair,²³ premetastatic niche formation and metastasis,²⁴ and angiogenesis.²⁰⁻²²

1.3 VASCULAR GROWTH AND REMODELING

Angiogenesis, or the growth of new blood vessels from pre-existing vessels, is one means by which the vasculature remodels as a means to meet the continuously changing metabolic demands of organisms. Blood vessels can also adaptively remodel through the processes of vasculogenesis and/or arteriogenesis. Vasculogenesis, or the *de novo* production of endothelial cells, is mostly confined to embryonic development but also occurs to a lesser degree in adult tissues.²⁵ Arteriogenesis is defined as the outward remodeling of existing collateral vessels. It involves an increase in fluid shear stress upstream of an arterial occlusion. This leads to endothelial activation, monocyte recruitment, breakdown of the basement membrane, SMC proliferation, and ultimately an increase in vessel diameter to restore downstream blood flow.^{26,27}

1.3.1 Angiogenesis

Research over the last few decades has led to a detailed model of angiogenesis. There are multiple stimuli that promote angiogenesis, but one of the most potent inducers is hypoxia. Under hypoxic conditions, hypoxia-inducible factors (HIFs) become stable, permitting them to drive transcriptional networks in EC that promote survival and proliferation. Vessel growth requires degradation of the shared basement membrane between EC and SMC-P, mediated by matrix metalloproteinases produced by both cell types. Angiopoietin 2 (ANG2) at least in part mediates SMC-P detachment from EC. Liberated EC respond to a host of angiogenic cues, the most well-studied of which is vascular endothelial growth factor (VEGF). VEGF binds principally to VEGFR-2 present on ECs, stimulating sprouting, proliferation, and migration. VEGF also promotes expression of the Notch ligand, DLL4. EC that respond to VEGF most quickly, and therefore upregulate DLL4 expression, are termed tip cells. DLL4 in tip cells binds to Notch1 receptors in neighboring EC, which inhibits VEGFR-2 signaling in these EC, termed stalk cells. This process is dynamic, with tip and stalk cells constantly shuffling position based on VEGFR-2 and DLL4

expression, controlled largely by tightly regulated VEGF gradients in the extracellular space. In addition to VEGF, cells respond to a number of other ligands including ephrins, neuropilins, semaphorins, and slits. Tip cells eventually contact other tip cells, which fuse with the help of macrophages and formation of VE-cadherin (Cdh5)-containing junctions. Stalk cells help generate a new lumen to form patent vessels, allowing blood flow to continue to shape the remodeling vessel.^{28,29} Deposition of a basement membrane and coordinated migration and recruitment of perivascular cells are required to ensure vessel stability.³⁰

1.3.2 Mechanisms of angiogenesis

Multiple pathways mediate SMC-P proliferation, migration, and recruitment to EC during angiogenesis. A key regulator of EC and SMC-P crosstalk during angiogenesis is the PDGF-BB/PDGFRB signaling pathway. Sprouting endothelium releases PDGF-BB as a homodimer, which binds to heparan sulfate proteoglycans (HSPGs) and signals to PDGFRB on mural cells. Global knockout of the ligand or receptor results in perinatal lethality due to perivascular cell deficiency.^{31,32} EC-specific deletion of PDGF-BB generates viable mice, but they have decreased SMC-P density in multiple vascular beds.^{33,34} Knockout of either the PDGF-BB retention motif³⁵ necessary for binding to HSPG, or NDST, an enzyme that causes N-sulfation of proteoglycans,³⁶ leads to decreased SMC-P recruitment and investment of EC tubes, demonstrating that HSPGs are a critical component in EC-mural cell signaling. Other well-studied pathways that mediate EC-SMC-P crosstalk during development and/or angiogenesis include ANG/Tie, Sphingosine 1-phosphate, TGF β , and Notch, among others. Intact signaling of each of these pathways is critical for coordinated growth of EC and mural cells necessary for formation of stable, non-leaky vasculature.^{28,37}

1.4 ANGIOGENESIS IN DISEASE

Dysregulated angiogenesis plays a role in numerous disease pathologies. These include ischemic occlusive diseases such as myocardial infarction, stroke, and peripheral arterial disease (PAD), where angiogenesis positively correlates with functional performance measures.^{38,39} Aberrant and/or excessive angiogenesis are also critical factors in the progression of diseases of the eye, such as diabetic retinopathy and corneal neovascularization (CNV), as well as cancer. We consider below, in more detail, the role of angiogenesis in a few of these pathologic states: PAD, CNV, and tumor growth and metastasis.

1.4.1 Angiogenesis in PAD

Peripheral arterial disease (PAD) is caused by occlusive atherosclerosis in vascular beds other than the heart, with the lower limbs being the most common vascular bed affected. The disease is defined by a reduced ankle brachial index (ABI), which is itself defined as the ratio of the blood pressure in the dorsalis pedis or posterior tibial artery compared to the blood pressure in the brachial artery. The disease, though often underdiagnosed, has a prevalence nearly equal to that of coronary artery disease (CAD), affecting 8.5 million people in the U.S.^{40,41} Smoking and diabetes are two of the principal risk factors, so prevalence is likely only going to continue to rise. Clinical symptoms of PAD are due to reduced blood flow to the lower limb, which manifests as either intermittent claudication (IC) or critical limb ischemia (CLI). In IC, reduced blood flow leads to calf or buttock pain that is relieved with rest. In CLI, this pain occurs even at rest and can additionally result in ulcers and/or gangrene. CLI is the more severe clinical outcome but somewhat paradoxically, the degree of reduced ABI does not correlate with the severity of clinical symptoms. Treatment of PAD is aimed at reducing the manifestations of atherosclerosis. Although some patients are candidates for stent or catheter-based revascularization, some have numerous blockages or co-morbidities that make them poor candidates for revascularization. Additionally,

restenosis following surgical revascularization can occur. Of major importance, there is currently no medical therapy that is capable of improving perfusion to the lower limbs. Therefore, treatment of the causal role of PAD remains an unmet clinical need.^{40,41}

The mouse model commonly used to study PAD is the hindlimb ischemia (HLI) model. There are a number of variations of this model, including the femoral artery ligation/excision (FAL/E) model, originally developed in 1998.⁴² This model attempts to mimic the human disease, which in many patients involves total or near total occlusion along the single path of blood flow to the distal leg.⁴⁰ Therefore, the model involves proximal ligation of the femoral artery just underneath the inguinal ligament, followed by excision of the artery from the proximal ligation to just proximal to the bifurcation of the popliteal artery. Although like any mouse model it has its limitations, the HLI FAL/E model mimics key aspects of the human disease. For instance, ligation and excision of a large segment of the femoral artery creates severe ischemia in downstream muscle, with an approximately 80% reduction in blood flow to the plantar sole. Additionally, patient-to-patient variability observed in PAD is mimicked by distinct rates of perfusion recovery between in-bred strains of mice. For instance, C57Bl/6 mice mount a stronger recovery response than BALB/c mice.⁴³

A number of clinical trials to treat patients with IC and/or CLI by inducing therapeutic angiogenesis have been undertaken over the past two decades. Many of these approaches have built on findings from studies using HLI preclinical models. The TRAFFIC, TALISMAN 201, and TAMARIS trial are a few examples of placebo-controlled clinical trials involving administration of angiogenic growth factors to stimulate angiogenesis in IC or CLI patients.⁴⁴⁻⁴⁶ Overall, these clinical trials have achieved limited success and have largely failed to reproduce more encouraging results observed in preclinical studies. There are a number of potential causes for this, including site of delivery, dosing strategy, an over-emphasis on stimulation of EC growth, and failure to fully consider responses of other critical cell types such as ischemic muscle cells and perivascular cells.

Taken together, there is a dire need to develop new therapeutic approaches for treating IC and CLI patients. One potential approach to improve therapeutic angiogenesis is through enhancing SMC-P phenotypic switching. This requires a better understanding of perivascular cell-specific mechanisms needed to mount a more effective angiogenic response.

1.4.2 Angiogenesis in CNV

Corneal neovascularization (CNV) is a major cause of corneal blindness, the fourth leading cause of blindness in the world.⁴⁷ CNV results when angiogenesis and lymphangiogenesis proceed from the limbal vascular network that resides between the sclera and cornea. CNV is a pathologic condition, since the cornea is normally angiogenic and immunogenically privileged because its transparency is essential for maintaining visual acuity.⁴⁸ This angiogenic privilege is normally actively maintained by anti-angiogenic signaling, including soluble VEGFR-1.⁴⁹ However, following injury or inflammation, there is a disruption of anti-angiogenic signaling, coupled with increased concentrations of pro-angiogenic signaling molecules such as VEGF-A.⁵⁰ This tips the angiogenic balance and allows vessel growth into the cornea, resulting in corneal opacity, fibrosis, and edema. The healthy cornea's avascular nature makes it a useful tissue in which to study angiogenesis *in vivo*, since actively remodeling vessel networks can be readily visualized migrating into a previously avascular region. This allows for detailed analysis of cell-specific mechanisms critical for *in vivo* angiogenesis.

There are a number of mouse models used to study corneal neovascularization. A detailed comparison of *in vivo* models of corneal angiogenesis can be found in Kelly-Goss et al, Scientific Reports, 2017.⁵¹ In brief, these include suturing of the cornea or implanting growth-factor containing-pellets into the cornea. Other methods involve application of chemical alkali burns to the cornea, including use of filter paper soaked with NaOH⁴⁸ or applicator rods coated with silver nitrate.⁵¹ All of these methods induce angiogenesis into the cornea. For our studies in Chapter 3,

we use applicator rods coated with silver nitrate for a variety of reasons including low cost, ease of reproducibility, and reliable formation of an angiogenic network.

1.4.3 Angiogenesis in tumor growth and metastasis

In 1971, Dr. Judah Folkman's group made the seminal discovery that tumors cannot enlarge beyond a certain size without forming new blood vessel networks.⁵² Indeed, angiogenesis is a critical step in tumor growth and metastasis. For many cancers, tumor vascularity inversely correlates with patient survival.⁵³ However, tumor vasculature is highly abnormal. It is characterized by increased diameter, tortuosity, and permeability, as well as decreased perivascular cell investment and differentiation.⁵⁴

Phenotypically modulated SMC-P are also a key component of the premetastatic niche (PMN), where they proliferate, migrate, and secrete extracellular matrix proteins such as fibronectin that enhance tumor cell extravasation into lung tissue. Knockout of the stem cell pluripotency gene *Klf4* specifically in SMC-P impairs SMC-P phenotypic switching in the lung and significantly reduces metastasis to the lungs in several orthotopic tumor models.²⁴ Additionally, four out of nine genes identified as being downregulated in metastatic versus non-metastatic adenocarcinomas are SMC differentiation genes.⁵⁵ Together, these studies demonstrate that altered perivascular cell phenotypic state is a key component of the vasculature in both primary tumors and at metastatic sites.

The combined therapeutic effort aimed at correcting abnormal features of tumor vasculature is termed vascular normalization.⁵⁶ One angle to approach vascular normalization is through the promotion of increased SMC-P investment and differentiation, thereby increasing vessel maturation and limiting vascular leak. Given the clear role of altered SMC-P phenotype in the vasculature of both primary tumors and metastatic sites, a better understanding of mechanisms

controlling SMC-P phenotypic states may provide insights into how to more effectively normalize tumor vasculature.

1.4.4 Summary-Angiogenesis in disease

In summary, angiogenesis is a critical component of numerous pathologic states, including PAD, CNV, and cancer. In PAD, total or near total occlusion of the inflow vessels is accompanied by angiogenesis in distal hypoxic tissue. Excessive and/or dysregulated angiogenesis are characteristic of pathologies such as CNV and cancer. Since SMC-P phenotypic switching is a hallmark of angiogenesis, a better understanding of mechanisms that control SMC-P phenotypic plasticity are required to understand how to manipulate SMC-P functions critical for effective blood vessel remodeling.

1.5 SMC-P PHENOTYPIC SWITCHING IN ANGIOGENESIS

Indeed, the critical role of proper SMC-P function in blood vessel formation and maintenance is well-appreciated. This has been established through a number of *in vivo* approaches, including global knockout of genes such as PDGF-BB that are required for SMC-P recruitment to nascent blood vessels³ as well as diphtheria toxin mediated-ablation of SMC-P.⁵⁷ More recently, studies have begun to dissect SMC-P signaling pathways critical for vascular remodeling in the setting of injury and disease. This is primarily achieved through knock out of genes of interest in SMC-P and rigorous analysis of the resultant phenotypes. For instance, conditional deletion of VEGFR-1 in PDGFRB+ SMC-P results in decreased EC sprouting and increased EC proliferation at the angiogenic front.⁵⁸ Deletion of Tie2 in NG2+ cells, including SMC-P, results in increased SMC-P migration and increased tumor angiogenesis.²¹ Our lab used Myh11-CreERT2 ROSA26 STOP-floxed eYFP lineage tracing, coupled with inducible, SMC-P-specific knockout of the stem cell pluripotency gene Oct4, to show that Oct4 signaling specifically in SMC-P is critical for SMC-P migration and investment into the lesion and fibrous cap of advanced atherosclerotic lesions.⁵⁹

This work was a major impetus for the studies reported in Chapter 3. As such, extensive background will now be provided on Oct4.

1.6 THE STEM CELL PLURIPOTENCY GENE OCT4

1.6.1 Structure of Oct4

Octamer binding transcription factor 4 (Oct4), also known as Pou5f1, is a 360 amino acid sequence encoded on human chromosome 6 and mouse chromosome 17. Oct4 is a member of the Pit-Onc-Unc family of transcription factors. As such, it contains a POU domain, which confers DNA-binding ability by recognizing and binding the octameric sequence AGTCAAAT contained in the promoter and/or enhancer region of its downstream targets.⁶⁰ It also contains an N-terminal transactivation domain and a C-terminal domain.

1.6.2 Role of Oct4 in stem cells

A well-established role of Oct4 is to establish and maintain pluripotency in the developing embryo. Oct4-deficient embryos proceed to the blastocyst stage but die at the time of implantation due to a lack of pluripotent cells in the inner cell mass (ICM).⁶¹ As a master regulator of pluripotency, Oct4 activates pluripotency-associated networks. Activation is achieved through individual or cooperative binding with other pluripotency factors, including Sox2 and Nanog. Together, the three transcription factors bind to and activate their own promoters as well as other key pluripotency-associated genes. They can also individually or cooperatively bind to promoters and repress activation of differentiation-associated genes.

1.6.3 Regulation of Oct4

Oct4 can be regulated through a number of mechanisms, including phosphorylation or ubiquitination, which decrease stability. In contrast, sumoylation increases protein stability and DNA-binding activity.⁶² Oct4 levels must be tightly controlled during the establishment and

maintenance of pluripotency. Reduction of Oct4 levels by half triggers differentiation to trophoblasts, whereas two-fold overexpression induces specification to primitive endoderm and mesoderm.⁶³ Upon induction of differentiation, the Oct4 locus becomes epigenetically silenced through the action of the histone methyltransferase G9a and the *de novo* DNA methyltransferases DNMT3a and DNMT3b.⁶⁴ However, this process can be reversed through the administration of exogenous factors, initially demonstrated by the seminal discovery that fibroblasts can be reprogrammed to induced pluripotent stem cells (iPSCs) through delivery of Oct4, Sox2, Klf4, and c-Myc.⁶⁵ Continued modification and optimization of the reprogramming protocol revealed that Oct4 activation is required to induce reprogramming to ESC-like cells.⁶⁶ Indeed, hypomethylation of the Oct4 promoter is often used to indicate a fully reprogrammed state.⁶³

Given the critical role of Oct4 in establishing and maintaining pluripotency both in the ICM and in reprogrammed somatic cells, the long-standing dogma in the stem cell field was that Oct4 is permanently epigenetically silenced during gastrulation.⁶⁴ Endogenous Oct4 expression was thought to be restricted to pluripotent stem cells and germline cells. Throughout the last few decades, however, numerous groups have reported Oct4 expression in a variety of stem, progenitor, and somatic cell compartments. Many of these results have been challenged though, because of several nuances involving the Oct4 gene, including the presence of at least three alternative transcripts, five protein products, and eight pseudogenes.⁶⁷

1.6.4 Isoforms and pseudogenes of Oct4

The three alternative Oct4 transcripts are termed Oct4A, Oct4B, and Oct4B1 and are generated by alternative splicing of the four exons within the Oct4 locus. This alternative splicing results in different 5' termini but identical 3' termini. Exon 1 is unique to Oct4A, and therefore Oct4A is the only transcript that contains the N-terminal transactivation domain necessary for establishment of pluripotency. In contrast, Oct4B and Oct4B1 lack exon 1 and thus lack pluripotent capacity. The Oct4B transcript contains an internal ribosome entry site (IRES) and is capable of

producing at least three protein products.⁶⁰ Oct4B1 also appears capable of producing a functional protein product.⁶⁸ Adequately distinguishing between Oct4A transcript and Oct4B and Oct4B1 transcripts requires rigorous primer design, including intron-spanning forward primers that recognize sequences specific to exon1. Identification of Oct4A protein, and not Oct4B or Oct4B1, requires use of an antibody specific to the N-terminus.

There are also at least eight identified Oct4 pseudogenes, which share high sequence homology with the full length Oct4A protein. In particular, pseudogenes 1, 3, and 4 share the unique N-terminal domain that is missing in Oct4B and Oct4B1 protein products. By definition, pseudogenes do not share exact sequence identity, lack full functionality, and are devoid of introns. However, they are remarkably similar in sequence and are still capable of performing regulatory functions.⁶⁹ Therefore, they are another potential source of false positives in previous studies claiming Oct4A expression in non-pluripotent stem cell sources, including in studies using antibodies specific to the N-terminus.

1.6.5 Dogma: Oct4 expression is limited to pluripotent stem cells and germline cells

In light of numerous publications reporting Oct4 expression in various stem, progenitor, and somatic cell compartments, Lengner et al. performed a functional study using a Cre-lox based approach. Specifically, Oct4 floxed mice were crossed with mice containing inducible Cre transgenes. Importantly, loxP sites were designed around exon 1 of the Oct4 locus,⁷⁰ thus specifically deleting the pluripotent capacity of Oct4 following Cre induction. This allowed for deletion of the Oct4 locus in a number of tissues including intestine, bone marrow, brain, liver, and hair follicles. In all tissues examined, there were no significant effects on tissue homeostasis or regeneration following Oct4 knockout. Additionally, this study utilized an Oct4-EGFP mouse, in which EGFP is expressed from the endogenous Oct4 locus, to test whether Oct4 was expressed in any of the aforementioned tissues. The group found no evidence for Oct4 activation in any of the tissues tested. Therefore, the group concluded that the Oct4 locus is permanently epigenetically

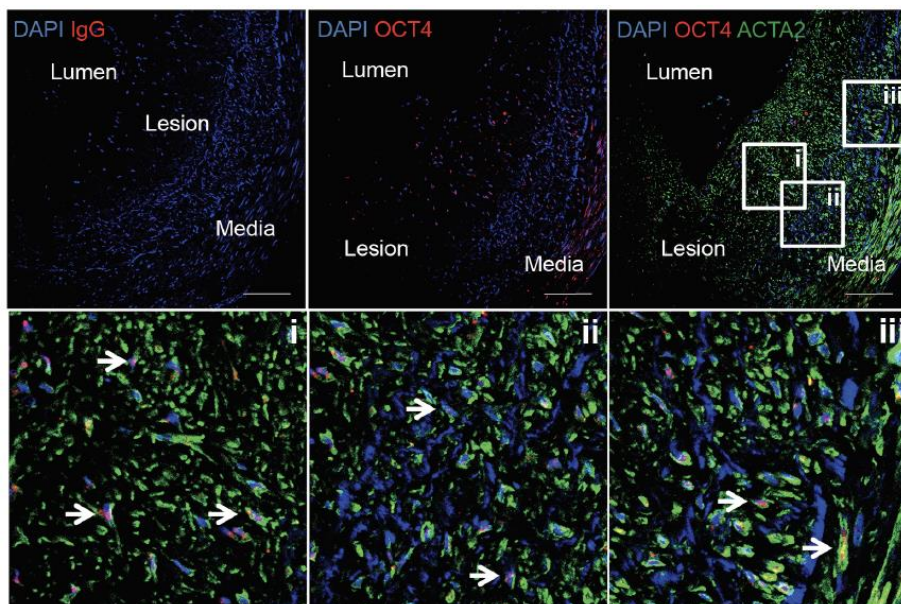
silenced and is dispensable for somatic stem cell self-renewal and tissue regeneration in the adult mouse.⁶⁷ This study has called into question many, if not all, of the reports of Oct4 expression in various somatic cells. Indeed, it is likely that at least some of these results are false positives, due to detection of non-pluripotent isoforms and/or pseudogenes. Prior to work from our lab, Lengner et al. was the only study to utilize a loss-of-function approach to specifically test whether Oct4A plays a functional role in somatic cells.⁶⁷

1.6.6 Detection of Oct4 in mouse and human atherosclerotic lesions

Dr. Olga Cherepanova, a former research scientist in the Owens Lab, also detected Oct4 protein in eYFP+ cells of atherosclerotic lesions of Myh11 eYFP mice. To determine whether Oct4 was also expressed in SMC-like cells in human atherosclerotic lesions, I performed Oct4 immunostaining in cross-sections of human coronary arteries with atherosclerotic lesions. I observed numerous OCT4+ACTA2+ cells, suggesting Oct4 expression in SMC-like cells (

Figure 1-2a-b). Importantly, I used an Oct4 antibody that recognizes the N-terminus and therefore detects Oct4A protein and not Oct4B or Oct4B1. This data is shown below, adapted from Cherepanova et al, Nature Medicine, 2016.⁵⁹

a



b

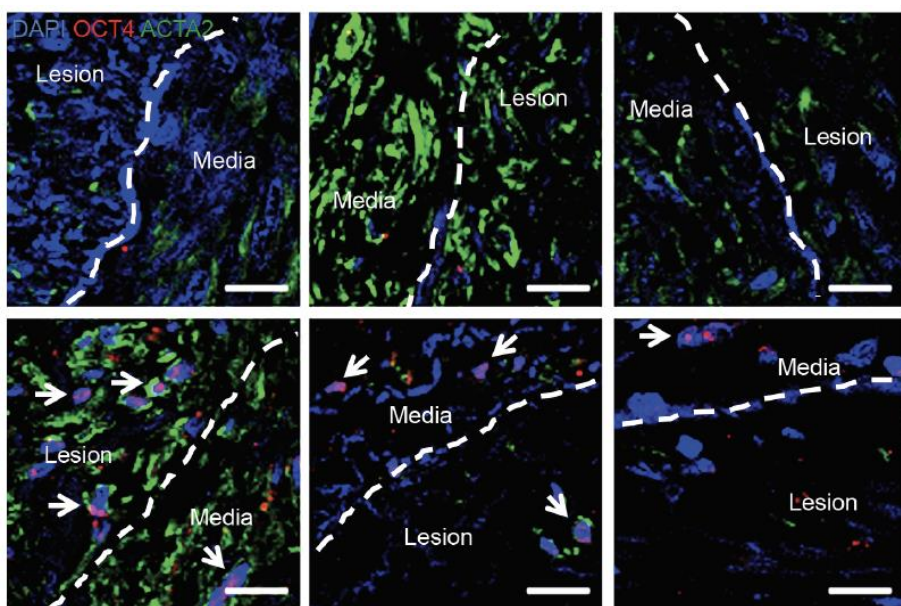


Figure 1-2

Activation of OCT4 within human atherosclerotic lesions. a,b, OCT4 was activated within advanced atherosclerotic lesions of the left anterior descending (LAD) coronary artery. Immunofluorescence staining for OCT4, ACTA2 and DAPI revealed Oct4+ nuclei/ACTA2+ cells

(white arrows). The examples shown in panel **a** were from a 53-year-old male subject. Panels **i**, **ii** and **iii** represent magnified boxed areas from the upper panels. Scale bar = 100 μm . **b**, Upper panels – 3 representative human LAD coronary artery samples from 3 different subjects with less than 20% occlusive lesions; lower panels – 3 human LAD coronary samples from 3 different subjects with >80% occlusive atherosclerotic lesions. Oct4⁺ nuclei/ACTA2⁺ cells are indicated with white arrows. Scale bar = 10 μm .

To determine whether Oct4 plays a functional role in SMC, we used a Cre-lox based loss-of-function approach, utilizing the same Oct4 floxed mouse described in Lengner et al.⁶⁷ Specifically, we crossed this Oct4 floxed mouse with our Myh11-CreERT2 ROSA26 STOP-floxed eYFP mouse. Following tamoxifen injections between 6-8 weeks of age, this allowed for permanent deletion of exon 1 of the Oct4 locus specifically in Myh11-expressing SMC. Using an ApoE^{-/-} mouse model of atherosclerosis combined with 18 weeks of high fat western diet feeding, we then conducted an extensive analysis of atherosclerotic lesions in Oct4 WT Myh11 eYFP^{+/+} ApoE^{-/-} and Oct4 KO Myh11 eYFP^{+/+} ApoE^{-/-} mice.⁵⁹

1.7 ROLE FOR OCT4 IN SMC IN ATHEROSCLEROSIS

1.7.1 Oct4 in SMC is atheroprotective

Analysis of cross-sections of the brachiocephalic arteries (BCA) revealed increased lesion area, increased vessel size, and decreased lumen area in Oct4 KO mice relative to Oct4 WT littermate controls. Additionally, lesions from Oct4 KO mice had increased necrotic core area, increased rates of hemorrhaging, and increased lipid content, but decreased collagen maturation. Immunofluorescence and confocal analysis revealed decreased numbers of eYFP⁺ cells in both the lesion and fibrous cap. All of these changes are consistent with decreased lesion stability.

Therefore, Oct4 signaling in SMC is critical for atherosclerotic lesion stability, at least in the BCA.⁵⁹

1.7.2 Oct4 promotes SMC migration

To determine whether the reduced number of eYFP+ cells in the lesion and fibrous cap was due to decreased proliferation and/or increased apoptosis, our lab performed immunostaining for KI67 and cleaved caspase-3. However, we observed no significant difference in KI67 or cleaved caspase-3 staining in eYFP+ cells between Oct4 WT and Oct4 KO lesions, suggesting that differences may instead be due to altered migration of eYFP+ cells. Because there are no specific *in vivo* markers of migration, our lab then performed *in vitro* SMC migration studies. Using both siRNA-mediated knockdown of Oct4, as well as isolated Oct4 WT and KO aortic SMC, we demonstrated that migration of SMC is reduced following Oct4 knockdown or knockout. qRT-PCR analysis of Oct4 WT and Oct4 KO SMC identified several genes downregulated in Oct4 KO SMC relative to Oct4 WT SMC, including osteopontin, MMP3, and MMP13. Additionally, *in vivo* and *in vitro* RNA-Seq analysis identified a number of genes and pathways dysregulated following Oct4 knockout, including genes and pathways implicated in cell migration. Taken together, results suggest that Oct4 expression in SMC promotes their migration in the setting of atherosclerosis.⁵⁹

1.7.3 Oct4 is reactivated in SMC through hydroxymethylation

To determine mechanisms of Oct4 reactivation in SMC, our lab performed bisulfite sequencing of the Oct4 promoter-enhancer region in cells treated with hypoxia plus the oxidized phospholipid POVPC, conditions that we showed activate Oct4 expression. We observed no significant difference in methylation status. However, we demonstrated that increased Oct4 expression correlated with increased hydroxymethylation of the Oct4 promoter-enhancer, both in cultured SMC and *in vivo* in atherosclerotic lesions. Site-directed mutagenesis of HIF1A and/or KLF4 binding sites within the Oct4 promoter-enhancer led to reduced Oct4 activation. Enrichment

of HIF1A and KLF4 binding to the Oct4 promoter-enhancer also occurred *in vivo* in ApoE^{-/-} mice following 18 weeks of western diet feeding. Together, these results revealed that Oct4 reactivation in SMC in the setting of atherosclerosis occurs at least in part through increased hydroxymethylation of the Oct4 promoter-enhancer, allowing for epigenetic de-repression and increased binding of HIF1A and KLF4.⁵⁹

Of note, it was demonstrated that this increased binding of KLF4 to the Oct4 promoter-enhancer was specific to eYFP⁺ cells using a novel *in situ* hybridization-proximity ligation assay (ISH-PLA) developed in our lab. This technique allows for the detection of protein binding or histone modifications at specific gene loci at single cell resolution. We originally used this technique to discover that phenotypically modulated SMC-P retain the H3K4diMe mark at the *Myh11* locus. Importantly, this retention of the H3K4diMe mark also occurs in SMC in human tissues and therefore ISH-PLA allows for the identification of phenotypically modulated SMC-P in human tissue.¹⁴

1.7.4 Is Oct4 function in SMC unique to the setting of advanced atherosclerosis?

By demonstrating that Oct4 plays a critical atheroprotective role in SMC, Cherepanova et al. overturned the long-standing dogma that Oct4 function is limited to pluripotent stem cells.⁶⁷ Of note, Lengner et al. did not delete Oct4 in the vasculature and therefore the conclusion that Oct4 does not play a functional role in any somatic cell appears to have been overly conclusive.⁶⁷ Indeed, Oct4 reactivation in SMC plays an essential functional role in promoting migration of SMC into the lesion and fibrous cap, which is essential for the stability of atherosclerotic lesions. However, with this important discovery, Cherepanova et al.⁵⁹ raised a number of additional questions warranting future study. First of all, is Oct4 reactivation unique to the setting of advanced atherosclerosis, or is it also reactivated in SMC in other pathologic disease states? For instance, a number of studies have detected expression of Oct4 within tumors.⁶⁷ It is possible that at least some of these reports are due to Oct4 expression in SMC of the tumor vasculature. In support of this, the

tumor microenvironment of actively growing tumors is typically highly vascular, hypoxic, and inflammatory. Hypoxia or the TLR3 agonist poly I:C are sufficient to activate Oct4 in SMC, at least *in vitro*, so perhaps they are also sufficient *in vivo*.⁵⁹ A similar, not mutually exclusive, idea is that Oct4 actually evolved to play a functional role in processes critical for survival and reproductive success. By this logic, reactivation of Oct4 in pathologic states such as atherosclerosis may be unintended secondary consequences of its evolved role in these processes. Indeed, end-stage complications of atherosclerosis, including myocardial infarction and stroke, typically occur in individuals well after their reproductive years. As such, there would have been no selective pressure for Oct4 reactivation in SMC to have evolved in the setting of atherosclerosis. Therefore, a key unresolved question is whether Oct4 reactivation in SMC is unique to advanced atherosclerosis or whether Oct4 evolved a functional role in SMC to enhance processes critical for survival and reproductive success, such as angiogenesis. In Chapter 3, I test the hypothesis that Oct4 plays a critical functional role in SMC-P during angiogenesis using two different *in vivo* angiogenesis models: corneal alkali burn and hindlimb ischemia.

1.8 SMC-P PHENOTYPIC SWITCHING IN CANCER

Our lab and others have demonstrated that SMC-P play critical functional roles in the setting of atherosclerosis, as evidenced by SMC-P-specific KO of *Klf4* or *Oct4*.^{15,59} Of major importance, Murgai et al. recently demonstrated, using rigorous *Myh11* and *NG2* lineage tracing, that SMC-P undergo extensive *Klf4*-dependent phenotypic switching in the pre-metastatic lungs. Knock out of *Klf4* in *Myh11* or *NG2*-expressing SMC-P impaired SMC-P phenotypic switching and resulted in significantly decreased metastasis of tumor cells to the lung.²⁴ Furthermore, gene expression analysis of hundreds of adenocarcinomas revealed that SMC differentiation genes are downregulated in highly metastatic tumors relative to non-metastatic tumors.⁵⁵ Therefore, SMC-P phenotypic switching plays critical roles not only in atherosclerosis and angiogenesis following

injury but also in cancer pathogenesis. Another critical observation from Murgai et al. was that IL-1 β induces Klf4 expression in SMC-P²⁴, at least *in vitro*, raising the possibility that at least some of the changes leading to enhanced SMC-P phenotypic switching and metastasis were due to increased IL-1R signaling in SMC-P. Together, these findings led us to the hypothesis that SMC-P IL-1R signaling promotes tumor growth and metastasis. We test this hypothesis in Chapter 4 using SMC-P KO of IL-1R in multiple orthotopic tumor models.

1.9 IL-1 SIGNALING IN CANCER

Interleukin 1-signaling occurs through binding of the agonistic proteins IL-1 α or IL-1 β to the IL-1R, leading to activation of interleukin 1-receptor associated kinases (IRAKs), ultimately resulting in NF κ B and MAPK-dependent signaling pathways critical in inflammation and immunity. IL-1R is expressed by a number of cell types including bone marrow derived cells (BMDCs), EC, and SMC.⁷¹ IL-1 α and IL-1 β are upregulated in a number of human tumors.⁷² Global knockout of IL-1 β results in decreased primary tumor growth and decreased metastasis in multiple tumor models, and global knockout of IL-1 α results in similar, albeit more modest, effects.⁷³ Treatment of mice with anakinra, a recombinant IL-1R antagonist which mimics naturally occurring IL-1Ra, leads to decreased breast tumor growth and metastasis to bone.⁷⁴ Taken together, there is a clear link between IL-1R signaling in tumor growth and metastasis. As further support of this, the Canakinumab Antiinflammatory Thrombosis Outcomes Study (CANTOS) phase III clinical trial recently reported that high-risk atherosclerotic patients treated with the IL-1 β neutralizing antibody, canakinumab, had a roughly 70% reduction in lung cancer incidence and fatality, compared to patients receiving placebo.⁷⁵ While this finding corroborates previous basic science studies and establishes a clear clinical effect, the critical cell types that mediate IL-1R signaling in cancer pathogenesis remain unknown.

1.9.1 IL-1 signaling in BMDCs

BMDCs are a key component of the tumor microenvironment and directly participate in IL-1 signaling. IL-1 β induces recruitment and maturation of BMDCs. For example, neutralization of IL-1 β reduced infiltration of VEGFR1+ BMDCs into Matrigel plugs containing B16 melanoma cells.⁷⁶ Interestingly, VEGFR1+ BMDCs are present in the pre-metastatic lungs and neutralization of VEGFR1 signaling inhibits pre-metastatic niche formation and metastasis.⁷⁷ Of note, these VEGFR1+ BMDCs express VLA-4, which binds to fibronectin upregulated by tumor-specific growth factors, allowing for extravasation into the lung and establishment of the pre-metastatic niche.⁷⁷ Therefore, BMDCs are critical for both primary tumor growth and subsequent metastasis, likely at least in part through IL-1 dependent signaling.

1.9.2 IL-1 signaling in EC

Endothelial cells and perivascular cells are both necessary for angiogenesis, one of the hallmarks of tumor progression. IL-1 β can induce phenotypic changes in each of these cell types. For instance, studies have shown that treatment of cultured EC with recombinant IL-1 β leads to increased tube formation.⁷⁸ Additionally, global knockout of IL-1 β results in decreased recruitment of endothelial progenitor cells (EPCs), decreased VEGFR-2 expression, and decreased VCAM1 expression in ECs following HLI.⁷⁹ The effects of IL-1 on EC are likely both direct and indirect. There is evidence that IL-1 β indirectly affects EC growth by acting on myeloid cells to stimulate them to produce pro-angiogenic cytokines including VEGF. For instance, neutralization of IL-1 β in macrophage-derived supernatants resulted in decreased VEGF and angiogenesis in Matrigel plugs.⁸⁰ IL-1 β and VEGF synergistically function to induce an angiogenic response in Matrigel plugs, with inhibition of either cytokine leading to reduced expression of the other, concomitant with decreased vascular density.⁷⁶

1.9.3 IL-1 signaling in SMC-P

IL-1 β stimulation of SMC *in vitro* induces SMC phenotypic switching, including downregulation of contractile proteins such as ACTA2 and SM-MHC and upregulation of multiple inflammatory markers.¹¹ Additionally, IL-1 β induces SMC proliferation and migration.⁸¹ IL-1R signaling is also relevant *in vivo*, as studies from our lab have shown IL-1R signaling in SMC is critical for promoting investment of SMC-P into the lesion and fibrous cap.¹⁷

1.10 OVERALL SUMMARY

SMC-P phenotypic switching occurs extensively in the setting of injury and disease, including atherosclerosis, angiogenesis, as well as tumor growth and metastasis. Conditional knockout of single genes in SMC-P can significantly impact SMC-P phenotypic switching, resulting in profoundly altered responses to injury and disease. For instance, previous work from our lab in the setting of atherosclerosis demonstrated that SMC KO of Oct4 leads to decreased indices of lesion stability, at least in part due to impaired SMC migration.⁵⁹ In Chapter 3, we test the hypothesis that this role for Oct4 is conserved, and indeed likely evolved, in the setting of angiogenesis following HLI or corneal burn. Additionally, we have shown that SMC-P phenotypic switching promotes PMN formation and tumor metastasis. Of major interest, the CANTOS trial recently demonstrated a clear link between IL-1 signaling and cancer pathogenesis. In Chapter 4, we test the hypothesis that IL-1R signaling in SMC-P promotes tumor growth and metastasis.

2 CHAPTER 2: MATERIALS AND METHODS

2.1 MICE

Myh11-CreER^{T2} ROSA floxed STOP eYFP Oct4^{FL/WT} mice were generated as previously described.⁵⁹ Briefly, we first bred Oct4^{FL/FL} (Pou5f1^{tm1Scho})⁷⁰ mice with Myh11-CreER^{T2} (Tg(Myh11-cre/ERT2)1Soff)⁸² mice to generate Oct4^{FL/WT} Myh11-CreER^{T2} mice. The Myh11-CreER^{T2} transgene is on the Y chromosome, precluding the use of Cre-negative mice as controls. We then bred Myh11-CreER^{T2} Oct4^{FL/WT} males with Oct4^{FL/WT} females to generate Myh11-CreER^{T2} Oct4^{FL/FL} and Myh11-CreER^{T2} Oct4^{WT/WT} male littermates. We then crossed ROSA26-STOP^{fllox}YFP^{+/+} mice (B6.129X1-Gt(ROSA)26Sortm1(eYFP);Cos/J) with Myh11-CreER^{T2} mice to yield Myh11-CreER^{T2} ROSA26-STOP^{fllox}YFP^{+/+} mice using the same strategy described above. We then crossed Oct4^{FL/FL};Myh11-CreER^{T2} male mice with Myh11-CreER^{T2} ROSA26-STOP^{fllox}YFP^{+/+} mice to generate Oct4^{FL/WT} Myh11-CreER^{T2} ROSA floxed STOP eYFP males and Oct4^{FL/WT} ROSA floxed STOP eYFP female mice. The resulting mice were then backcrossed nine generations to the C57BL/6 line (Jackson Labs; Bar Harbor, ME). We then used these mice as breeders to generate Myh11-CreER^{T2} ROSA floxed STOP eYFP Oct4^{WT/WT} and Myh11-CreER^{T2} ROSA floxed STOP eYFP Oct4^{FL/FL} male littermate mice which were genetically identical other than containing WT versus floxed Oct4 alleles. We achieved Cre-mediated recombination via ten daily intraperitoneal injections of tamoxifen (Sigma-Aldrich; St. Louis, MO) (1mg in 100 μ l of peanut oil (Sigma-Aldrich; St. Louis, MO)) between 6-8 weeks of age. All experimental mice received identical amounts of tamoxifen. We only used male progeny for experiments, since the Myh11-CreER^{T2} transgene is located on the Y chromosome. Upon tamoxifen treatment, there is

simultaneous activation of eYFP and excision of the floxed Oct4 alleles, generating Myh11-CreER^{T2} ROSA eYFP Oct4^{WT/WT} and Myh11-CreER^{T2} ROSA eYFP Oct4^{Δ/Δ} mice. Henceforth, we refer to them as Oct4^{SMC-P WT/WT} and Oct4^{SMC-P Δ/Δ}, for simplicity. At 12-18 weeks of age, mice were used for experiments. We also crossed our Myh11-CreER^{T2} ROSA floxed STOP eYFP mice with NG2-DsRED (Tg(Cspg4-DsRed.T1)1Akik/J) (Jackson Labs; Bar Harbor, ME) mice to generate NG2-DsRED Myh11-CreER^{T2} ROSA floxed STOP eYFP mice. We treated these mice with the same tamoxifen protocol outlined above to generate NG2-DsRED Myh11-CreER^{T2} ROSA eYFP mice.

Myh11-CreER^{T2} ROSA26-STOP^{fllox}YFP^{+/+} mice were also crossed to ApoE^{-/-} mice, as previously described.^{15,59} These mice were then crossed with IL-1R^{FL/FL} mice, as previously described.¹⁷ Male ApoE^{-/-} Myh11 CreER^{T2} ROSA eYFP IL-1R^{FL/WT} mice were then bred with female ApoE^{-/-} IL-1R^{FL/WT} ROSA eYFP mice to generate ApoE^{-/-} Myh11 CreER^{T2} ROSA eYFP IL-1R^{WT/WT} or ^{FL/FL} male mice and ApoE^{-/-} ROSA eYFP IL-1R^{WT/WT} or ^{FL/FL} female mice. These ApoE^{-/-} Myh11 IL-1R^{WT/WT} and ApoE^{-/-} Myh11 IL-1R^{FL/FL} male and female mice were used to establish final IL-1R WT or KO breeder pairs, which were used to generate experimental mice. We treated experimental mice with the same tamoxifen protocol outlined above.

Cdh5-CreER^{T2} mice were a kind gift from Dr. Ralf Adams. These mice were crossed with ApoE^{-/-} ROSA26-STOP^{fllox}YFP^{+/+} mice to generate ApoE^{-/-} Cdh5-CreER^{T2} ROSA26-STOP^{fllox}YFP^{+/+} mice. These mice were then crossed with IL-1R^{FL/FL} mice to generate ApoE^{-/-} Cdh5-CreER^{T2} ROSA26-STOP^{fllox}YFP^{+/+} IL-1R^{FL/WT} mice. The Cdh5-CreER^{T2} transgene allows use of both male and female experimental mice. However, to limit potential recombination due to estrogen-mediated activation of ER^{T2}, we bred ApoE^{-/-} Cdh5-CreER^{T2} ROSA26-STOP^{fllox}YFP^{+/+} IL-1R^{FL/WT} male mice with ApoE^{-/-} ROSA26-STOP^{fllox}YFP^{+/+} IL-1R^{FL/WT} female mice. These ApoE^{-/-} Cdh5 IL-1R^{WT/WT} and ApoE^{-/-} Cdh5 IL-1R^{FL/FL} male and female mice were used to establish final IL-1R WT or KO breeder pairs, which were used to generate experimental mice. We treated

experimental mice with the same tamoxifen protocol outlined above. Protocols for experiments involving mice were approved by and performed in accordance with the University of Virginia Animal Care and Use Committee.

2.2 WHOLE MOUNT RETINA IMAGING

Thirty minutes prior to sacrifice, isolectin (IB4-Alexa647; Life Technologies; Carlsbad, CA) was injected into the mouse tail vein. Mice were euthanized by CO₂ asphyxiation and then whole retinas were removed and flat-mounted on slides to image isolectin plus endogenous NG2-dsRED and eYFP fluorescence. Images were taken on a Zeiss LSM700 scanning confocal microscope on 20x magnification.

2.3 EYFP+ CELL SORTING

Mice were euthanized with CO₂ asphyxiation and perfused with 10 ml PBS. Tissues were harvested and digested with 4 U/ml Liberase TM (Roche 05401119001) and 0.74 U/ml Elastase in RPMI-1640 for 1.5 hr at 37°C. Tissues were spun down at 1000g for 10 min, resuspended in FACS buffer and run through a 70µm cell strainer. Samples were run on a Becton Dickinson FACSVantage SE Turbo Sorter and sorted based on native eYFP expression.

2.4 BLOOD PRESSURE TELEMETRY

Blood pressure and heart rate were measured using radiotelemetry units (Data Sciences International; St. Paul, MN). The catheter of a radiotelemetry unit was inserted into the left carotid artery and the radiotransmitter was placed in a subcutaneous pouch on the right flank. Blood pressure was recorded for 5 minutes per hour for 2 days on, then five days off, for a total of 10 days of recording. Recordings were limited to weekend days to minimize noise and stress-related fluctuations in blood pressure.

2.5 CORNEAL ALKALI BURN

Corneal alkali burn surgery was performed as previously described.⁵¹ At 12-18 weeks of age, mice were anesthetized with isofluorane (2% isofluorane, 200 ml/min flow rate). A drop of sterile 0.5% Proparacaine Hydrochloride Ophthalmic Solution was added as a topical anesthetic to numb the eye two minutes prior to burn and another drop applied immediately prior to burn. Corneal alkali burn was induced by applying applicator sticks coated with 75% AgNO₃/25% KNO₃ (SnypStix by Graeco; Atlanta, GA) to the center of the right cornea for 10 seconds. An additional drop of Proparacaine was applied to the right cornea immediately post-burn, and mice received post-operative analgesic (buprenorphine 0.1-0.2 mg/kg subcutaneous). For each experimental mouse, the contralateral eye remained unburned and untreated.

2.6 INTRAVITAL CONFOCAL MICROSCOPY AND QUANTIFICATION

Intravital confocal microscopy of the cornea was performed as previously described.⁵¹ Briefly, animals were anesthetized with an intraperitoneal injection of ketamine/xylazine/atropine (60/4/0.2 mg/kg body weight) (Zoetis; Kalamazoo, MI/West-Ward; Eatontown, NJ/Lloyd Laboratories; Shenandoah, IA). A drop of sterile 0.5% Proparacaine Hydrochloride Ophthalmic Solution was added as a topical anesthetic to numb the eye before imaging. Ophthalmic lubricant Genteal gel (Alcon; Fort Worth, TX) was applied to the eye during imaging to prevent drying. Mice were placed on a microscope stage that contained a warming pad to maintain a constant body temperature of 37°C, eyelashes and whiskers were gently pushed back with ophthalmic lubricant Genteal gel, and the snout was gently restrained with a nosecone. Mice were imaged immediately (within ten minutes) prior to injury (day 0), and then at days 3, 7, and 21 post-injury on a confocal microscope (Nikon Instruments Incorporated, Melville, NY; Model TE200-E2; 10X, 20X, and 60X objectives optimized for 3 channels-laser excitation wavelengths at 488, 543, and 632). Immediately prior to each round of imaging, mice were perfused with isolectin GS-IB4 (lectin) or rhodamine-dextran

(MW 70 kDa, Sigma-Aldrich) via retro-orbital injection into the contralateral eye to visualize perfusion-competent vasculature. During imaging, the right eye was placed against a coverslip that rested on the stage of the inverted confocal microscope. The entire portion of the eye that rested on the stage, or approximately one quarter of the entire corneal circumference, was imaged on 20x or 60x magnification by taking multiple fields of view (FOV) using Z-stack imaging through the entire cornea thickness. Each FOV was then compressed into a maximum intensity projection. All FOV from each eye were stitched together into montages using Adobe Illustrator and then analyzed. To rigorously quantify the number of eYFP⁺ cells within each montage, the corneal vascular networks were divided into distinct regions. The number of cells on the arteriole-venule (A-V) pair was counted to determine the number of eYFP⁺ cells per A-V pair. To quantify number of eYFP⁺ cells beyond the A-V pair in the direction of the center of the cornea, we divided the vascular network into 50 μm regions, where 50 μm was measured from the A-V pair towards the cornea center along the entire length of the montaged image. The number of eYFP⁺ cells in each of these regions was counted and normalized to the area of the respective region. Researchers were blinded to the genotype of the animals until the end of analysis.

2.7 BRIGHT FIELD IMAGING AND QUANTIFICATION OF HEMORRHAGING

Bright field images of corneas under 4X magnification were obtained using a Nikon Digital Sight DS-L2 Camera Controller (Nikon Instruments Inc, Melville, NY; Model 214602) to assess the network-wide hierarchy of neovessels and determine the macrostructural health of the tissue (Figure 4c). For each mouse, multiple fields of view were taken encompassing the entire circumference of the eye. Corneal hemorrhaging in bright field montages was graded on a scaled score from 0-7, adapted from Kisucka et al.⁸³

2.8 RHODAMINE DEXTRAN INJECTIONS

Mice were imaged at day 3 post corneal-burn. Following anesthetization with ketamine/xylazine/atropine, mice were administered a retro-orbital injection of 70kDa rhodamine-dextran (Sigma-Aldrich) immediately prior to imaging, such that movie recording started < 3 minutes post-injection. Consequently, the perfusion and leak of dextran have just begun at the onset of recording. Digital images of the vascular networks were acquired using a NikonTE200-E2 confocal microscope, as described above. One field of view per cornea was imaged with full-thickness Z-stacks (25-30 slices at 3 μm between each slice) on repetition for 90 minutes. Volume renders of z-stacks, using the maximum intensity projection, were used to capture the entire corneal vascular network in the field of view. Movie files were analyzed in ImageJ, where we measured the mean pixel intensity in three equal-size regions of interest (ROIs) that were evenly distributed across three different areas in the field of view (above limbus, in vascular loops within the limbus, and below the A-V pair defining the start of the limbus), for a total of nine ROIs analyzed per frame. The three ROIs within a given area were then averaged for each frame and recorded as a single value. These values were then plotted against time. Finally, we quantified the Area Under the Curve to capture the total leak of dextran from the mouse over time. Researchers were blinded to the genotype of the animals until the end of analysis.

2.9 WHOLE MOUNT CORNEA IMMUNOSTAINING

Mice were euthanized by CO₂ asphyxiation and then whole corneas, including the limbus, were removed and washed in phosphate-buffered saline (PBS; Life Technologies; Carlsbad, CA). Corneas were then fixed in 1% paraformaldehyde (PFA; Electron Microscopy Sciences; Hatfield, PA) for 45 min, followed by blocking for 1 hour in blocking buffer containing 10% horse serum. Primary anti-GFP antibody (Abcam ab6673, 1:100) was added overnight at 4°C in blocking buffer. Corneas were then washed and stained for 1.5 hours in blocking buffer with CD31 (Dianova 310,

1:250) and/or Slit3 (Sigma SAB2104337, 1:50). Corneas were then washed in PBS+0.1% Tween-20, followed by staining with appropriate secondary antibodies (Alexafluor, 1:250) for 1.5 hours in blocking buffer. Corneas were washed in PBS+0.1% Tween-20, stained with DAPI (1:100) for 10 min, washed with PBS, and then flat-mounted on slides using 50/50 PBS/Glycerol. Images were acquired at 10x magnification on a Zeiss LSM700 scanning confocal microscope using full-thickness Z stacks (approximately 15-20 slices at 5 μ m between each slice). For each cornea a minimum of 2 FOV from different leaflets were used for analysis. Individual slices were then collapsed into maximum intensity projections for analysis using Zen 2009 Light Edition Software or Image-Pro Plus. Researchers were blinded to the genotype of the animals until the end of analysis.

2.10 HARVESTING, IMMUNOSTAINING, AND ANALYSIS OF TISSUE

Mice were euthanized by CO₂ asphyxiation and then perfused through the left ventricle with 5 ml of PBS, followed by 10 ml of 4% Periodate-Lysine-Paraformaldehyde (PLP), followed by 5 ml of PBS. Whole eyes were fixed for an additional 2 hours in 4% PLP. Tissues were then processed through a sucrose gradient and embedded in OCT compound, frozen in liquid nitrogen, and stored at -80°C until sectioning. Eyes, calf muscle, and/or thigh muscle was serially sectioned at 5-10 μ m thickness on a cryostat. For immunohistochemical staining, slides were blocked for 1 hour in blocking buffer containing 10% horse serum + 0.6% fish skin gelatin in PBS. Primary antibodies were added overnight in blocking buffer at 4°C, and then tissues were washed 2x with PBS-Tween (0.1%). Secondary antibodies were added for 1 hour at room temperature in blocking buffer. Tissues were then washed 2x with PBS-Tween (0.1%), counterstained with DAPI, and cover slipped using Prolong Gold mounting medium. Slides were stained using combinations of the following primary antibodies: GFP (Abcam ab6673, 1:250), CD31 (Dianova 310; 1:250), KI67 (abcam ab15583, 1:500), NG2 Chondroitin Sulfate Proteoglycan (Millipore AB5320, 1:500),

PDGFR β (abcam ab32570, 1:500), and Slit3 (Sigma SAB2104337, 1:50). For TUNEL staining, dUTP conjugated to CF 640R dye (Biotium, 1:50) was used. DAPI (1:100) was used to label nuclei and Alexafluor 555 Phalloidin (1:1000) was used to label muscle fibers. Isotype-matched IgG antibodies were used as a negative control for all antibodies. All secondary antibodies were Alexafluor and used at 1:250 concentration. No TdT enzyme was used as a negative control for TUNEL staining. Images were acquired using a Zeiss LSM700 scanning confocal microscope. A minimum of 3 FOV from multiple locations throughout the tissue were analyzed. High-resolution Z-stack analysis was performed using Zen 2009 Light Edition Software to ensure staining was limited to a single cell. For analysis of eye cross-sections, quantification was limited to cells comprising the corneal vasculature. For pixel analysis, Z-stack slices were collapsed into maximum intensity projections and analyzed using Image-Pro Plus. Researchers were blinded to the genotype of the animals until the end of analysis.

2.11 HINDLIMB ISCHEMIA MODEL

Hindlimb ischemia surgery was performed as previously described.⁸⁴ At 12-18 weeks of age, mice were anesthetized with ketamine (90 mg/kg) and xylazine (10 mg/kg) and then subjected to unilateral femoral artery ligation and resection. Blood flow in the plantar soles was monitored with a laser Doppler perfusion imaging system (Perimed, Inc, Ardmore, PA) immediately after surgery (day 0) and then at days 3, 7, 14, and 21 post-surgery. Mice were placed on a warming pad during surgery and during laser doppler image acquisition to maintain a constant body temperature of 37°C. Perfusion was expressed as the ratio of the left (ischemic) to right (nonischemic) hindlimb. The right hindlimb served as an internal control for each mouse. Animals received buprenorphine (intraperitoneal) immediately after surgery and every 8-12 hours thereafter until 48 hours post-surgery.

2.12 RNA-SEQ ANALYSIS

Genes differentially expressed in hypoxic with respect to normoxic conditions were found for both Oct4 knockout (comparison 1) and wild-type (comparison 2) cultured mouse aortic SMC. Genes differentially expressed in comparison 1 with respect to comparison 2 were found. Since this comparison yielded a high number of genes, strict cuts of 5 in the absolute value of log₂ fold change and 0.01 in False Discovery Rate were applied. oPOSSUM web-based tool⁸⁵⁻⁸⁷ was used to find transcription factors targeting the resulting list of genes (193 genes after the cuts). The tool was run with the following parameters: all 29347 oPOSSUM database genes used as a background; all vertebrate profiles with a minimum specificity of 8 bits used; Transcription factor binding site search parameters: conservation cutoff of 0.3, matrix score threshold of 85%, amount of upstream/downstream sequence of 5000/5000. 96 transcription factors, including Oct4, targeting the top genes with $|Z| > 2$ were found.

2.13 CELL CULTURE

Oct4^{+/+} and Oct4^{Δ/Δ} mouse aortic SMC were isolated and cultured as previously described.⁵⁹ Cells were maintained in 10% serum-containing media (DMEM/F12 (Gibco), Fetal bovine serum (FBS; GE Healthcare Bio-Sciences; Pittsburgh, PA), 100 U/ml penicillin/streptomycin (Gibco), 1.6 mM/L L-glutamine (Gibco)). Mouse aortic EC were purchased from Cell Biologics (C57-6052) and maintained in complete mouse endothelial cell medium plus kit (M1168). For experiments, cells were grown to 80-100% confluency and then switched to serum-free media SFM for at least 24 hours prior to harvest and/or treatment. The B16 F10 and M3-9M cancer cell lines were a kind gift from our collaborators at the National Cancer Institute, Dr. Rosandra Kaplan and Dr. Meera Murgai. Both lines were transduced with a lentivirus expressing an mCherry-Luciferase fusion protein, as previously described.²⁴ B16 F10 cells were grown in DMEM with 10% FBS plus 1%

penicillin-streptomycin-glutamine. M3-9M cells were grown in RPMI with 10% FBS plus 1% penicillin-streptomycin-glutamine.

2.14 RNA ISOLATION, cDNA PREPARATION, AND qRT-PCR

Total RNA was harvested using phenol-chloroform extraction (TRIzol, Life Technologies, Grand Island, NY). 0.5-1 µg of RNA was reverse-transcribed with iScript cDNA synthesis kit (Bio-Rad).

Real-time qRT-PCR was performed on a C1000 Thermal Cycler CFX96 (Bio-Rad) using SensiFAST SYBR NO-ROX mix (Bioline) and primers specific for mouse *Robo2*, *Slit3*, and *B2M*. Expression of genes was normalized to *B2M*.

Robo2 For: CGAGCTCCTCCACAGTTTGT

Rev: GTAGGTTCTGGCTGCCTTCT

Slit3 For: AGTTGTCTGCCTTCCGACAG

Rev: TTTCCATGGAGGGTCAGCAC

B2M For: ATGGCTCGCTCGGTGACCCT

Rev: TTCTCCGGTGGGTGGCGTGA

2.15 SCRATCH WOUND ASSAY

Scratch wound assays were performed in 6 well plates. Once cells were 100% confluent, cells were washed 2x with 1xPBS and placed in serum-free media (SFM) for 24 hours. A scratch down the middle of each well was made using a p200 pipet tip and then media was immediately replaced with SFM containing 1nmol/L SLIT3 (MyBioSource.com, MBS2010323) or Vehicle (PBS). Images were taken immediately after scratch and every 24 hours thereafter for 72 hours post-scratch on 4x magnification using an inverted microscope. Prior to cell plating, horizontal lines were made

on the underside of each well at 12 mm, 20 mm, and 28 mm from the bottom of each well to ensure the same FOV was imaged at each time point. Numbers of cells that migrated into the scratch were counted in each FOV using ImageJ analysis software. Counts were then averaged together across 9 FOV per condition (3 wells with 3 FOV each).

2.16 ORTHOTOPIC TUMOR MODELS

For orthotopic tumor cell injections, B16 F10 or M3-9M tumor cells were harvested and resuspended at 5×10^6 cells/ml in Hank's balanced salt solution (HBSS). Mice were then anesthetized under 2% isoflurane, and 100 μ l of cell suspension was injected into the right flank (B16 F10) or right gastrocnemius muscle (M3-9M) using a sterile 27g needle. Primary tumor volume was measured with a caliper at multiple time points throughout tumor development. Volume was calculated using the formula $(\text{length} \times \text{width})^2$ divided by 2. For tail vein injections, 2.5×10^4 M3-9M cells were injected directly into the tail vein using a sterile 27g needle. Metastatic end point was determined for each experiment based on both maximum primary tumor volume and the appearance of moribund mice.²⁴

2.17 BIOLUMINESCENCE IMAGING AND ANALYSIS

At metastatic end point, mice were euthanized and perfused with PBS through the right ventricle. Primary tumor and lung tissue were harvested. Lungs were incubated in 1 μ g/ml D-luciferin. Luminescence readings were collected for 4-5 minutes, in 30 second or 1 minute intervals, on a Xenogen IVIS 200. Analysis of images was conducted using the Xenogen Living Image software package.²⁴ Primary tumors and lung tissue were embedded in OCT or paraffin for potential future histologic analysis.

2.18 STATISTICAL ANALYSIS

Statistical analysis was performed using GraphPad Prism Version 7 software. Normality of the data was determined using a Kolmogorov-Smirnov test. For comparison of two groups with normal distribution, an unpaired two-tailed *t*-test was used. For comparison of two groups with non-normal distribution, a Mann-Whitney *U* test was used. For analysis of three or more groups with normal distribution, a two-way ANOVA was used. All results are presented as mean \pm SEM. $P < 0.05$ was considered significant. For all *in vivo* experiments, each 'n' refers to a biologically independent animal. For all *in vitro* experiments, each experiment was performed in triplicate and repeated independently three times. Specific statistical tests and number of mice used for each *in vivo* analysis are reported in the figure legends.

3 CHAPTER 3: PERIVASCULAR CELL-SPECIFIC KNOCKOUT OF THE STEM CELL PLURIPOTENCY GENE OCT4 INHIBITS ANGIOGENESIS

Disclaimer: This chapter was adapted from a manuscript currently under revision at *Nature Communications*; re-submitted on November 6, 2018

Authors: Daniel L. Hess,* BS, Molly R. Kelly-Goss,* PhD, Olga A. Cherepanova, PhD, Anh T. Nguyen, PhD, Richard A. Baylis, Svyatoslav Tkachenko, PhD, Brian H. Annex, MD, Shayn M. Peirce^{1,3}, PhD, Gary K. Owens, PhD

*These authors contributed equally to this article

3.1 ABSTRACT

We recently showed that the stem cell pluripotency factor Oct4 serves a critical protective role by promoting smooth muscle cell (SMC) investment during atherosclerotic plaque development. Those were the first studies to show that Oct4 is reactivated and plays a functional role in somatic cells. However, since the lethal consequences of atherosclerosis occur well after our reproductive years, herein, we sought to identify a functional role for Oct4 in perivascular cells that is likely to have been highly conserved through evolution. We used Myh11-CreER^{T2} eYFP lineage-tracing, combined with tamoxifen-inducible smooth muscle cell and pericyte (SMC-P) knockout of Oct4, to test the hypothesis that SMC-P Oct4 regulates perivascular cell migration and recruitment necessary for angiogenesis. SMC-P Oct4 wild type and knockout Myh11-CreER^{T2} eYFP mice had no detectable differences in vasculature at baseline. In contrast, following corneal angiogenic stimulus, SMC-P Oct4 knockout mice had significantly impaired eYFP⁺ cell migration, increased eYFP⁺ cell death, delayed CD31⁺ endothelial cell migration, and increased vascular

leak. SMC-P Oct4 knockout mice also had impaired perfusion recovery and decreased angiogenesis following hindlimb ischemia. RNA-Seq analysis and validation by qRT-PCR demonstrated that the migration gene *Slit3* was reduced following loss of Oct4 in cultured SMC. Interestingly, SLIT3 was expressed in eYFP+ perivascular cells in both injured cornea and ischemic hindlimb muscle, and its expression decreased with SMC-P Oct4 knockout. Taken together, these results provide compelling evidence that expression of the stem cell pluripotency gene *Oct4* within perivascular cells plays an essential role in injury- and hypoxia-induced angiogenesis, which are critical processes for survival, growth, and reproduction of all organisms.

3.2 INTRODUCTION

Octamer-binding transcription factor 4 (Oct4) is a stem cell pluripotency gene critical for maintenance of pluripotency in the inner cell mass of the blastocyst.⁶¹ Oct4 expression is tightly regulated during embryogenesis and declines during germ layer specification through epigenetic repression via DNA and histone methylation.⁶⁴ The long-standing dogma in the field was that this epigenetic silencing is permanent in all adult somatic cells.^{64,70,88} Contrary to dogma, a number of studies have reported Oct4 expression in a variety of stem and progenitor cell populations.⁸⁸ However, these studies failed to provide evidence that Oct4 had a functional role in these cells, and were viewed with extensive skepticism due to a number of potential false positives associated with Oct4 transcript and protein detection, including the presence of multiple Oct4 non-pluripotent isoforms and pseudogenes.⁸⁸ Our lab also detected Oct4 expression in somatic cells, namely in smooth muscle cells (SMC) in mouse and human atherosclerotic lesions, and utilized a murine genetic loss-of-function approach to conditionally and specifically delete the pluripotency isoform of Oct4 in SMC.⁵⁹ We found that Oct4 plays a critical protective role in SMC, in that Oct4 deletion impaired investment of SMC into both the lesion and fibrous cap during atherosclerosis, and was associated with increased atherosclerotic burden and decreased indices of plaque stability.⁵⁹ Of

major significance, this was the *first direct evidence that Oct4 plays a functional role in any somatic cell*. Therefore, despite epigenetic silencing during gastrulation, the Oct4 locus evolved the capacity to be reactivated and serve a function in SMC.

Interestingly, the clinical manifestations of atherosclerosis, including thromboembolic complications such as stroke and myocardial infarction, affect individuals well after their reproductive years, and as such there would have been no selective pressure for Oct4 to evolve a role to combat atherosclerosis development or end stage complications. Therefore, Oct4 reactivation in SMC may be an anomaly unique to pathological states as has been surmised by numerous investigators claiming it is re-activated in cancer stem cells.⁸⁹ Alternatively, *Oct4 may have evolved a protective role in SMC to enhance processes critical for survival and reproductive success* and only secondarily developed a role during atherosclerosis development. Angiogenesis, or the growth of new blood vessels from a pre-existing vasculature, is essential for survival and reproduction, as it is responsible for supply of oxygen and nutrients.^{28,29} Since angiogenesis requires perivascular cell investment for formation of functional vascular networks, we postulated that Oct4 evolved to play a critical role in this process.

Angiogenesis requires coordinated migration of the two major cell types of the blood vessel wall: 1) endothelial cells (EC), which line the inner lumen, and 2) perivascular cells [smooth muscle cells (SMC) and pericytes], which envelop EC. In general, SMC concentrically wrap arteries, arterioles, veins, and venules which have diameters >10 μm , while pericytes extend longitudinally along capillaries <10 μm in diameter. Despite these distinct anatomical differences, SMC and pericytes often express many common proteins including ACTA2, MYH11, and PDGFR- β , which vary in expression across different vascular beds under both normal and pathologic conditions.⁹⁰ Indeed, no marker or set of markers has been able to unequivocally distinguish SMC from pericytes.⁹⁰ For this reason, and due to their shared contributions to angiogenic perivascular populations,⁹¹ we henceforth refer to them together as smooth muscle cells and pericytes (SMC-P).

During angiogenesis, EC and SMC-P communication is essential for new blood vessel formation.⁹² Global genetic knockout (KO) studies have identified a number of pathways critical in EC-SMC-P cross-talk, including PDGF-B/PDGF-R β , ANG/TIE2, TGF β , S1P, and Notch signaling.^{37,92-94} Manipulating these pathways results in improper EC and SMC-P function, including their decreased association with one another,⁹⁵⁻⁹⁹ often leading to increased vascular leak and hemorrhage.^{100,101} Therefore, perivascular cell investment of EC tubes is critical for normal function and stability of vascular networks.¹⁰⁰⁻¹⁰² However, cell-specific loss-of-function studies are required to determine which cell type(s) and gene(s) drive specific phenotypes.

EC-specific deletion of genes, such as *Pdgfb*^{33,34}, *Notch*^{103,104}, and others¹⁰⁵⁻¹⁰⁷ result in impaired angiogenesis, demonstrating that EC play a critical role in regulating this process. Similarly, perivascular cell-selective knockout of various genes including *Ephrin-B2*,¹⁰⁸ *CD146*,¹⁰⁹ *Tie2*,²¹ and *VEGFR1*⁵⁸ result in impaired angiogenesis, including defective SMC-P investment of EC tubes and increased vascular leak. However, despite these insights into mechanisms by which perivascular cells contribute to functional vascular networks, dysregulated angiogenesis continues to play a major role in numerous disease processes including cardiovascular disease and cancer, the two leading causes of death in the US.¹¹⁰ Numerous cardiovascular clinical trials for peripheral arterial disease (PAD), heart failure, and stroke have sought to augment angiogenesis by administering growth factors that promote EC proliferation and migration (e.g. VEGF and bFGF) as a means to increase tissue perfusion and recovery.^{46,111-113} However, the majority of these studies have failed to meet their primary endpoints, which is at least partially due to EC growth without coordinated SMC-P migration and investment.¹¹⁴ Thus, further insight into the mechanisms regulating perivascular cell involvement in angiogenesis is critical for developing therapies to modulate functional vascular growth and remodeling.

Herein, we tested the hypothesis that SMC-P derived Oct4 is essential for angiogenesis following *in vivo* injury, including corneal burn and hindlimb ischemia (HLI). We demonstrate

that SMC-P conditional deletion of the stem cell pluripotency factor Oct4 results in markedly impaired angiogenesis, at least in part through defective SMC-P migration leading to increased vascular leak. This study identifies a novel pathway implicating the key stem cell factor Oct4 in regulation of perivascular cell investment and vascular network remodeling following tissue injury or hypoxia.

3.3 RESULTS

3.3.1 Myh11-CreER^{T2} eYFP efficiently labeled SMC and a large subset of pericytes in multiple tissues

We previously developed a Myh11-CreER^{T2} ROSA floxed STOP eYFP inducible lineage tracing mouse that specifically labels >95% of SMC within large conduit arteries with eYFP following tamoxifen injection between 6-8 weeks of age. Recently, using this mouse, we demonstrated that a subset of eYFP⁺ cells in the pre-metastatic lungs express the pericyte markers NG2 and PDGFR- β .²⁴ To determine whether the Myh11-CreER^{T2} system also labels pericytes in a number of other microvascular beds, we crossed our Myh11-CreER^{T2} ROSA floxed STOP eYFP mice to NG2-DsRED reporter mice to generate Myh11-CreER^{T2} ROSA eYFP NG2-DsRED mice (**Figure 3-1a**). We examined whole mounts of the retina, which has the highest pericyte density in the body,⁹² and observed eYFP⁺ cells surrounding isolectin⁺ EC tubes, including those of capillary size diameter (**Figure 3-1b**). There was co-localization of eYFP and NG2-DsRed in pericytes surrounding isolectin⁺ EC tubes, demonstrating eYFP efficiently labels NG2⁺ pericytes in the retina (**Figure 3-1c**). We also examined the limbal vasculature of the cornea and observed labeling of NG2-DsRED⁺ cells with eYFP (**Figure 3-1d**). We next used our Myh11-CreER^{T2} ROSA eYFP lineage tracing mice (**Figure 3-1e**) to quantify the efficiency of eYFP labeling of pericytes in calf muscle vasculature. We found that approximately 80% of eYFP⁺ cells surrounding CD31⁺ capillaries express multiple pericyte markers, including NG2 and PDGFR- β (**Figure 3-1f-h**). Over

90% of NG2⁺ cells, and 80% of PDGFR- β ⁺ cells, express eYFP (**Figure 3-1i**). Taken together, our results demonstrate that the Myh11-CreER^{T2} system labels both SMC¹¹⁵ and a large subset of pericytes within multiple tissues. Using Myh11-CreER^{T2}, we can therefore conditionally delete *Oct4* in both SMC and pericytes (SMC-P) to test for a functional role during angiogenesis following injury.

3.3.2 SMC-P knockout of Oct4 in young, healthy mice had no discernable effect on microvascular phenotype

To knock out *Oct4* and determine its role in Myh11-expressing SMC-P, we injected Myh11-CreER^{T2} ROSA floxed STOP eYFP Oct4^{WT/WT} and Myh11-CreER^{T2} ROSA floxed STOP eYFP Oct4^{FL/FL} male littermate mice with tamoxifen from 6-8 weeks of age, as previously described.⁵⁹ This induces permanent lineage tagging of Myh11-expressing cells with eYFP, without and with *Oct4* knockout, respectively, exclusively in SMC-P (**Figure 3-2a**). Henceforth, we refer to them as Oct4^{SMC-P WT/WT} and Oct4^{SMC-P Δ/Δ} mice. To ensure *Oct4* knockout, we tested recombination at the *Oct4* locus in a number of tissues, including aorta, liver, lung, diaphragm, skeletal muscle, and blood. Following tamoxifen administration, we observed *Oct4* recombination in Oct4^{SMC-P Δ/Δ} tissues but not in Oct4^{SMC-P WT/WT} tissues. Additionally, no *Oct4* recombination was observed in blood, which we previously showed contains no eYFP⁺ cells (**Figure 3-8a,b**).¹⁵ As further validation, we sorted eYFP⁺ and eYFP⁻ cells from calf muscle of Oct4^{SMC-P WT/WT} and Oct4^{SMC-P Δ/Δ} mice (**Figure 3-8c**). We observed *Oct4* recombination only in the eYFP⁺ population sorted from Oct4^{SMC-P Δ/Δ} mice (**Figure 3-8d**).

We then determined whether loss of *Oct4* in Myh11-expressing SMC-P results in any effect prior to an angiogenic stimulus. Twelve to eighteen-week-old Oct4^{SMC-P Δ/Δ} mice did not show any significant changes in total body weight, blood pressure, or heart rate, compared to littermate controls (**Figure 3-9**). We administered Alexaflour-647-labeled isolectin GS-IB4 (lectin) via retro-orbital injection ten minutes prior to imaging in order to visualize perfusion-competent blood

vessels. We then used intravital confocal microscopy to image the corneal limbal vascular bed of Oct4^{SMC-P WT/WT} and Oct4^{SMC-P Δ/Δ} mice for injected isolectin and native eYFP expression (**Figure 3-2b,c**). The corneal limbal vasculature consists of an arteriole-venule (A-V) pair encircling the cornea circumference as well as a vascular network that extends approximately 200 μm away from the main A-V pair towards the center of the cornea. We divided the limbal vasculature into 50 μm regions and assessed a number of vascular parameters at baseline, i.e. immediately prior to injury (**Figure 3-2d**). We observed no significant differences in eYFP+ vascular length density, number of eYFP+ vascular segments, eYFP+ cell coverage, or eYFP+ cell density between Oct4^{SMC-P WT/WT} and Oct4^{SMC-P Δ/Δ} corneas immediately prior to injury (**Figure 3-2e-h**). We then assessed the baseline vasculature in hindlimb muscle of Oct4^{SMC-P WT/WT} and Oct4^{SMC-P Δ/Δ} mice. We saw no difference in capillary density or number of eYFP+ vessels within the hindlimb (**Figure 3-2i,j**). Taken together, results show that, in the absence of injury, conditional knockout of Oct4 within perivascular cells has no effect on corneal limbal or hindlimb vasculature.

3.3.3 SMC-P knockout of the stem cell pluripotency gene Oct4 resulted in impaired angiogenesis following corneal burn, including reduced migration and increased cell death of SMC-P

To test whether Oct4 plays a functional role in SMC-P during angiogenesis following injury, we subjected twelve to eighteen-week-old Oct4^{SMC-P WT/WT} and Oct4^{SMC-P Δ/Δ} mice to corneal alkali burn injury (**Figure 3-3a**), as previously described.⁵¹ Following corneal burn, the limbal vasculature gives rise to angiogenic sprouts that extend towards the alkali burn in the center of the cornea (**Figure 3-10**). We used intravital confocal microscopy to visualize isolectin+ vessel lumens and eYFP+ cells during angiogenesis towards the burn site at days 3, 7, and 21 post-corneal burn. We divided the network area into defined regions, including the A-V pair and 50 μm regions extending away from the A-V pair towards the burn (**Figure 3-10**). We then calculated the number of eYFP+ cells within each region and normalized to area.

By day 3 post-corneal burn, the distribution of eYFP⁺ cells throughout the remodeling vascular network was significantly different in Oct4^{SMC-P Δ/Δ} corneas relative to Oct4^{SMC-P WT/WT} corneas. Moreover, there was a significant decrease in eYFP⁺ cell density throughout the angiogenic network in Oct4^{SMC-P Δ/Δ} corneas (**Figure 3-11a**). At day 7 post-corneal burn, eYFP⁺ cell distribution throughout the remodeling corneal network was also significantly different between Oct4^{SMC-P Δ/Δ} and Oct4^{SMC-P WT/WT} corneas. Specifically, in Oct4^{SMC-P WT/WT} corneas at day 7 post-burn, eYFP⁺ cells migrated away from the limbal vasculature to form a dense neovascular area extending approximately 600 μm away from the limbal A-V pair. In Oct4^{SMC-P Δ/Δ} corneas, however, there were very few eYFP⁺ cells that had migrated >350 μm away from the limbal A-V pair (**Figure 3-3d,e**). At day 21 post-corneal burn, eYFP⁺ cell distribution remained significantly different across genotypes. In Oct4^{SMC-P WT/WT} corneas, numerous eYFP⁺ cells migrated out to 900 μm away from the A-V pair. In contrast, in Oct4^{SMC-P Δ/Δ} corneas, there were very few eYFP⁺ cells that had migrated >450 μm away from the limbus (**Figure 3-3f,g**). The altered distribution of eYFP⁺ cells throughout the remodeling angiogenic network at all time points post-burn suggests eYFP⁺ cells lacking Oct4 may be unable to effectively migrate following corneal burn.

In addition to significantly altered distribution of eYFP⁺ cells following loss of Oct4, there was also significantly decreased eYFP⁺ cell density throughout the entire network area in Oct4^{SMC-P Δ/Δ} corneas (**Figure 3-3h**). This suggests that, in the absence of Oct4, eYFP⁺ cells undergo increased cell death and/or decreased proliferation following corneal burn, resulting in decreased cell density. To test whether eYFP⁺ cells lacking Oct4 are more susceptible to apoptosis following burn, we measured apoptotic DNA fragmentation with TUNEL. At day 1 post-injury, Oct4^{SMC-P Δ/Δ} corneas had significantly increased ratios of TUNEL⁺eYFP⁺ cells to total eYFP⁺ cells, when compared to Oct4^{SMC-P WT/WT} corneas. However, at days 2 and 5 post-injury, there was no significant difference in TUNEL staining of eYFP⁺ cells between Oct4^{SMC-P WT/WT} and Oct4^{SMC-P Δ/Δ} corneas (**Figure 3-11b**). To determine whether eYFP⁺ cell proliferation was altered as a function of loss of

Oct4, we stained for KI67 at days 2 and 5 post-corneal burn and found approximately 18% and 35% of eYFP+ cells, respectively, were in active phases of the cell cycle. However, rates of eYFP+ cell proliferation were similar between Oct4^{SMC-P WT/WT} and Oct4^{SMC-P Δ/Δ} corneas (**Figure 3-11c**). Therefore, Oct4 knockout leads to increased apoptosis of eYFP+ cells at day 1 post-burn, contributing to significantly reduced eYFP+ cell density at day 3 post-burn. Oct4 knockout also reduced the distance of eYFP+ cells from the corneal limbus, likely due in part to impaired eYFP+ cell migration. However, we cannot rule out additional changes in eYFP+ proliferation or apoptosis that we failed to detect. Taken together, these data suggest that SMC-P Oct4 is critical for effective angiogenesis following corneal burn.

3.3.4 SMC-P knockout of the stem cell pluripotency gene Oct4 resulted in increased vascular leakage from angiogenic vessels

We then tested if changes in eYFP+ cells due to SMC-P knockout of *Oct4* played a role in the patency and functionality of the angiogenic vessels, as well as the overall health of the healing cornea post-alkali burn. Therefore, we examined vascular leakage, incidence of hemorrhage, and cornea tissue damage.

To assess vascular leakage, we administered a retro-orbital injection of 70 kDa rhodamine-dextran into the contralateral eye immediately (< 3 minutes) prior to live confocal imaging at day 3 post-corneal burn. We observed very little dextran leak in Oct4^{SMC-P WT/WT} corneas (**Figure 3-4a**). However, in Oct4^{SMC-P Δ/Δ} corneas, there was extensive accumulation of 70 kDa rhodamine-dextran in the interstitial space, indicative of vascular leakage (**Figure 3-4a**). Indeed, when we quantified fluorescence intensity of dextran in regions outside the vasculature, vascular leak was increased more than four-fold in Oct4^{SMC-P Δ/Δ} corneas compared to Oct4^{SMC-P WT/WT} corneas (**Figure 3-4b**).

To evaluate the extent of hemorrhaging in Oct4^{SMC-P Δ/Δ} corneas, we took bright field images of Oct4^{SMC-P WT/WT} and Oct4^{SMC-P Δ/Δ} corneas at days 0, 3, 7, and 21 post-corneal burn and quantified

the number of hemorrhages, or areas of blood not confined to the vasculature, using a semi-quantitative scoring system based on a clinical scale (**Figure 3-4c**). The scoring also assessed the health of the corneal tissue, i.e. whether it was healthy, torn, or ruptured, which directly correlated with the extent of hemorrhaging. We observed increased hemorrhaging in $Oct4^{SMC-P \Delta/\Delta}$ mice, indicative of increased vascular leak and consistent with reduced eYFP⁺ cell migration and investment of nascent EC tubes (**Figure 3-4d**).

3.3.5 SMC-P knockout of the stem cell pluripotency gene Oct4 resulted in delayed EC migration, but did not affect EC sprouting, apoptosis, or proliferation

Given the important role of SMC-P/EC crosstalk during angiogenesis, we asked whether SMC-P *Oct4* knockout results in secondary changes in EC. Thus, we performed whole mount immunostaining of post-burn corneas for the EC marker CD31. In $Oct4^{SMC-P \Delta/\Delta}$ corneas at day 3 post-burn, there was a significant decrease in CD31⁺ migration distance, defined as the maximum distance CD31⁺ cells extended away from the A-V pair (**Figure 3-5a-c**). However, sprout formation at day 3 was unaffected by loss of Oct4 in SMC-P (**Figure 3-5d**). By day 7 post-corneal burn, CD31⁺ distance from the A-V pair was not significantly different between $Oct4^{SMC-P WT/WT}$ and $Oct4^{SMC-P \Delta/\Delta}$ corneas (**Figure 3-5e**). We then assessed EC apoptosis (**Figure 3-5f**) and proliferation (**Figure 3-5g**) at days 2 and 5, which could possibly contribute to the changes at days 3 and 7, respectively, but observed no significant difference between genotypes. Taken together, results indicate that loss of Oct4 within perivascular cells results in a transient delay in EC migration at day 3 post-burn that is compensated for by day 7 post-burn.

This compensation in EC migration, along with no other detectable changes in EC function despite significant eYFP⁺ cell dropout, raised the possibility that eYFP⁻ populations of SMC-P may compensate for the loss of eYFP⁺ cells following Oct4 knockout. To test this hypothesis, we stained eye cross-sections at day 5 post-burn for CD31, eYFP, and NG2, an additional pericyte marker. In $Oct4^{SMC-P WT/WT}$ corneas, eYFP⁺ and NG2⁺ cells invested CD31⁺ EC tubes throughout

the proximal and distal corneal vascular network (**Figure 3-12a**). However, in Oct4^{SMC-P Δ/Δ} corneas, we observed CD31⁺ tubes devoid of eYFP⁺ cells at distal regions of the remodeling vasculature, consistent with our earlier observations (**Figure 3-3b-g**). Interestingly, many of the CD31⁺ EC that lacked eYFP⁺ cell investment were invested with eYFP⁻/NG2⁺ cells (**Figure 3-12b**). These cells represent a SMC-P population that lacked Myh11 expression and/or failed to undergo recombination at the ROSA locus during the course of tamoxifen injections. This observation suggests that an eYFP⁻ SMC-P population may at least partially compensate for eYFP⁺ cell dropout following loss of Oct4 in eYFP⁺ SMC-P.

3.3.6 SMC-P *Oct4* knockout resulted in impaired angiogenesis and decreased perfusion recovery following hindlimb ischemia

Next, we sought to determine whether the impaired angiogenesis resulting from SMC-P *Oct4* knockout extended to other models of angiogenesis. We performed femoral artery ligation and resection (hindlimb ischemia (HLI)) surgery, a well-established mouse model of PAD, on Oct4^{SMC-P WT/WT} and Oct4^{SMC-P Δ/Δ} mice and monitored blood flow recovery over the course of 21 days post-HLI (**Figure 3-6a**), as previously described.¹¹⁶ There was no significant difference in perfusion recovery as assessed by Laser Doppler imaging at days 0 (immediately post-injury), 3, and 7 post-HLI (**Figure 3-6b,c**). To assess for baseline differences in vasculature, we measured vascular density in the calf muscle via immunostaining. At days 0 and 7 post-HLI, there was no significant difference in capillary density, measured by counting the number of CD31⁺ cells per muscle fiber, between Oct4^{SMC-P WT/WT} and Oct4^{SMC-P Δ/Δ} mice (**Figure 3-6d**). However, Oct4^{SMC-P Δ/Δ} mice had significantly impaired perfusion recovery at days 14 and 21 post-HLI, compared to Oct4^{SMC-P WT/WT} littermate controls (**Figure 3-6b,c**). At day 21 post-HLI, there was also significantly reduced capillary density in SMC-P *Oct4* knockout calf muscle compared to control muscle, consistent with the perfusion deficit detected by Laser Doppler (**Figure 3-6d,e**). There was also a significant decrease in both CD31⁺ and eYFP⁺ pixel density, but no change in the ratio of

eYFP to CD31, at day 21 post-HLI (**Figure 3-6f-h**). To determine if differences in arteriogenesis, or collateral vessel remodeling, could contribute to the impaired perfusion recovery, we measured arteriogenesis by staining thigh muscle for eYFP and counting the number of vessels with a diameter $>10\mu\text{m}$. We did not detect any significant differences in the number of eYFP+ collateral vessels between Oct4^{SMC-P WT/WT} and Oct4^{SMC-P Δ/Δ} mice (**Figure 3-13**).

However, the femoral artery ligation and resection model HLI model is a poor model in which to study arteriogenesis, since it involves cauterization of collateral vessels that would otherwise contribute to arteriogenesis following disrupted blood flow. Therefore, to further determine whether SMC-P Oct4 plays a role in arteriogenesis, we used a femoral artery ligation (FAL) model, which involves ligation of the femoral artery just distal to the muscular branch. This stimulates robust remodeling of the collateral vessels of the gracilis muscle.^{117,118} Following FAL, we found that Oct4^{SMC-P Δ/Δ} mice had no significant difference in hindlimb perfusion recovery or collateral vessel diameter, compared to Oct4^{SMC-P WT/WT} mice (**Figure 3-14**). Therefore, SMC-P derived Oct4 plays a major role in angiogenesis, but not arteriogenesis, in mice recovering from hindlimb injury.

Taken together, our results demonstrate that loss of the stem cell pluripotency gene Oct4 in Myh11-expressing SMC-P results in marked impairment of angiogenesis in two distinct mouse models, corneal alkali burn and hindlimb ischemia.

3.3.7 SMC-P Oct4 knockout was associated with decreased expression of the guidance gene Slit3 both *in vivo* and *in vitro*.

To identify putative Oct4 target genes, we analyzed previous RNA-seq data from our lab to determine genes differentially expressed under normoxia versus hypoxia (1% O₂) in cultured Oct4^{WT/WT} and Oct4 ^{Δ/Δ} SMC. We used hypoxia as an *in vitro* stimulus because it is a potent activator of angiogenesis, and we previously showed it activates Oct4 expression.⁵⁹ We then determined

which of these hypoxia-regulated genes were differentially expressed in Oct4^{WT/WT} versus Oct4^{Δ/Δ} SMC. Finally, we compared the resulting list of genes with putative Oct4 ChIP-seq target genes using the oPOSSUM database. This analysis identified 38 genes that were common in both datasets (**Figure 3-7a**; Supplemental Table 1). Two of these, *Slit3* and *Robo2*, were of particular interest given that *Slit3* is a secreted glycoprotein that has been previously shown to promote migration of multiple cell types including SMC-P¹¹⁹, EC¹¹⁹, and macrophages¹²⁰ by binding to ROBO receptors on the cell surface.¹²¹ To validate these targets, we measured expression levels in Oct4^{WT/WT} and Oct4^{Δ/Δ} cultured SMC by qRT-PCR. Results showed that *Robo2* was decreased in Oct4 knockout SMC, although this did not reach statistical significance (**Figure 3-7b**). *Slit3*, however, was significantly decreased in *Oct4* knockout SMC relative to wild type (**Figure 3-7b**).

SLIT3 has been shown to promote angiogenesis in multiple *in vitro* and *in vivo* systems,^{119,122–124} suggesting its dysregulation might play a role in our phenotype. To test this, we performed SLIT3 immunostaining following both corneal burn and HLI. Interestingly, SLIT3 protein was expressed in eYFP+ cells of corneal blood vessels measuring approximately 10-20 μm in diameter (**Figure 3-7c**). In ischemic hindlimb, SLIT3 was expressed by many eYFP+ vessels, including small arterioles, venules, and capillaries (**Figure 3-7d**). SLIT3 levels, normalized to eYFP+ density, were significantly decreased in Oct4^{SMC-P Δ/Δ} hindlimb compared to Oct4^{SMC-P WT/WT} hindlimb following HLI (**Figure 3-7e**), providing further evidence that expression of *Slit3* is Oct4-dependent. Additionally, to test the role of SLIT3 on SMC and EC wound closure, we performed *in vitro* scratch wound assays, with or without exogenous Slit3. We found that Slit3 significantly increased the number of SMC or EC within the scratch wound, supporting a role for Slit3 in promoting cell migration and/or proliferation in SMC and EC (**Figure 3-7f-g**). Taken together, Oct4-dependent regulation of *Slit3* in SMC-P is one potential mechanism by which Oct4 promotes angiogenesis.

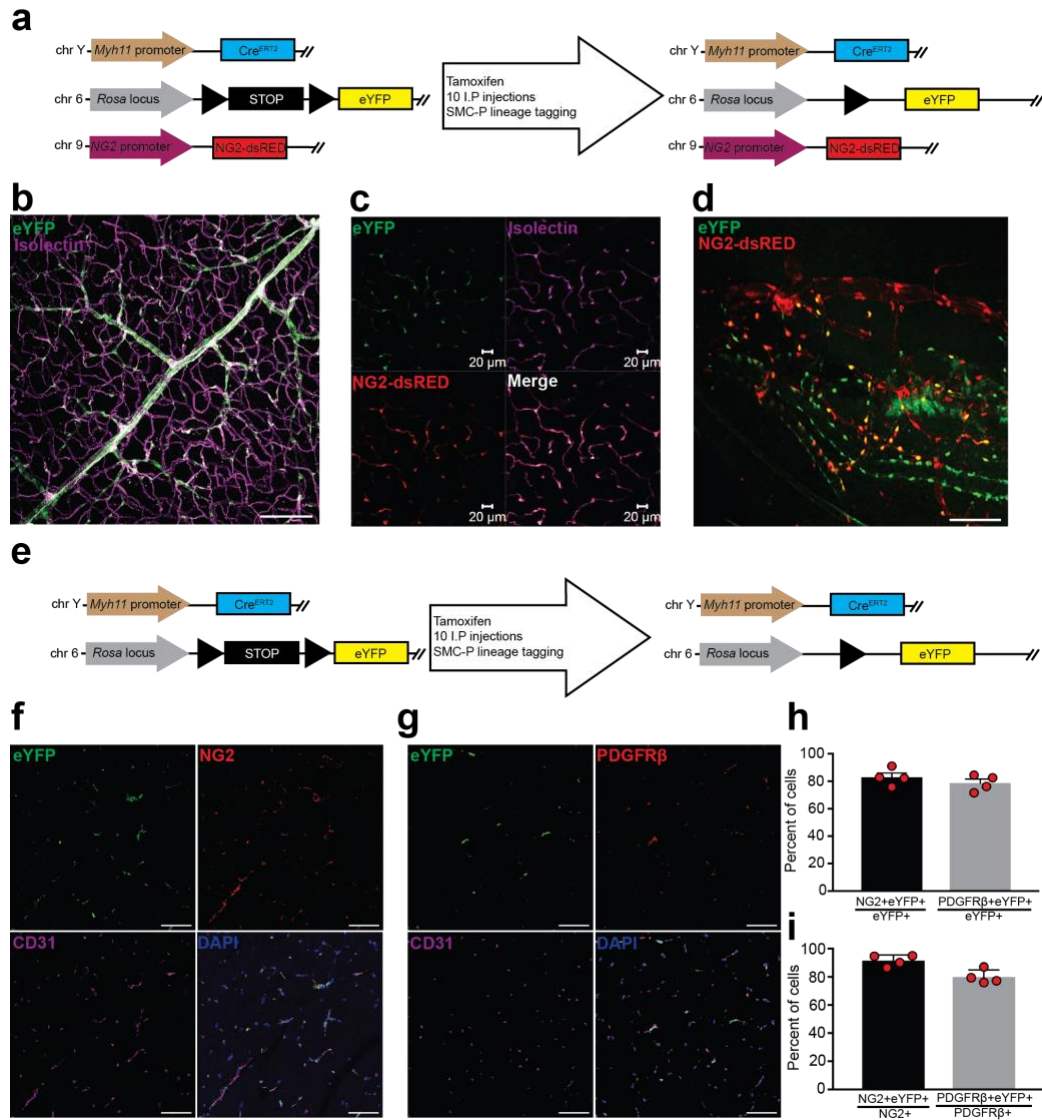


Figure 3-1

Myh11-CreERT2 ROSA eYFP efficiently labeled SMC and a large subset of pericytes in multiple microvascular tissue beds. a, Schematic showing crossing of Myh11-CreERT2 ROSA floxed STOP eYFP mice with NG2-DsRED mice plus tamoxifen injection to generate NG2-DsRED Myh11-CreERT2 ROSA eYFP mice. **b-c**, Imaging of retina whole mounts for eYFP, NG2-DsRED, and isolectin. Scale bar in **b** = 100 μ m. Scale bar in **c** = 20 μ m. **d**, Intravital microscopy of cornea limbal vasculature for eYFP and NG2-DsRED. Scale bar = 50 μ m. **e**, Schematic showing Myh11-CreERT2 ROSA eYFP mice. **f-g**, Co-staining of uninjured calf muscle cross sections from

Oct4^{SMC-P WT/WT} mice for DAPI, eYFP, and NG2 (f) or PDGFR- β (g). Scale bars = 50 μ m. **h-i**, Quantification of percentages of dual positive cells within calf muscle (n=4 mice). Values = mean \pm SEM.

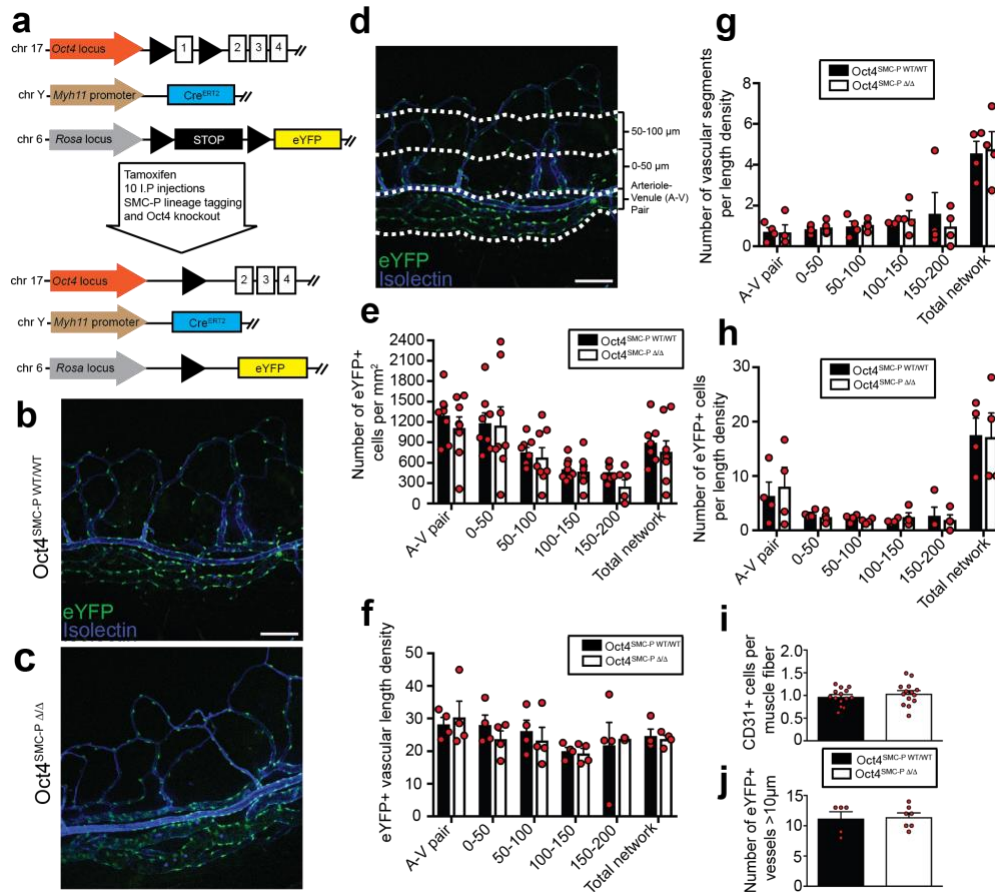


Figure 3-2

There were no differences in the corneal or hindlimb vasculature at baseline following SMC-P knockout of Oct4. **a**, Myh11-CreERT2 ROSA floxed STOP eYFP Oct4^{WT/WT} and Myh11-CreERT2 ROSA floxed STOP eYFP Oct4^{FL/FL} male littermate mice were injected with tamoxifen (10 intraperitoneal injections) from 6-8 weeks of age to induce simultaneous lineage tagging, without or with Oct4 KO, respectively. For simplicity, we refer to them henceforth as Oct4^{SMC-P WT/WT} and Oct4^{SMC-P Δ/Δ}, respectively. **b,c** Representative intravital confocal images of Oct4^{SMC-P WT/WT} and Oct4^{SMC-P Δ/Δ} corneas showing native eYFP (green) and perfused isolectin (blue). Scale bar = 50 μm. **d**, Prior to injury, there is limbal vasculature consisting of a main arteriole-venule (A-V) pair at the base of the vascular network as well as vessels extending approximately 200 μm away from the A-V pair toward the center of the cornea. To more rigorously quantify number of

cells in the limbal vasculature, we divided this region in to 50 μm regions, where 50 μm was measured from the edge of the A-V pair towards the center of the cornea along the total width of the montaged image. Scale bar = 50 μm . **e-h**, Quantification of eYFP+ cell density (e), eYFP+ vascular length density (f), eYFP+ vascular segments per length density (g), and number of eYFP+ cells per length density (h) in Oct4^{SMC-P WT/WT} and Oct4^{SMC-P Δ/Δ} corneas immediately prior to injury [n=8 WT, 8 KO (e); n=4 WT, 4 KO (f-h)]. **i-j**, Quantification of number of CD31+ cells per muscle fiber (i) and number of eYFP+ vessels > 10 μm diameter (j) in hindlimb muscle of Oct4^{SMC-P WT/WT} and Oct4^{SMC-P Δ/Δ} mice [n=14 WT, 14 KO (i); n=5 WT, 7 KO (j)]. Values = mean \pm SEM. Statistics were performed using two-way ANOVA (e-h), unpaired two-tailed t-test (i), or Mann-Whitney U test (j).

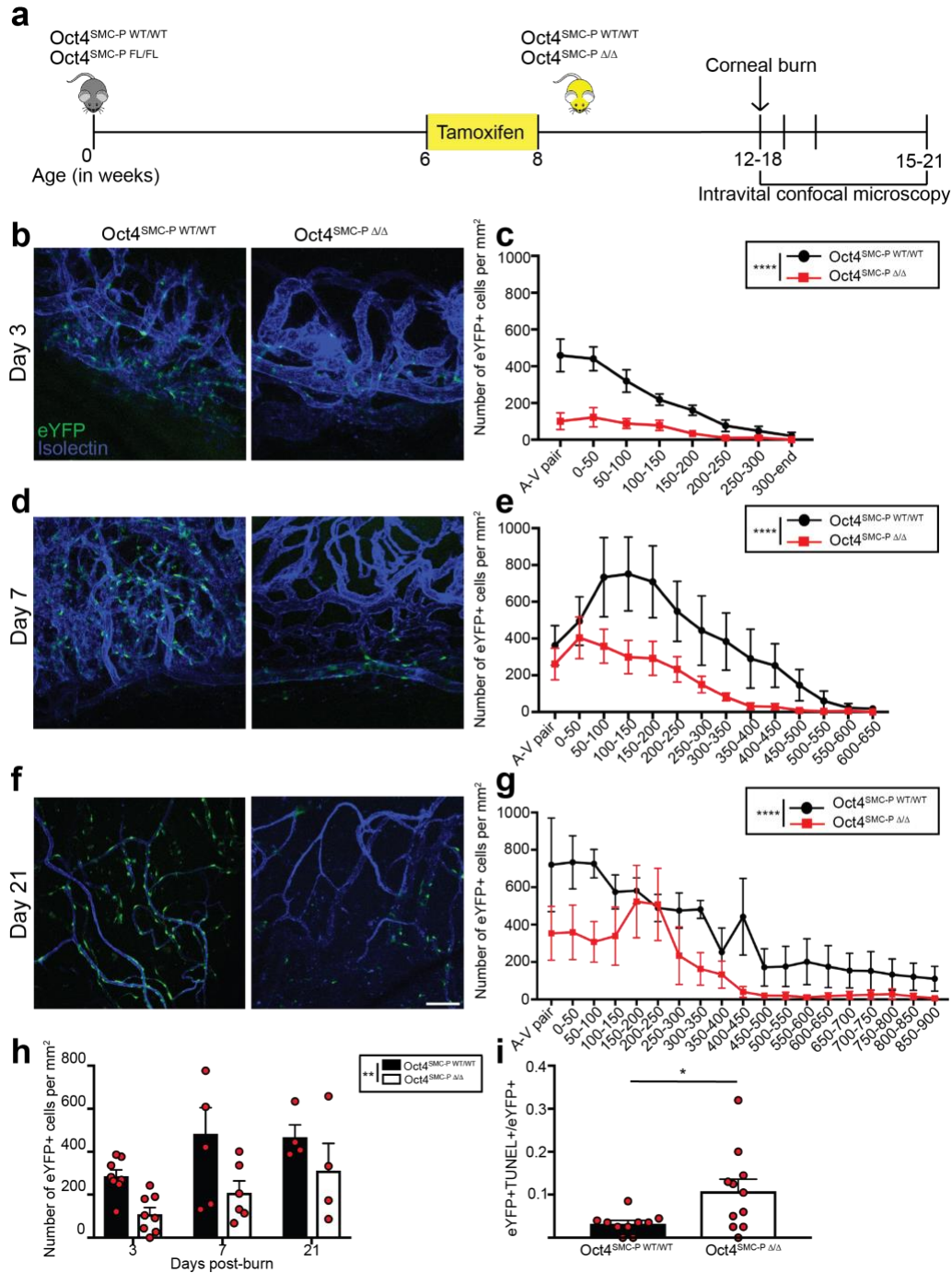


Figure 3-3

SMC-P conditional knockout of Oct4 resulted in impaired migration and increased cell death of eYFP+ cells following corneal burn. **a**, Schematic outlining experimental design. **b-g**, Representative intravital confocal microscopy images for native eYFP (green) and perfused

isolectin (blue) and quantification of the number of eYFP+ cells per area at days 3 (b,c) 7 (d,e), and 21 (f,g) post-corneal burn. Scale bar = 50 μ m. [n = 8 WT, 8 KO (c); n=6 WT, 6 KO (e); n=4 WT, 4 KO (g)]. **h**, Quantification of the number of eYFP+ cells throughout the entire network area at days 3, 7, and 21 post-burn. **i**, Quantification of the ratio of TUNEL+eYFP+ cells to total eYFP+ cells in cornea vasculature at day 1 (n=10 WT, 11 KO) post-burn. Values = mean \pm SEM. Statistics were performed using unpaired two-tailed t test (i) or two-way ANOVA (c,e,g,h). *P < 0.05, **P < 0.01, ****P < 0.0001

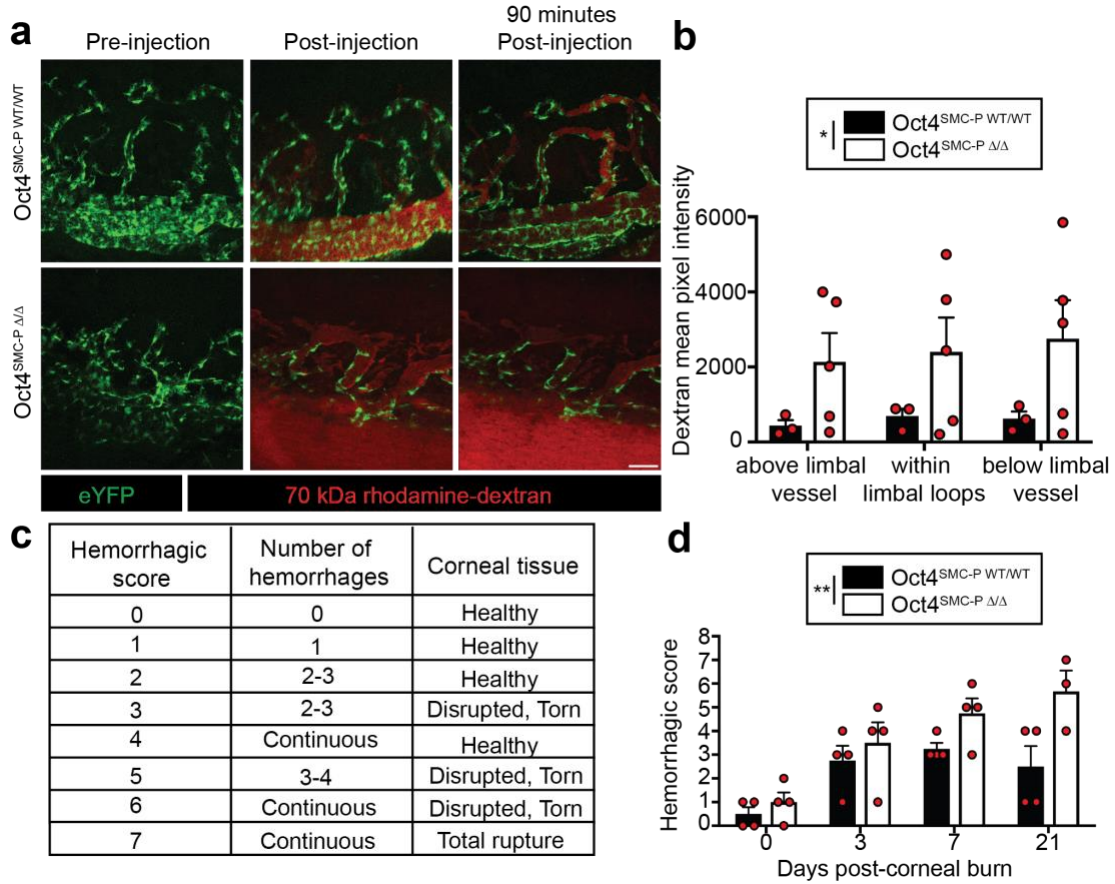


Figure 3-4

SMC-P knockout of Oct4 resulted in increased vascular leak and hemorrhaging following corneal burn. **a**, Representative still-frame images of Oct4^{SMC-P WT/WT} and Oct4^{SMC-P Δ/Δ} corneas pre-injection, immediately post-injection, and 90 minutes post-injection of 70 kDa rhodamine-dextran (red). Native eYFP expression is shown in green. **b**, Quantification of dextran mean pixel intensity of defined regions throughout the vascular network (n=3 WT, 5 KO). Scale bar = 50 μm. **c**, Scale used to quantify extent of hemorrhaging and health of corneal tissue following burn. **d**, Quantification of hemorrhaging and cornea integrity at each time point post-corneal burn (n=4 WT, 4 KO for D0, D3, D7; n=4 WT, 3 KO for D21). Values = mean ± SEM. Statistics were performed using two-way ANOVA (b,d). *P < 0.05 and **P < 0.01

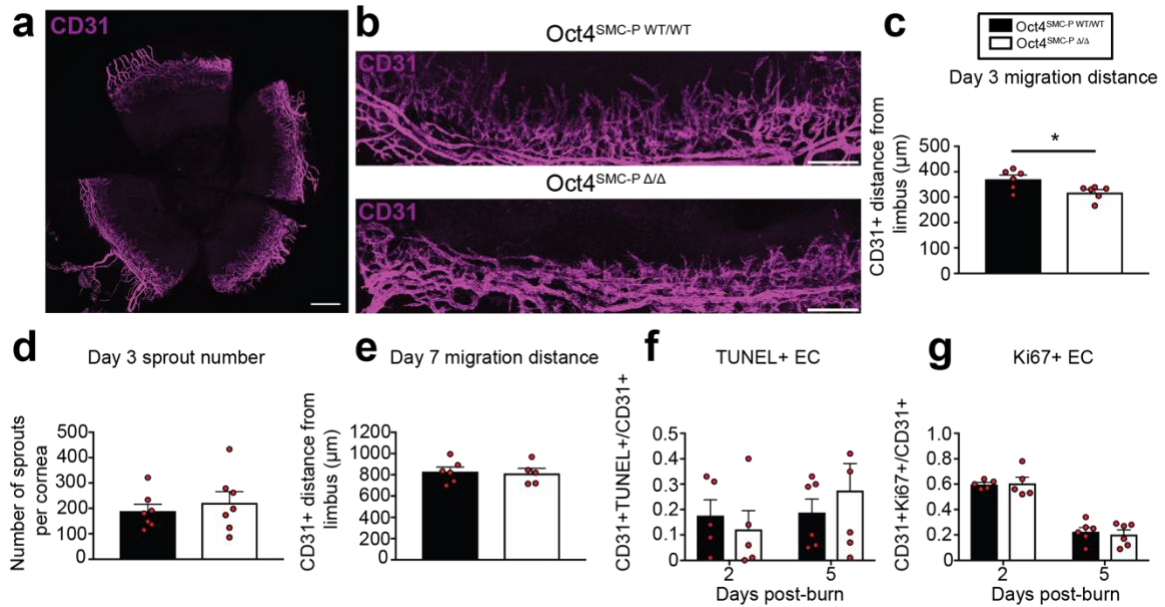


Figure 3-5

SMC-P Oct4 knockout resulted in delayed migration of CD31+ EC following corneal burn.

a, Whole mount immunostaining of a representative Oct4^{SMC-P WT/WT} cornea for CD31 (magenta) at day 3 post-corneal burn. Scale bar = 500 μm. **b**, Fields of view from Oct4^{SMC-P WT/WT} and Oct4^{SMC-P ΔΔ} mice stained with CD31 at day 3 post-corneal burn. Scale bar = 200 μm. **c**, Quantification of the average distance of CD31+ EC away from the A-V pair of the corneal limbus at day 3 post-burn. **d**, Quantification of EC sprout number throughout the cornea. **e**, Quantification of the average distance of CD31+ EC away from the A-V pair of the corneal limbus at day 7 post-burn ((c-e) n=6 WT, 6 KO). **f**, Quantification of the number of TUNEL+ EC in cornea at day 2 (n=5 WT, 5 KO) and day 5 (n=6 WT, 6 KO) post-burn. **g**, Quantification of the number of KI67+ EC in cornea at day 2 (n=5 WT, 5 KO) and day 5 post-burn (n=6 WT, 6 KO). Values = mean ± SEM. Statistics were performed using unpaired two-tailed t-test (c-g). *P < 0.05

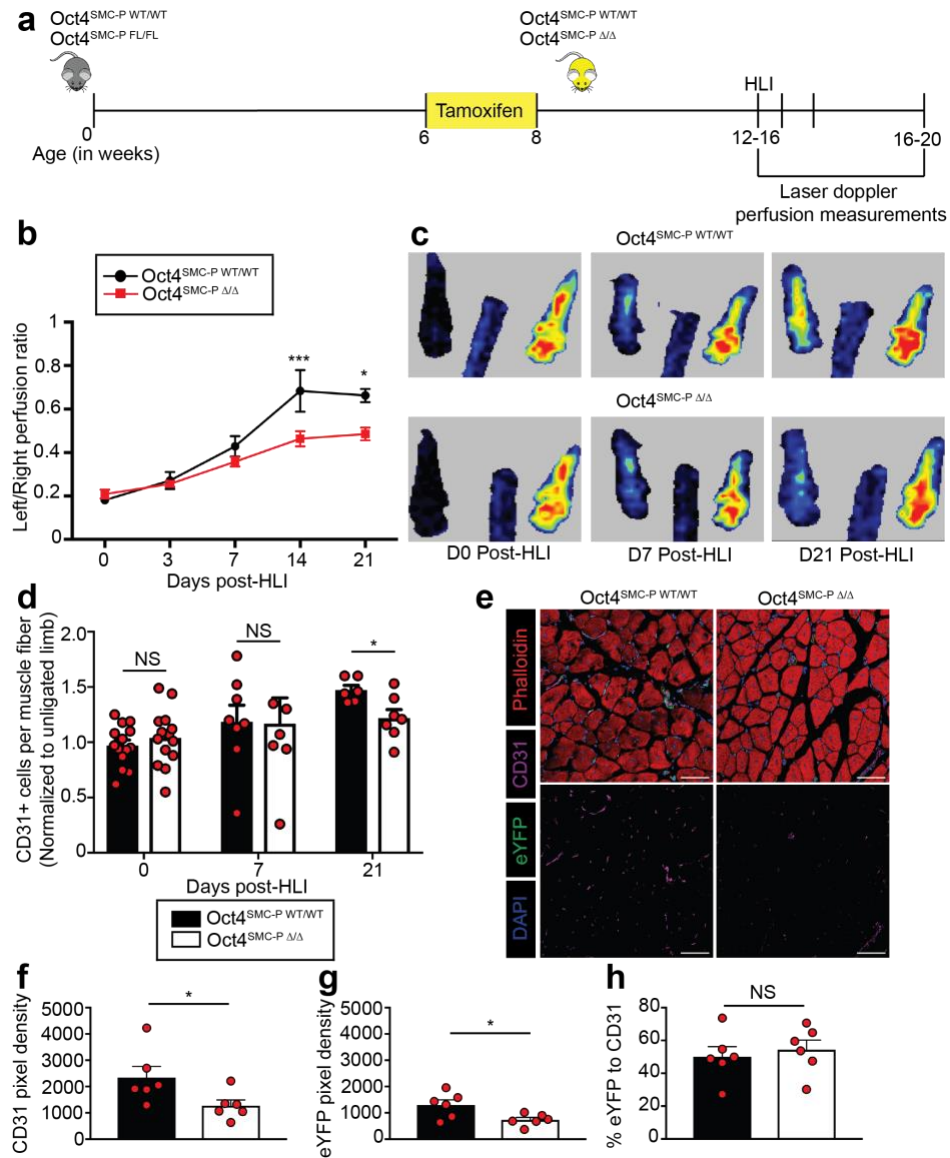


Figure 3-6

SMC-P knockout of Oct4 resulted in impaired perfusion recovery and angiogenesis at day 21 post-HLI. **a**, Schematic outlining experimental design. **b**, Perfusion recovery of Oct4^{SMC-P WT/WT} and Oct4^{SMC-P Δ/Δ} mice as assessed by Laser Doppler perfusion and expressed as left (ligated) over right (unligated) perfusion ratio of the plantar sole (n=8 WT, 9 KO). **c**, Representative images of perfusion to the plantar soles at days 0, 7, and 21 post-HLI. **d**, Quantification of number of CD31+ cells per muscle fiber at days 0, 7, and 21 post-HLI. For each mouse, data was normalized to the number of CD31+ cells per muscle fiber of the corresponding unligated muscle [n=14 WT, 14 KO

(D0); n=8 WT, 6 KO (D7); n=6 WT, 7 KO (D21)]. **e**, Representative images of calf muscle cross-sections at day 21 post-HLI stained for DAPI, eYFP, CD31, and Phalloidin. Scale bar = 50 μ m. **f-g**, Quantification of pixel density in calf muscle for CD31 (f) or eYFP (g) (n=6 WT, 6 KO). **h**, Percentage of eYFP to CD31 pixel density as measured in f-g (n=6 WT, 6 KO). Values = mean \pm SEM. Statistics were performed using two-way ANOVA with Sidak's multiple comparisons test (b) and unpaired two-tailed t-test (d,f-h). *P < 0.05 and ***P < 0.001

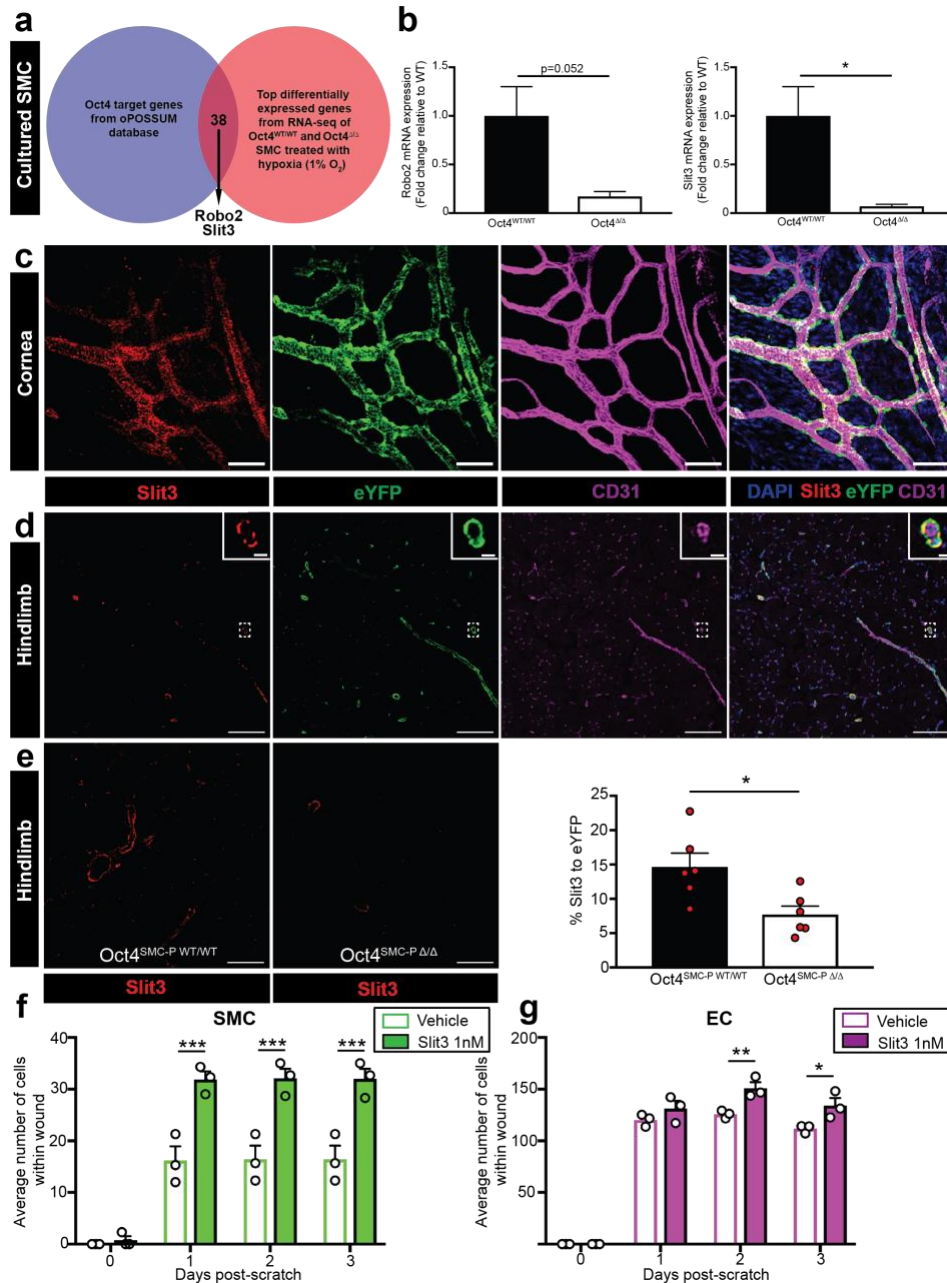


Figure 3-7

Slit3 was expressed in eYFP⁺ cells and was decreased following Oct4 knockout. **a**, We found 38 genes that were both differentially expressed in our RNA-seq analysis of cultured Oct4^{WT/WT} and Oct4^{Δ/Δ} SMC treated with hypoxia (1% O₂) as well as putative Oct4 target genes using the oPOSSUM database. Two of these genes (Robo2 and Slit3) were members of the Slit-Robo pathway of guidance genes. **b**, qRT-PCR of Oct4^{WT/WT} and Oct4^{Δ/Δ} cultured SMC for expression of

Robo2 and Slit3. Data is expressed as fold change relative to wild type. Data is from three independent experiments. **c**, Immunostaining of whole mount cornea at day 3 post-corneal burn for CD31, eYFP, and SLIT3. Scale bar = 50 μm . **d**, Immunostaining of ischemic calf muscle at day 7 post-HLI for DAPI, CD31, eYFP, and SLIT3. Scale bar = 100 μm . Zoom in scale bar = 10 μm . **e**, Representative images and quantification of SLIT3 pixel density, normalized to eYFP+ pixel density, in ischemic calf muscle at day 21 post-HLI. Scale bar = 50 μm . (n=6 WT, 6 KO). **f-g**, Scratch wound assays showing number of SMC (f) or EC (g) within the scratch wound following vehicle or Slit3 (1nM) treatment. Values = mean \pm SEM. Statistics were performed using unpaired two-tailed t-test (e) or two-way ANOVA with Sidak's multiple comparisons test (f-g). *P < 0.05, **P < 0.01, ***P < 0.001

270069I18Rik	Hoxc6
Acsbg2	Hoxc9
Adcy8	Il1rapl1
Ano4	Kcnt2
Ano5	Klhl6
Asxl3	Lphn3
Cdh8	Mef2c
Ctsk	Nrap
Dio2	Olf1317
Dlg2	Olf1318
Ebf1	Ppp1r9a
Elavl2	Prrt1
Etv1	Robo2
Gm10664	Slit3
Grm7	Sp8
Hoxa11	Sv2c
Hoxa11as	Tox
Hoxa7	Vwc2l
Hoxc4	Zfp385b

Table 1

A list of the 38 genes that were both differentially regulated in cultured Oct4^{WT/WT} and Oct4^{Δ/Δ} SMC treated with hypoxia (1% O₂) as well as putative Oct4 target genes using the oPOSSUM database.

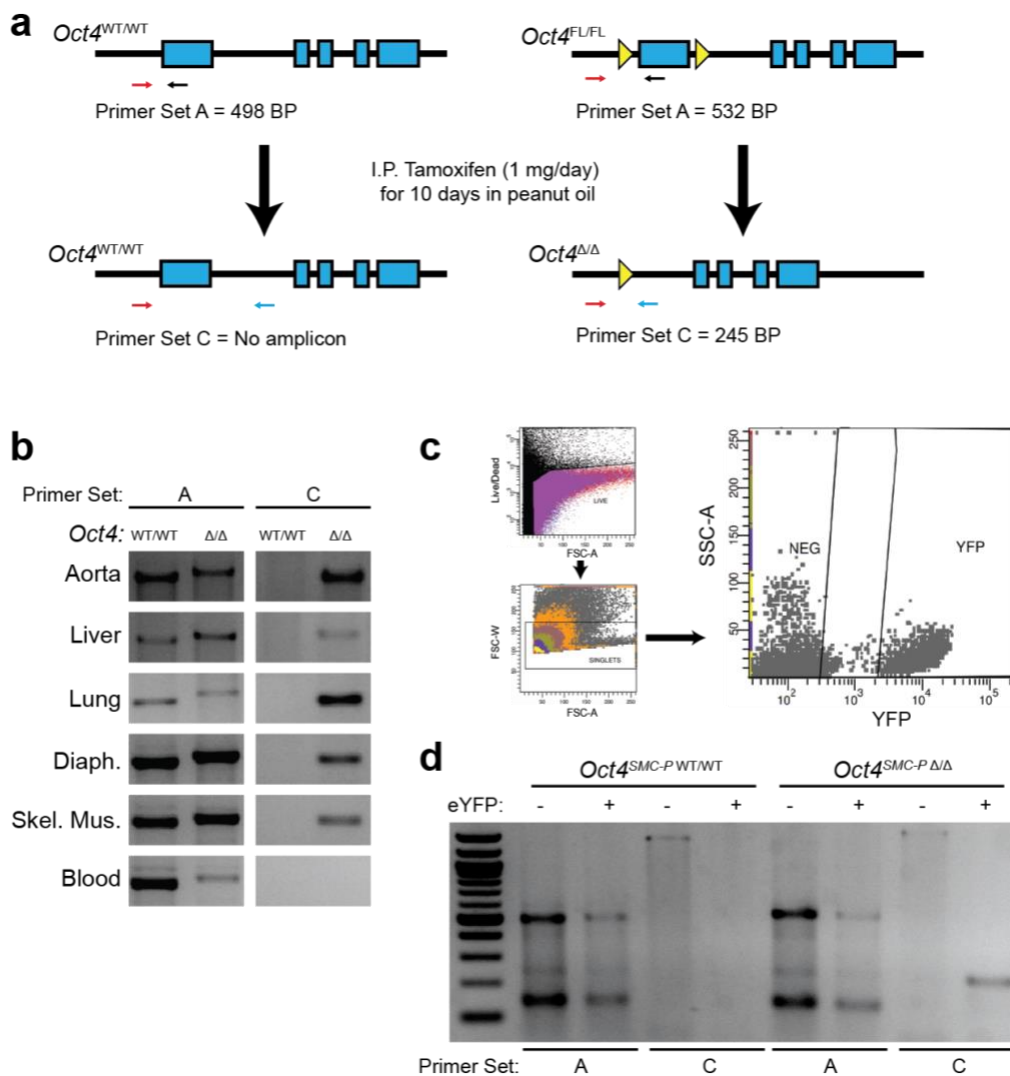


Figure 3-8

Oct4 recombination occurs in multiple tissues of *Oct4*^{SMC-P Δ/Δ} mice. **a**, Primer design for detecting non-recombined (Primer Set A) and recombined (Primer Set C) *Oct4* locus. **b**, PCR analysis using primer set A and primer set C on genomic DNA isolated from multiple tissues of *Oct4*^{SMC-P WT/WT} and *Oct4*^{SMC-P Δ/Δ} mice. **c**, Gating strategy used to sort eYFP⁻ and eYFP⁺ cells from the calf muscles of *Oct4*^{SMC-P WT/WT} and *Oct4*^{SMC-P Δ/Δ} mice. **d**, PCR analysis of sorted cells demonstrates recombination exclusively among eYFP⁺ cells harvested from *Oct4*^{SMC-P Δ/Δ} mice.

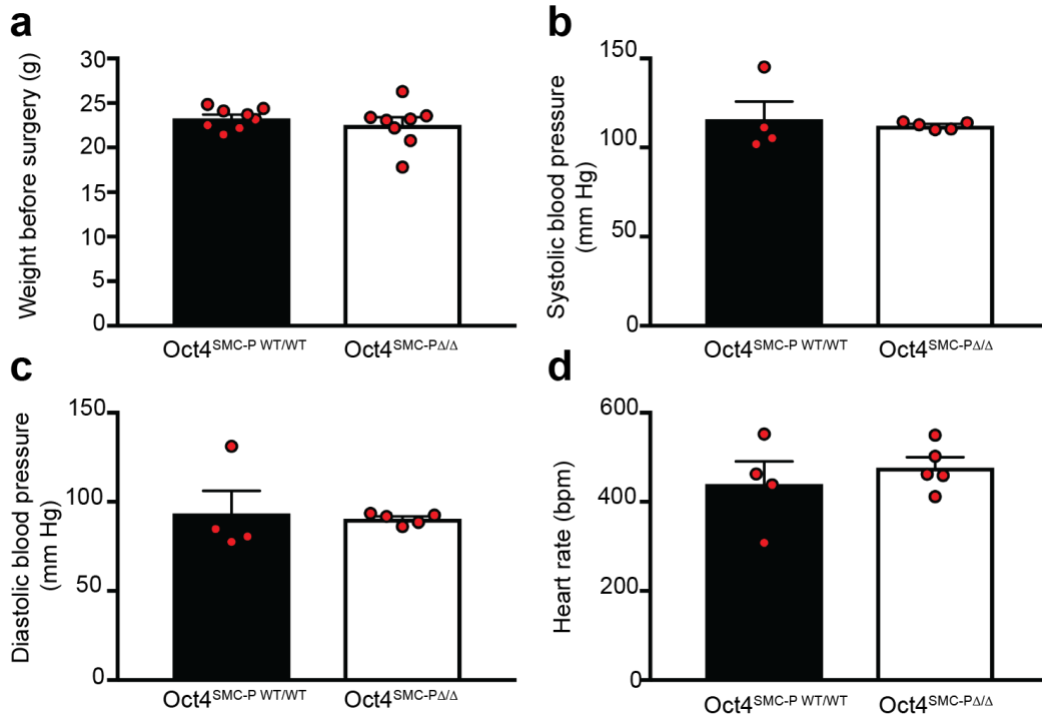


Figure 3-9

There were no differences in weight, blood pressure, or heart rate following SMC-P *Oct4* knockout. **a**, Weight of mice immediately prior to surgery (n=8 WT, 8 KO). **b-d**, A catheter-based radiotelemetry system was used to monitor systolic blood pressure (b), diastolic blood pressure (c), and heart rate (d) (n=4 WT, 5 KO). Values = mean ± SEM. Statistics were performed using unpaired two-tailed t-test (a) or Mann-Whitney U test (b-d).

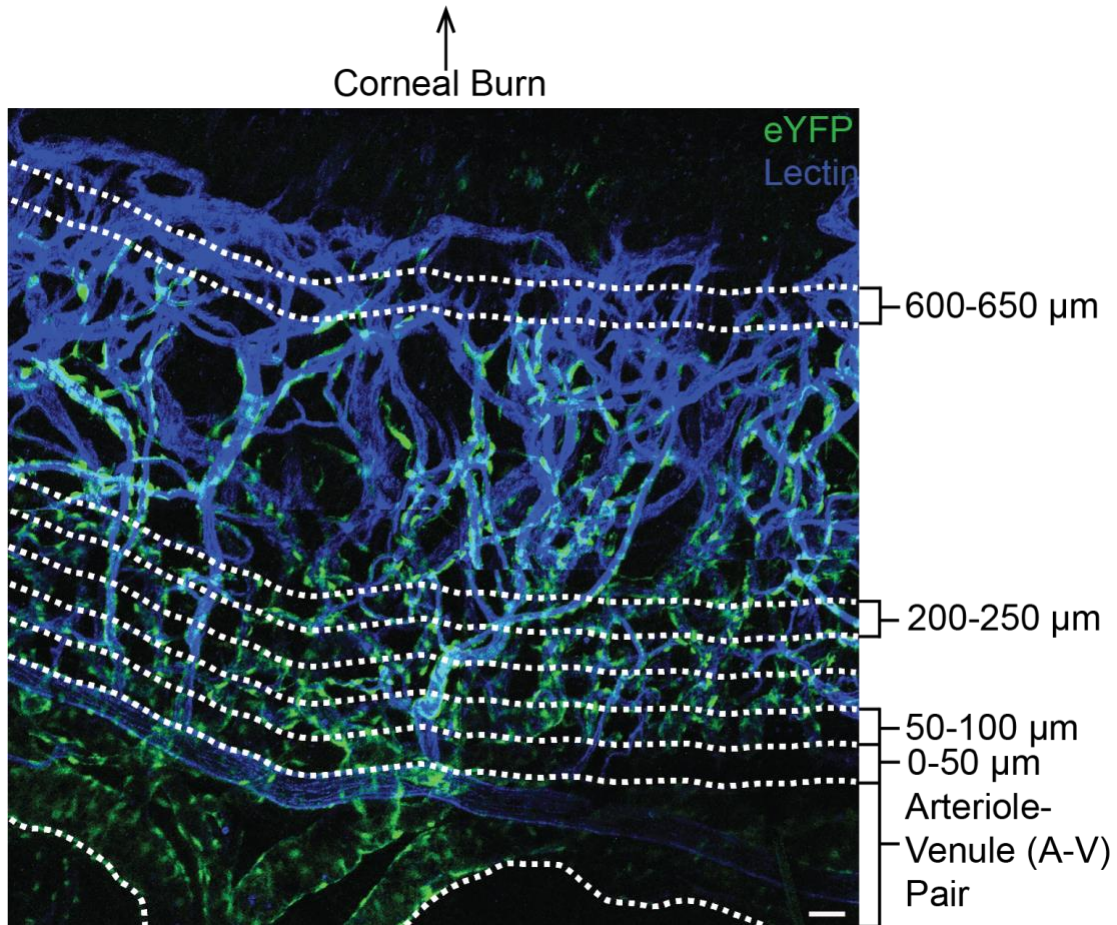


Figure 3-10

Intravital microscopy following corneal burn captures a robust angiogenic response, as visualized by eYFP+ cells along lectin-perfused vasculature. The area of new growth was divided into 50 μm regions for rigorous quantification of eYFP+ cell density. Shown is a representative montage (several fields of view stitched together) of an Oct4^{SMC-P WT/WT} cornea at day 7 post-corneal burn. eYFP is in green and perfused lectin is in blue. Scale bar = 50 μm.

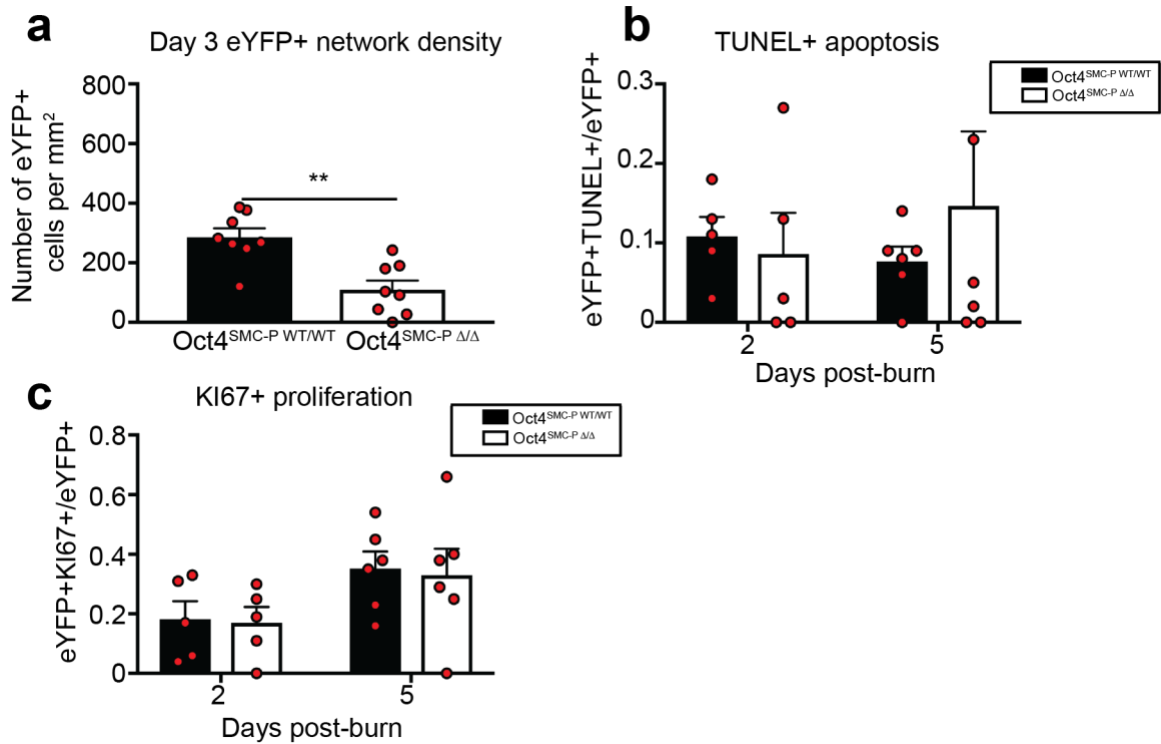


Figure 3-11

SMC-P Oct4 knockout resulted in decreased eYFP+ cell density. **a**, Quantification of eYFP+ cell density of the entire eYFP+ vascular network at day 3 post-burn (n=8 WT, 8 KO). **b**, Quantification of the ratio of eYFP+KI67+ cells to total eYFP+ cells at day 2 (n=5 WT, 5 KO) and day 5 (n=6 WT, 6 KO) post-burn. **c**, Quantification of the ratio of eYFP+TUNEL+ cells to total eYFP+ cells at day 2 (n=5 WT, 5 KO) and day 5 (n=6 WT, 6 KO) post-burn. Values = mean ± SEM. Statistics were performed using unpaired two-tailed t-test (a, b, c day2) or Mann-Whitney U test (c day 5). **P < 0.01

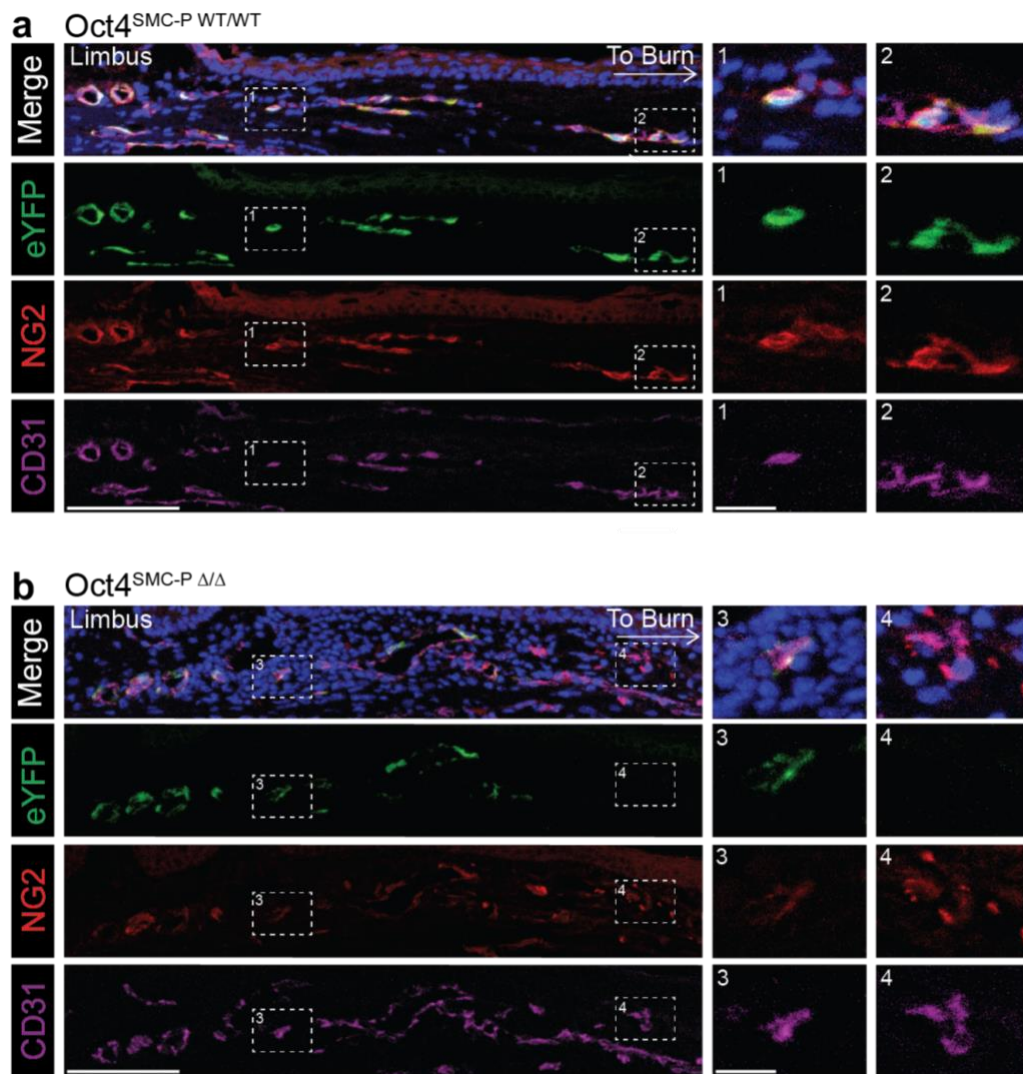


Figure 3-12

Distal CD31⁺ EC tubes from SMC-P Oct4 knockout corneas were not invested by eYFP⁺ SMC-P but were at least partially invested by eYFP⁻/NG2⁺ cells. a, Remodeling corneal vasculature from Oct4^{SMC-P WT/WT} mice at day 5 post-corneal burn stained for DAPI, eYFP, NG2, and CD31. Proximal vasculature (box 1) and distal vasculature (box 2) both contain CD31⁺ cells invested with eYFP⁺NG2⁺ cells. **b,** Remodeling corneal vasculature from Oct4^{SMC-P Δ/Δ} mice at day 5 post-burn stained for DAPI, eYFP, NG2, and CD31. Proximal vasculature (box 3) contains CD31⁺ cells invested with eYFP⁺NG2⁺ cells. Distal vasculature (box 4) contains CD31⁺ cells

invested with eYFP-/NG2+ cells. n= 3 WT, 3 KO. Representative images are shown. Scale bars = 100 μm , 20 μm (zoom-in regions).

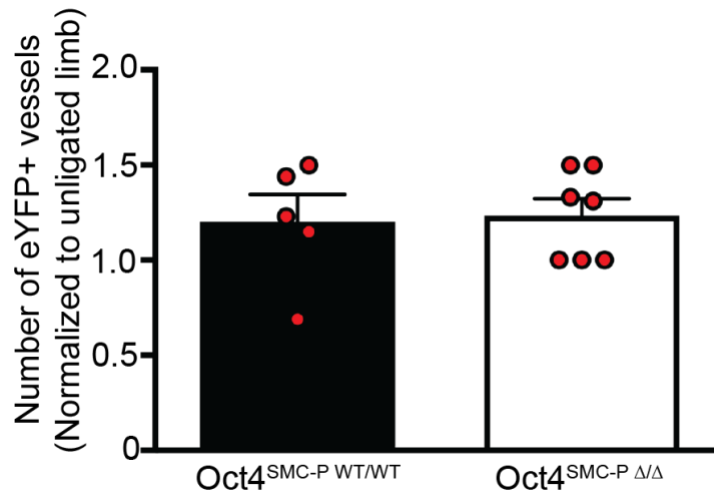


Figure 3-13

SMC-P Oct4 knockout did not affect arteriogenesis following HLI. Quantification of the number of eYFP+ vessels $> 10\mu\text{m}$ in diameter in ligated (left) thigh muscle at day 21 post-HLI normalized to the same parameter in the corresponding unligated (right) thigh muscle (n=5 WT, 7 KO). Values = mean \pm SEM. Statistics were performed using unpaired two-tailed t-test.

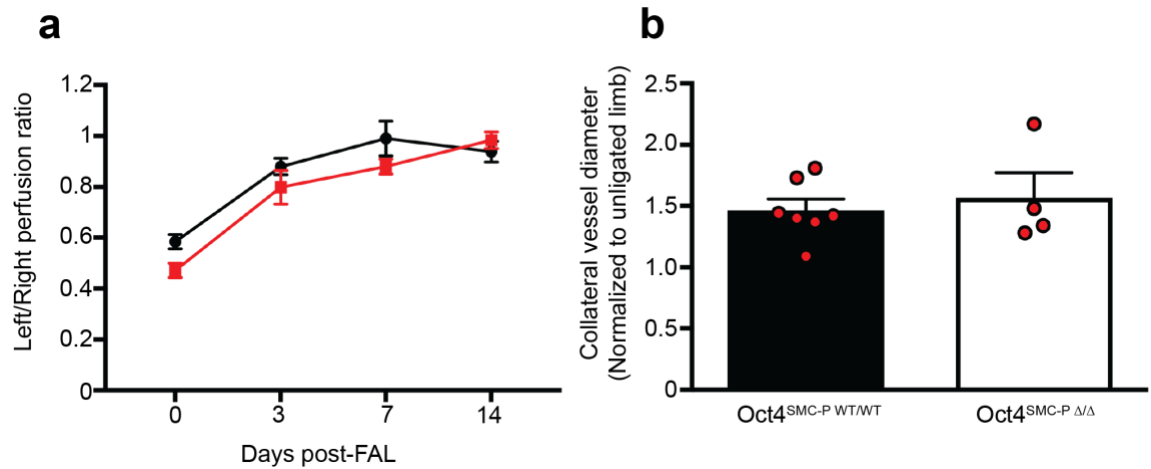


Figure 3-14

SMC-P Oct4 KO did not affect arteriogenesis in a femoral artery ligation (FAL) model. a, Perfusion recovery of Oct4^{SMC-P WT/WT} and Oct4^{SMC-P Δ/Δ} mice as assessed by Laser Doppler perfusion and expressed as left (ligated) over right (unligated) perfusion ratio of the plantar sole (n=7 WT, 6 KO). **b,** Average diameter of the collateral arteries traveling through the gracilis muscle, expressed as ratio of the diameter of those in the ligated limb to those in the unligated limb (n=7 WT, 4 KO).

3.4 DISCUSSION

In the present study, we identified a novel role for the stem cell pluripotency gene Oct4 in regulating perivascular cell function following tissue injury or hypoxia-induced angiogenesis. This is only the second report of a functional role for Oct4 in any somatic cell. The first was a previous study by our lab showing that Oct4 expression in SMC is required for formation of a fibrous cap in advanced atherosclerotic lesions. However, the present study is the first to demonstrate a protective role for Oct4 in a process, i.e. angiogenesis, that is critical for survival to and through one's reproductive years. Therefore, a functional role for Oct4 in perivascular cells likely evolved as a means to form new blood vessel networks, and/or repair damaged vessels, and only secondarily proved beneficial during atherosclerosis development.

Of interest, recent studies from our lab demonstrated that Klf4, another stem cell reprogramming factor,⁶⁵ is also active in SMC-P in a number of processes, including atherosclerosis development, maintenance of resistance arteriole diameter, and arteriole SMC-P coverage.^{15,125} It should be noted that Oct4 and Klf4 directly interact to maintain pluripotency of embryonic stem cells (ESCs) and promote reprogramming to induced pluripotent stem cells (iPSCs).¹²⁶ However, they play distinct roles within SMC-P in the microvasculature. Klf4 serves to stabilize the baseline microvasculature. In contrast, we found no role for Oct4 in baseline microvasculature. Rather, Oct4 serves to stabilize the angiogenic vasculature, as reflected by the significant functional changes we observed upon its loss, including increased leak following corneal burn and impaired perfusion recovery following HLI. The fact that SMC-P utilize two stem cell pluripotency factors may partially be a reflection of the plasticity of SMC-P, which are non-terminally differentiated cells that can undergo phenotypic modulation to less differentiated states, concomitant with increased proliferative and migratory capacity.¹ For example, roughly half of all eYFP+ cells in advanced atherosclerotic lesions express markers of other cell types including macrophages, myofibroblasts, and mesenchymal stem cells.¹⁵ Other groups have used lineage tracing to show SMC-P can adopt

features of other cell types in various disease models, such as beige adipocytes following cold stress.¹²⁷ However, SMC-P phenotypic switching is not an all-or-none response, and activation of Oct4 and/or Klf4 may be required at distinct stages of this process. In the future, it will be intriguing to test whether Oct4, like Klf4, also plays critical functional roles in other cell types, including EC.^{128,129} Of note, Klf4 was recently identified as a genetic risk locus for coronary artery disease.¹³⁰ In the future, it will be intriguing to determine whether polymorphisms in Oct4, or any downstream target genes including Slit3, are associated with cardiovascular disease or cancer. In summary, we have now shown that two stem cell pluripotency factors play distinct protective, rate-limiting roles in SMC-P in the microvasculature, such that conditional deletion of either leads to numerous deleterious downstream changes.

Interestingly, following SMC-P loss of Klf4 in young, healthy non-hyperlipidemic mice, multiple microvascular beds developed gaps in eYFP⁺ perivascular cell coverage that were filled by Acta2⁺Myh11⁺eYFP⁻ cells.¹²⁵ Based on bone marrow transfer experiments, we showed that these eYFP⁻ perivascular cells were not of myeloid origin, suggesting an alternative source including: 1) endothelial cells undergoing endothelial-to-mesenchymal transition,¹³¹ 2) Sca1⁺ adventitial progenitor cells,¹³² 3) other SMC-P progenitor populations not labeled by the Myh11-CreER^{T2} system, 4) Myh11⁻ SMC-P populations, and/or 5) Myh11⁺ SMC-P that failed to undergo recombination. In the present study, these same alternative sources of perivascular cells may partially compensate by activating a SMC-P-like program following eYFP⁺ cell dropout resulting from Oct4 knockout. In other words, when eYFP⁺ cells labeled by our Myh11-CreER^{T2} system lack Oct4 and are unable to appropriately function, alternative sources of perivascular cells may then have a selective advantage in investing nascent EC tubes and partially rescuing the angiogenic phenotype. Indeed, herein we have provided some evidence that this may occur. For example, by crossing our Myh11-CreER^{T2} ROSA eYFP lineage tracing mouse to an NG2-dsRED reporter mouse, we found that many of the NG2⁺ pericytes are eYFP⁺. However, there is a population of

NG2+ SMC-P that lack eYFP expression and as such, presumably retain the ability to activate Oct4 and adequately participate in angiogenesis (**Figure 3-1c**).²⁰ In remodeling corneal vasculature of Oct4^{SMC-P Δ/Δ} mice, we observed that, despite distal CD31+ tubes being virtually devoid of eYFP+ cells due to loss of Oct4, a population of eYFP-/NG2+ SMC-P were observed surrounding these same distal CD31+ EC tubes (**Figure 3-12b**). This means that eYFP- SMC-P populations likely partially compensate following loss of the eYFP+ population. Indeed, despite significant reductions in eYFP+ cell density and distribution resulting in increased vascular leak following corneal burn, there were relatively modest effects on EC. Loss of SMC-P coverage has previously been associated with increased EC proliferation¹⁰² and impaired EC sprouting.⁵⁸ In contrast, we observed no difference in EC proliferation (**Figure 3-11c**) or sprout number (**Figure 3-5d**). We did observe a delay in EC migration into the cornea at day 3, but this was completely resolved by day 7 (**Figure 3-5e**). This may be due in part to investment of EC by additional pericyte populations not labeled by our Myh11 lineage tracing system, including a subset of NG2+ pericytes.

However, our data cannot rule out the possibility of eYFP false negatives, or cells that express Myh11 at the time of tamoxifen injection but fail to undergo recombination and therefore are not labeled with eYFP. In Oct4^{SMC-P FL/FL} mice, these same cells would also presumably fail to undergo recombination at the Oct4 locus and would therefore likely have a survival advantage. With recent evidence demonstrating that pathologic remodeling may be due to clonal expansion of a few cells, SMC-P that fail to recombine at the Oct4 locus may then undergo selective expansion.^{133,134} Additionally, immunostaining is insufficient to determine cell of origin and can only determine positive or negative marker expression at the time of analysis. Rigorously testing the hypothesis that eYFP- cells compensate following loss of Oct4 in eYFP+ SMC-P would require development of dual conditional lineage tracing models. Importantly, this would require the use of a second, Cre-independent recombinase, such as Dre, since we utilize Myh11-CreER^{T2} to generate the Oct4 KO phenotype. Therefore, fully and rigorously addressing the possibility of compensation

by any of the aforementioned candidate cell types would require generating, validating, and repeating experiments in multiple Cre-independent lineage tracing models, coupled with Myh11-CreER^{T2} knockout of Oct4.

Activation of the pluripotency factor Oct4 leads to a multitude of downstream changes during its role as a master transcription factor in embryonic stem cells.¹³⁵ Interestingly, this is again reflected in adult SMC-P, as our previous *in vitro* and *in vivo* RNA-Seq analyses identified thousands of Oct4-dependent genes in SMC.⁵⁹ Clearly, the role of Oct4 in SMC-P is complex and our phenotype reflects the aggregate result of numerous Oct4-dependent gene modifications and subsequent downstream effects. In order to identify candidate genes contributory to our phenotype, we conducted RNA-Seq analysis of cultured Oct4 wild type and Oct4 knockout SMC treated with hypoxia and compared it with the publicly available Oct4 ChIP-seq ESC/iPSC datasets from the oPOSSUM database. Of major interest, this analysis revealed the guidance gene Slit3 as a top putative candidate. Indeed, both *in vitro* and *in vivo* validation demonstrated decreased Slit3 upon loss of Oct4. *In vitro* experimentation also demonstrated that exogenous Slit3 causes increased SMC and EC wound closure. Therefore, the impaired SMC-P and EC migration in our studies may be due, at least in part, to dysregulated Slit3 signaling in SMC-P. Consistent with these data, numerous studies have previously shown that cell types critical for angiogenesis, including SMC-P^{136,137} and EC^{107,138-140}, as well as macrophages^{120,141} and nerve cells,¹⁴² all express ROBO receptors and would therefore be impacted by altered Slit3 levels in the extracellular space. In the future, it would be interesting to generate SMC-P Slit3 knockout mice to test whether this would recapitulate the phenotype observed in our SMC-P Oct4 knockout mice. However, testing this idea will be extraordinarily difficult for the following reasons: First, there are multiple SLIT ligands, including Slit1 and Slit2, that have both overlapping and distinct functions that may compensate for the loss of SLIT3. Second, SLIT3 is produced by multiple cell types in our tissues of interest, including epithelial cells and endothelial cells¹⁴² which may upregulate expression in response to altered Slit3

gradients resulting from decreased production by SMC-P. Third, it is highly unlikely that the phenotype we report here is due exclusively to loss of only one of the many known OCT4-dependent genes. For instance, we also show that Oct4 loss in SMC-P leads to increased cell death one day after corneal burn, similar to the pro-survival role for Oct4 previously described in murine ESCs.^{143,144} Furthermore, we have previously shown that numerous other genes previously implicated in control of angiogenesis, including matrix metalloproteinases 3 and 13, multiple collagens, and osteopontin are also Oct4-dependent.⁵⁹ Taken together, our results suggest that Oct4 in SMC-P leads to numerous downstream changes, including altered Slit3 levels, which in aggregate contribute to the angiogenic phenotype observed in two different *in vivo* models.

In conclusion, this study provides multiple lines of evidence that SMC-P Oct4 is critical for angiogenesis following either corneal alkali burn or HLI. Results are of major interest and significance since they indicate that the reactivation of Oct4, which we previously demonstrated occurs in SMC during development of atherosclerotic lesions, is not exclusive to that pathological state.⁵⁹ Rather, we show that Oct4 reactivation within perivascular cells is required for functional network formation in response to tissue injury or hypoxia. Moreover, whereas Oct4 has been shown to be essential for maintenance of the pluripotency state of embryonic stem cells, herein we describe a novel role for this factor in regulating cell survival, cell migration, investment of endothelial tubes, and vessel permeability. Future studies will be required to better understand the mechanisms regulating these effects, as well as to determine how this information might be exploited to either inhibit or promote effective angiogenesis in different disease states.

4 CHAPTER 4: INTERLEUKIN 1-RECEPTOR SIGNALING IN ENDOTHELIAL CELLS, BUT NOT PERIVASCULAR CELLS, PROMOTES PRIMARY TUMOR GROWTH

4.1 ABSTRACT

A recently released secondary analysis of the phase III clinical trial, CANTOS, showed that treatment with the IL-1 β neutralizing antibody, canakinumab, reduced lung cancer incidence and fatality by approximately 70%, compared to placebo.⁷⁵ While this corroborates basic science studies and solidifies a clear link between IL-1 signaling and cancer pathogenesis, the cell types mediating these effects are unknown and unexplored. Tumor growth and metastasis are highly dependent on blood vessels, which consist of both EC and SMC-P. Herein, we utilize Cdh5 or Myh11 lineage tracing, coupled with IL-1R knockout in EC or SMC-P, to test the hypothesis that IL-1R signaling in EC and/or SMC-P promotes primary tumor growth and metastasis. Cdh5 IL-1R KO, but not Myh11 IL-1R KO, resulted in significantly decreased primary tumor growth in both B16 F10 and M3-9M orthotopic tumor models. Neither Cdh5 IL-1R KO nor Myh11 IL-R KO significantly affected metastasis of M3-9M cells to the lung. These initial studies suggest that IL-1R signaling in EC promotes primary tumor growth. Future studies will focus on further characterizing the role of IL-1R signaling in EC and SMC-P, using murine cancer models that more closely mimic the CANTOS study design.

4.2 INTRODUCTION

The Canakinumab Anti-Inflammatory Thrombosis Outcomes Study (CANTOS) trial was a large-scale clinical trial designed to treat high-risk atherosclerotic patients with the IL-1 β neutralizing antibody, canakinumab, or placebo.¹⁴⁵ Although the study was originally designed to assess primary endpoints of non-fatal myocardial infarction, non-fatal stroke, or cardiovascular death, a highly intriguing secondary analysis of the collected data was published shortly after release of the primary endpoint results. Strikingly, Ridker et al. reported that patients receiving canakinumab experienced a significant reduction in both lung cancer incidence and fatality by approximately 70%.⁷⁵ These results corroborate several studies suggesting a link between IL-1R signaling and tumor pathogenesis. For instance, IL-1 is upregulated in numerous human tumors, and global knockout of IL-1 α or IL-1 β leads to decreased primary tumor growth and metastasis.^{72,73} Additionally, polymorphisms within the IL-1 β gene are associated with increased risk of non-small cell lung cancer.^{146,147} However, while IL-1 signaling correlates with cancer pathogenesis, the critical cell types mediating IL-1 signaling in both tumor growth and tumor metastasis remain largely unknown and unexplored.

Angiogenesis, or the growth of new blood vessels, is a hallmark of tumor progression. Increased tumor growth results in hypoxia which induces an ‘angiogenic switch,’ characterized by perivascular cell detachment, EC sprouting, and pericyte recruitment during vessel maturation.¹⁴⁸ This tumor vasculature is typically abnormal, characterized by leaky, dilated blood vessels with reduced perivascular cell coverage and investment.^{54,56} As tumors continue to grow, tumor cells eventually intravasate into blood vessels and/or lymphatics, enter the systemic circulation, and ultimately extravasate to metastatic sites.¹⁴⁹ Since tumor growth and metastasis are highly dependent on blood vessel growth, these processes require extensive involvement of both EC and perivascular cells, the two major cell types of blood vessels. Of major interest, four out of nine genes downregulated in highly metastatic tumors are SMC contractile genes that are also

downregulated during SMC phenotypic switching,⁵⁵ suggesting that SMC differentiation state inversely correlates with metastasis. Building on this idea, we recently showed that phenotypically modulated SMC-P are a key component of the pre-metastatic niche in multiple orthotopic tumor models. Knockout of the stem cell pluripotency gene *Klf4* specifically in SMC-P resulted in significantly decreased metastasis to the lungs, demonstrating that SMC-P are essential for premetastatic niche formation and subsequent metastasis.²⁴ While some key signaling molecules have been elucidated, our understanding of mechanisms promoting tumor growth and metastasis, particularly in vascular cells, is incomplete. Cancer remains the second leading cause of death in the U.S.¹⁵⁰ Therefore, identification of novel signaling pathways critical for tumor angiogenesis, growth, and metastasis in EC and SMC-P is essential for developing new therapeutic approaches to curb the cancer epidemic.

IL-1 β has previously been shown to induce phenotypic changes in EC including increased proliferation, migration, and upregulation of adhesion molecules.^{71,78} IL-1 β also induces phenotypic switching of SMC, including downregulation of contractile genes and upregulation of inflammatory genes,¹¹ as well as increased proliferation and migration.⁸¹ However, the functional role of IL-1 signaling in EC and SMC-P in the context of tumor growth and metastasis remains unknown. Herein, we utilize *Cdh5* and *Myh11* lineage tracing, combined with EC and SMC-P specific knockout of IL-1R, to test the hypothesis that IL-1 signaling in EC and/or SMC-P promotes primary tumor growth and/or metastasis.

4.3 RESULTS

4.3.1 IL-1R signaling in EC, but not SMC-P, promotes primary tumor growth of B16 F10 melanoma

To determine whether IL-1R signaling in EC promotes primary tumor growth, we first utilized an orthotopic B16 F10 melanoma model. Briefly, B16 F10 melanoma cells, previously

stably transduced with a construct expressing an mCherry-Luciferase fusion protein to allow detection via fluorescence or luminescence, were injected intradermally into the right flank of Cdh5 IL-1R WT ApoE^{-/-} or Cdh5 IL-1R KO ApoE^{-/-} mice. We henceforth refer to these mice as IL-1R^{EC WT/WT} and IL-1R^{EC Δ/Δ}, respectively. Of note, we found that tumor volume in IL-1R^{EC Δ/Δ} mice was significantly decreased compared to IL-1R^{EC WT/WT} controls (**Figure 4-1a**), suggesting that IL-1R signaling in EC may promote primary tumor growth.

To determine whether IL-1R signaling in SMC-P promotes primary tumor growth, we performed the same B16 F10 orthotopic tumor model in Myh11 IL-1R WT ApoE^{-/-} and Myh11 IL-1R KO ApoE^{-/-} mice. We henceforth refer to these mice as IL-1R^{SMC-P WT/WT} and IL-1R^{SMC-P Δ/Δ} mice, respectively. However, we observed no difference in primary tumor volume between IL-1R^{SMC-P WT/WT} and IL-1R^{SMC-P Δ/Δ} mice, (**Figure 4-1b**), demonstrating that IL-1R signaling in SMC-P does not play a significant role in growth of B16 F10 primary tumors.

We attempted to measure metastasis of B16 F10 cells to the lungs using bioluminescence. Although B16 F10 is reportedly a highly metastatic variant of B16 melanoma cells which readily metastasizes to the lungs, we did not observe a rate of metastasis that was sufficiently high to allow for reliable quantification in either the Cdh5 or Myh11 mice.

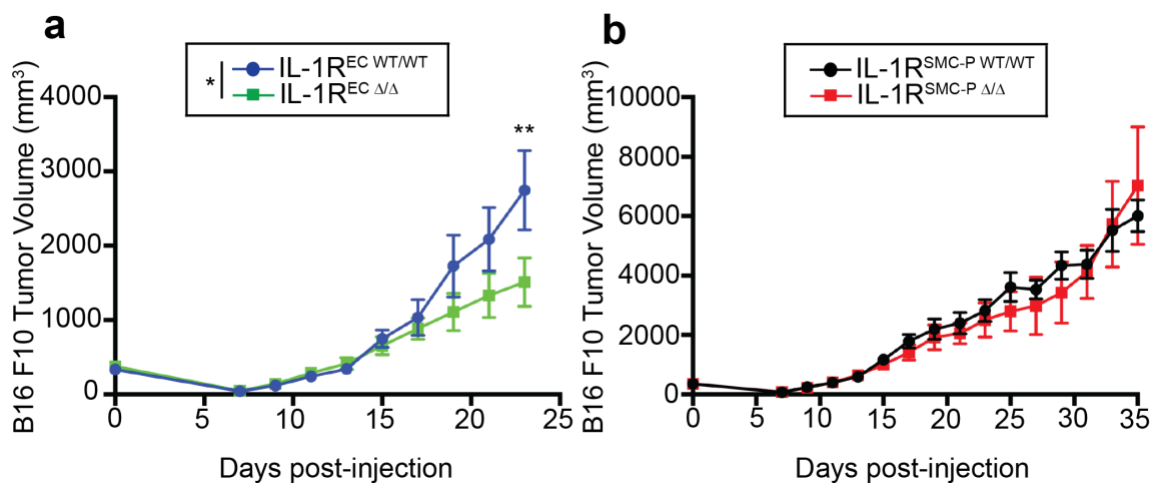


Figure 4-1

a,b, 5×10^5 B16 F10 melanoma cells were injected into the right flank of $IL-1R^{EC\ WT/WT}$ and $IL-1R^{EC\ \Delta/\Delta}$ mice (a) or $IL-1R^{SMC-P\ WT/WT}$ and $IL-1R^{SMC-P\ \Delta/\Delta}$ mice (b). Primary tumor volume was measured with a caliper at various time points throughout tumor growth.

4.3.2 IL-1R signaling in EC promotes primary tumor growth, but not metastasis, of M3-9M rhabdomyosarcoma

To determine whether IL-1R signaling in EC promotes primary tumor growth in an additional tumor model, we injected M3-9M rhabdomyosarcoma cells, also expressing mCherry-Luciferase, orthotopically into the right gastrocnemius muscle of $IL-1R^{EC\ WT/WT}$ and $IL-1R^{EC\ \Delta/\Delta}$ mice. We observed that primary tumor volume was significantly decreased in KO mice relative to WT mice (**Figure 4-2a**). Taken together with previous results, IL-1R signaling in EC promotes primary tumor growth in two different orthotopic tumor models, B16 F10 and M3-9M. We then measured metastasis of M3-9M cells to the lungs at day 30 post-tumor injection using bioluminescence imaging. We observed no significant difference in metastasis, expressed as average radiance, between $IL-1R^{EC\ WT/WT}$ and $IL-1R^{EC\ \Delta/\Delta}$ mice (**Figure 4-2b**). Therefore, at least in the M3-9M orthotopic model, IL-1R signaling in EC does not play a significant role in metastasis.

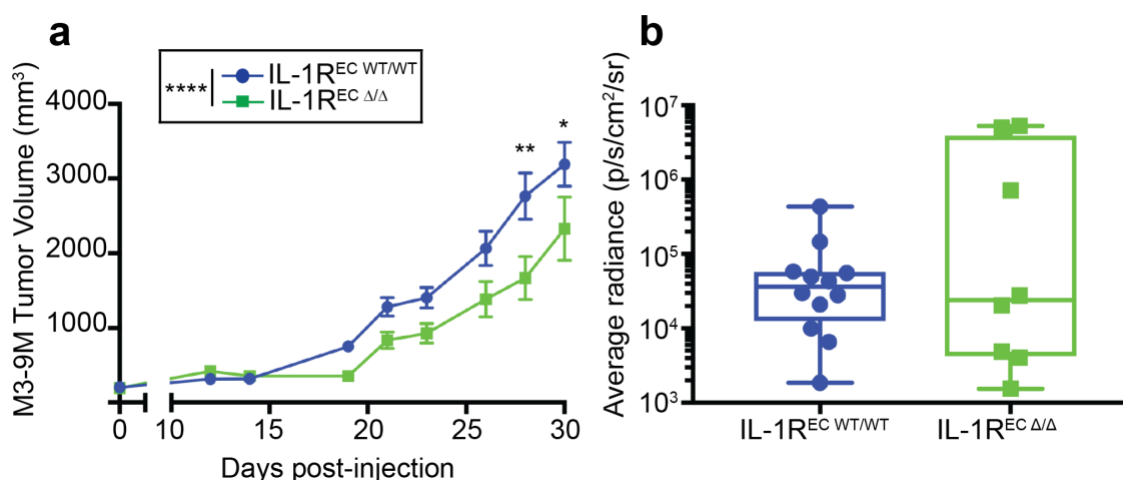


Figure 4-2

a, 5×10^5 M3-9M rhabdomyosarcoma cells were injected into the right gastrocnemius muscle of IL-1R^{EC WT/WT} and IL-1R^{EC Δ/Δ} mice. Primary tumor volume was measured with a caliper at various time points throughout tumor growth. **b**, At day 30 post-tumor injection, lungs were harvested and incubated *ex vivo* with luciferin. Average radiance of the lungs was measured using bioluminescence imaging.

4.3.3 IL-1R signaling in SMC-P does not significantly affect primary tumor growth or metastasis of M3-9M rhabdomyosarcoma

We next performed the M3-9M orthotopic tumor model in IL-1R^{SMC-P WT/WT} and IL-1R^{SMC-P Δ/Δ} mice to determine whether IL-1R signaling in SMC-P promotes primary tumor growth and/or metastasis. We observed no significant difference in either primary tumor volume (Error! Reference source not found.**a**) or metastasis to the lungs (Error! Reference source not found.**b**) between IL-1R^{SMC-P WT/WT} and IL-1R^{SMC-P Δ/Δ} mice. However, there was a trending decrease in metastasis to the lungs in IL-1R^{SMC-P Δ/Δ} mice ($p=0.135$), warranting further investigation. To model later stages of metastasis including tumor cell extravasation, colonization, and growth in metastatic lung tissue, we injected M3-9M cells directly into the tail vein of IL-1R^{SMC-P WT/WT} and IL-1R^{SMC-P Δ/Δ} mice. We observed no significant difference in mouse survival, defined as time of humane death or decline, between genotypes (Error! Reference source not found.**c**). Therefore, IL-1R signaling in SMC-P does not play a major role in primary tumor growth or metastasis, at least in the M3-9M orthotopic model.

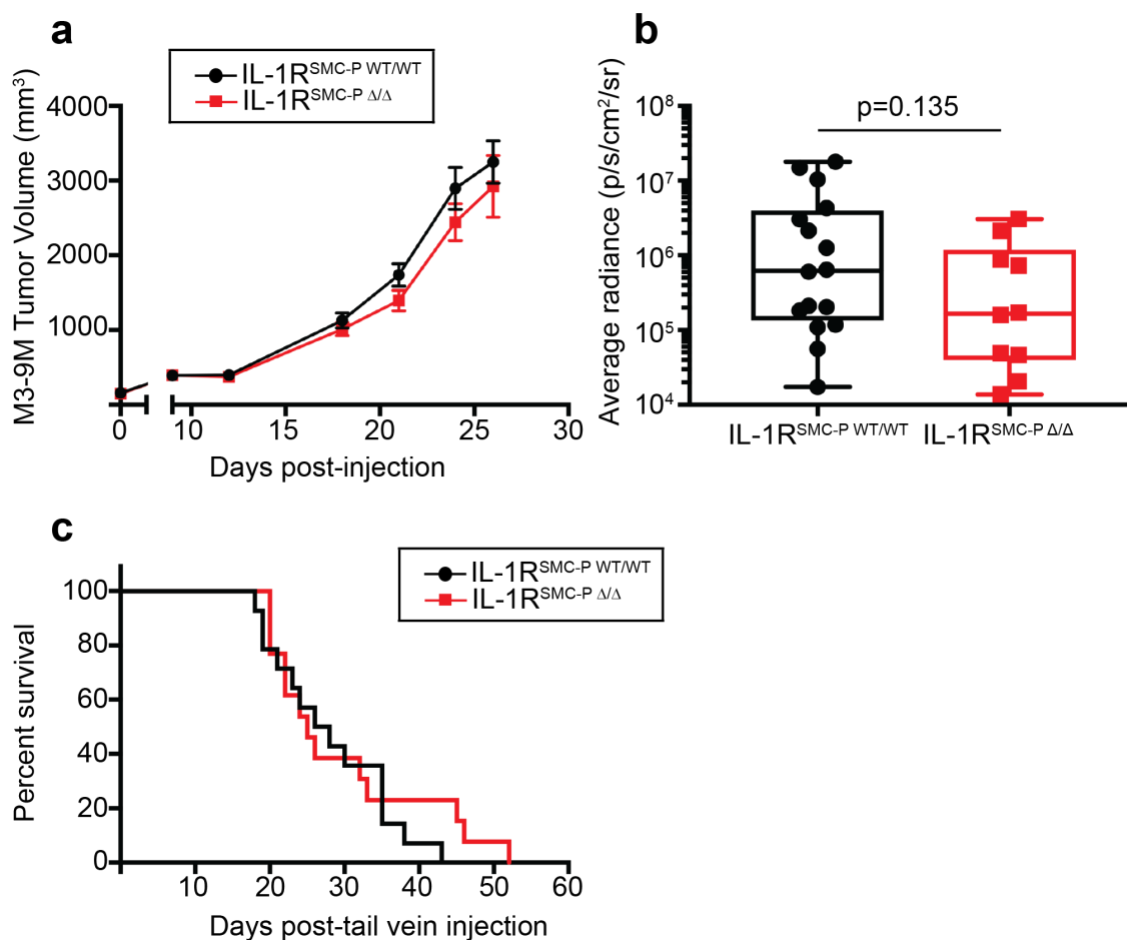


Figure 4-3

a, 5×10^5 M3-9M rhabdomyosarcoma cells were injected into the right gastrocnemius muscle of IL-1R^{SMC-P WT/WT} and IL-1R^{SMC-P Δ/Δ} mice. Primary tumor volume was measured with a caliper at various time points throughout tumor growth. **b**, At day 26 post-tumor injection, lungs were harvested and incubated *ex vivo* with luciferin. Average radiance of the lungs was measured using bioluminescence imaging. **c**, 2.5×10^4 M3-9M rhabdomyosarcoma cells were injected directly into the tail vein of IL-1R^{SMC-P WT/WT} and IL-1R^{SMC-P Δ/Δ} mice. Mice were monitored until point of humane death or decline.

4.4 DISCUSSION

In the present study, we found that IL-1R signaling in EC, but not SMC-P, promotes primary tumor growth in two different orthotopic tumor models, B16 F10 and M3-9M. Additionally, we found that IL-1R signaling in neither EC nor SMC-P plays a major role in metastasis of M3-9M cells to the lung. These initial studies raise a number of points warranting further discussion and investigation.

First, what is the mechanism of decreased primary tumor growth following loss of IL-1R in EC? One possibility is that the decreased tumor size is due to decreased angiogenesis resulting from loss of IL-1 signaling in EC. In support of this idea, IL-1 β induces EC migration and tube formation *in vitro*.⁷⁸ Additionally, IL-1 β neutralization leads to impaired BrdU incorporation into EC and impaired outgrowth of EC from aortic rings.⁷⁶ Another, not mutually exclusive possibility, is that IL-1R signaling in EC promotes primary tumor growth through indirect effects on other cell types, including tumor cells and/or BMDCs. For instance, IL-1 β secreted by VEGFR1+ BMDCs induces production of VEGF and other pro-angiogenic factors by EC. In addition to increasing EC functions necessary for angiogenesis, this also leads to increased recruitment of VEGFR1+ BMDCs, which aid in tumor growth.⁷⁶ A third possible contributor to tumor growth is increased vasculogenesis due to IL-1 β -mediated maturation of EPCs into EC.¹⁵¹ Defects in any combination of these processes could contribute to decreased primary tumor growth in IL-1R^{EC Δ/Δ} mice.

Second, the results of this study indicate that IL-1R signaling in SMC-P does not play a major role in tumor growth or metastasis. This is in contrast to previous observations in SMC-P Klf4 KO mice, where we observed no change in primary tumor growth but significantly decreased metastasis to the lungs in multiple orthotopic tumor models, including B16 F10 and M3-9M.²⁴ We previously demonstrated that IL-1 β induces Klf4 expression in SMC-P,¹¹ leading us to hypothesize that IL-1 signaling in SMC-P might play a similar role to Klf4. However, multiple other mitogens

present in the tumor stroma and premetastatic niche, including, PDGF-DD, WISP-1, and ANG-2 also induce Klf4 in SMC-P^{11,24} and may be sufficient for activation even in the absence of SMC-P IL-1R signaling. Additionally, IL-1R is a receptor as opposed to a transcription factor like Klf4, which can activate or repress numerous downstream target genes and therefore have much broader effects. IL-1R signaling in SMC-P is critical in atherosclerosis pathogenesis, as our lab recently reported that SMC-P IL-1R KO results in multiple changes consistent with decreased lesion stability.¹⁷ In contrast, our preliminary studies suggest that IL-1R signaling in SMC-P may be dispensable for tumor growth and metastasis. Further studies are needed, but it is possible that tumor pathogenesis is instead mediated by IL-1R signaling in EC and as well as tumor cells and/or BMDCs. We could examine the contributions of the latter using LysMCre and/or Cx3Cr1CreER^{T2} mediated knockout of IL-1R.

Third, although these preliminary studies are informative, it is important to note the advantages and limitations of the models used, particularly in light of the CANTOS results.⁷⁵ The advantages of the orthotopic models used in this study are their compatibility with genetically modified mice and their relative speed of completion. However, future studies using mouse models that more closely mimic the CANTOS study design might yield different results. To be included in the CANTOS trial, patients must have had a history of myocardial infarction (MI) and an elevated C-reactive protein >2mg/L, despite aggressive treatment with statins to normalize lipid levels. Importantly, they must also have been previously undiagnosed of cancer (other than basal cell skin carcinoma). Patients who went on to develop lung cancer had higher hsCRP and IL-6 and were significantly more likely to be current smokers. Specifically, more than 90% of patients who developed lung cancer were former or current smokers.⁷⁵

The strong correlation with inflammation and primary lung cancer makes it more likely that the decreased lung cancer incidence and fatality observed in CANTOS were most likely due to effects on primary lung tumor growth, as opposed to metastasis from other tissues to the lung.

Furthermore, the median follow-up time was only 3.7 years, making it more likely that canakinumab reduced progression of tumors undetectable at trial entry, rather than the development of new cancer.⁷⁵ Despite elevated markers of inflammation, the CANTOS cohort was aggressively treated with lipid-lowering agents, resulting in a median LDL cholesterol of 82.4 mg/dL, well within normal limits.¹⁴⁵

In light of these factors, future studies will attempt to more closely model the CANTOS study design, including: 1) The use of primary lung tumor cell lines, such as Lewis Lung carcinoma, to test the effects of loss of IL-1R signaling in EC or SMC-P on primary lung tumor growth. 2) Stimulation of lung injury and inflammation, using bleomycin,¹⁵² lipopolysaccharide (LPS),¹⁵³ and/or cigarette smoke extract (CES)¹⁵⁴ to mimic the elevated inflammatory profile of CANTOS patients. Indeed, the CANTOS population consisted of 24% current smokers, 47% past smokers, and a median hsCRP of 4.2 mg/L.⁷⁵ 3) Seeding of the lung with primary lung cancer cells, followed by delayed tamoxifen administration and/or use of IL-1 β neutralizing antibody, to better mimic the late-stage intervention in CANTOS. 4) High-fat western diet feeding for several weeks, followed by switching to chow diet, to generate systemic atherosclerosis and then normalize lipid levels.¹⁴⁵ Future experimentation using these mouse models will be more therapeutically relevant and shed light on whether the profound results of CANTOS occur at least in part through IL-1R signaling in the vasculature.

Our initial experiments demonstrated a role for Cdh5 IL-1R, but not Myh11 IL-1R signaling, in promoting primary tumor growth. Future studies will determine whether this is due, at least in part, to impaired angiogenesis in IL-1R^{EC Δ/Δ} mice. In contrast, we did not detect any significant role for EC or SMC-P IL-1R signaling in metastasis of M3-9M cells to the lung. While these results are informative, it is important to note that metastasis was measured using a single tumor cell line and that cancer is an extremely heterogenous disease. Future studies will attempt to better model the CANTOS trial, including testing the effects of IL-1 intervention on primary lung

tumor growth in mice with elevated inflammation. Utilization of these mouse models will help answer whether the profound results of CANTOS occur at least in part through IL-1R signaling in EC and/or SMC-P.

5 CHAPTER 5: SUMMARY, DISCUSSION AND FUTURE DIRECTIONS

5.1 SUMMARY OF CHAPTERS 3 AND 4

The studies reported in Chapters 3 and 4 examined the role of perivascular cells in angiogenesis and cancer pathogenesis using several different mouse models including corneal burn, hindlimb ischemia, and orthotopic tumor models. Chapter 3 demonstrated a critical role for Oct4 in SMC-P in angiogenesis following either corneal burn or hindlimb ischemia. Chapter 4 demonstrated no significant role for IL-R in SMC-P during primary tumor growth or metastasis but showed that IL-1R signaling in EC is critical for primary tumor growth. Taken together, results demonstrate a number of important points: 1) Numerous physiologic and pathophysiologic responses require proper functioning of the vasculature, including an appropriate angiogenic response. 2) Proper functioning of the vasculature, including an appropriate angiogenic response, requires proper function of both EC and SMC-P. 3) Loss of a single gene in either cell type can impair proper functioning of the vasculature, leading to altered disease progression and outcome.

Studies in Chapters 3 and 4 have raised a number of broad questions: 1) How far does a functional role for Oct4 and IL-1R in the vasculature extend? 2) What are the changes resulting from loss of Oct4 in the vasculature? 3) What are the changes resulting from loss of IL-1R in the vasculature? 4) How can Oct4 and IL-1R signaling in vascular cells inform future therapeutic approaches in a number of disease contexts? In the subsequent pages, I will address each of these questions in detail.

5.2 HOW FAR DOES A FUNCTIONAL ROLE FOR OCT4 AND IL-1R IN THE VASCULATURE EXTEND?

5.2.1 Evolutionary function of SMC-P

SMC-P are unique in that they are a critical cell type of blood vessels and are therefore located in nearly every tissue throughout the body. Additionally, they display remarkable phenotypic plasticity, particularly in the setting of injury and disease. Their location and high degree of plasticity confer SMC-P the ability to respond to tissue injury and contribute to wound repair in a number of physiologic and pathologic processes. From an evolutionary perspective, mutations which conferred any sort of advantage in the ability of SMC-P to contribute to injury and wound repair would be selected for over time, and conversely, mutations that impaired this process would not persist. Because of this, a broad hypothesis of our lab and others is that organisms have evolved, and are continually evolving, so that SMC-P are able to maximally respond to tissue injury and contribute to the repair process. A major aspect of this growth and repair process is the formation of new vasculature and remodeling of existing vasculature in the setting of angiogenesis.

5.2.2 Why did Oct4 evolve a function in SMC-P?

In Chapter 3, we demonstrated that Oct4 signaling in perivascular cells is one mechanism by which SMC-P are able to more robustly contribute to angiogenesis following injury, at least in the setting of corneal burn or hindlimb ischemia. Previous work from our lab demonstrated that Oct4 signaling in SMC is one mechanism by which SMC invest into atherosclerotic lesions. From an evolutionary perspective, it is far more likely that Oct4 evolved a role in SMC-P because it proved advantageous in the setting of angiogenesis, since this would lead to increased survival and reproductive success. Its role in atherosclerosis is likely an unintended secondary but beneficial consequence of its evolved role in angiogenesis. The fatal consequences of atherosclerosis, including MI and stroke, typically occur in aged individuals with long-standing atherosclerosis,

well after their reproductive years. Excluding atypical causes of thrombosis such as congenital disease or pharmacologic agents, there would have been no selective pressure for Oct4 to evolve a role to combat late-stage thrombotic or embolic events.

As of now, there is only one other described report for a functional role of Oct4 in somatic cells. A recent report demonstrated that Oct4 in EC and in SMC promotes cell quiescence, thereby preventing cell senescence.¹⁵⁵ All of the functional data was generated *in vitro*, so it remains unknown what relevance this finding might have to *in vivo* growth and disease. Regardless, it seems unlikely that there would have been sufficient selective pressure for Oct4 to have evolved a role in this context, as cell senescence is associated with aging, or prevention thereof, rather than survival.

5.2.3 Potential role of Oct4 in developmental or postnatal angiogenesis

An additional possibility is that Oct4 evolved a function in SMC-P in an as yet undescribed context, and only secondarily proved beneficial in the settings of both angiogenesis following injury as well as atherosclerosis. Angiogenesis is also essential for the initial vascularization of nearly all tissues, including developmentally and postnatally, such as during retinal angiogenesis. Rigorous examination of the role of SMC-P Oct4 in developmental angiogenesis could be achieved through tamoxifen administration to pregnant females. *Myh11* expression in SMC in mice appears around embryonic day 14.5, so initiation of tamoxifen at this time point would be ideal.¹⁵⁶ To examine post-natal retinal angiogenesis in tamoxifen-inducible mouse lines, there are established protocols involving tamoxifen administration to pups at either P1-P3 or P5-P7 to measure sprouting angiogenesis or vessel remodeling and maturation, respectively.¹⁵⁷ The roles of SMC-P Oct4 in developmental as well as postnatal retinal angiogenesis are worth future investigation, since these processes are both essential for survival and reproductive success. However, it is possible that Oct4 in SMC-P may not be rate-limiting in developmental or postnatal angiogenesis. There is precedent for differential effects observed in post-natal versus pathologic angiogenesis. For instance, *Tie2* deletion in NG2+ cells, including SMC-P, impairs post-natal retinal angiogenesis but promotes

tumor angiogenesis.²¹ Additionally, our data to this point indicates that Oct4 in SMC-P is not rate-limiting in baseline vasculature, but only in the setting of injury/disease.

5.2.4 Why did IL-1R evolve a function in SMC-P?

Regardless of whether organisms first evolved a functional role for Oct4 in SMC-P in the setting of angiogenesis following injury or in some other process critical for survival and reproductive success, this role appears to be beneficial across multiple contexts, at least in the settings of both angiogenesis and atherosclerosis. Interestingly, the phenotypes resulting from SMC-P Oct4 KO and SMC-P IL-1R KO in the setting of atherosclerosis are similar in that both ultimately lead to reduced investment of eYFP+ cells into the lesion and fibrous cap.^{17,59} Like Oct4 though, clearly IL-1R signaling in SMC-P did not evolve because it proved beneficial during atherosclerotic plaque development. It is interesting to speculate that IL-1R in SMC-P also evolved to promote SMC-P phenotypic switching and confer increased survival and reproductive success. It appears this role did not evolve to combat cancer pathogenesis though, since SMC-P IL-1R signaling appears to be dispensable in tumor growth and metastasis, at least in models tested in Chapter 4. However, more work still needs to be done to definitively address whether IL-1R in SMC-P plays a major role in other models of cancer pathogenesis (**discussed further in 5.4.3**). Instead, did SMC-P IL-1R signaling evolve to promote efficient angiogenesis following injury, including corneal burn and HLI, similar to its role in atherosclerosis? IL-1 β is upregulated following injury and inflammation, so it is less likely to have evolved a role in baseline function and/or post-natal retinal angiogenesis, as discussed for Oct4 above.

A related idea is that IL-1R signaling in SMC-P could become detrimental in other disease contexts, and in fact, this was part of the rationale for studies in Chapter 4. Indeed, we have previously shown that other SMC-P mechanisms of phenotypic switching can be beneficial or detrimental depending on context. For instance, SMC-P activation of the stem cell pluripotency gene *Klf4* is critical for baseline function of the microvasculature and likely evolved a role in that

context.¹²⁵ However, this function becomes secondarily maladaptive and actually promotes disease progression in the settings of atherosclerosis as well as cancer.^{15,24} In summary, SMC-P regulation of phenotypic state by a number of different genes including Oct4, Klf4, or IL-1R, can result in profound beneficial or detrimental effects on tissue repair and disease pathogenesis.

5.2.5 Potential role of Oct4 in tumor growth and metastasis

Continuing that line of logic then, did a functional role for Oct4 in SMC-P become secondarily adaptive, or maladaptive, in the setting of cancer? A role for Oct4 in SMC-P in the setting of cancer pathogenesis is currently being investigated by Dr. Meera Murgai, a postdoctoral researcher at the National Cancer Institute and a collaborator on studies performed in Chapter 4. I am unaware of the timeline and results of these studies, but they will be highly intriguing to this body of work since they bridge the gap between gene and models. Some of the questions that these studies could answer include: 1) Is Oct4 expression in SMC-P upregulated in primary tumors, PMNs, and/or sites of metastasis? A number of papers have reported Oct4 expression in the tumor microenvironment over the last decade.⁶⁷ Immunostaining for eYFP and Oct4 in SMC-P Oct4 WT and KO tissue would allow us to ascertain if at least some of those reports are potentially due to Oct4 expression in SMC-P. There would still be no way to rule out false positives from Oct4 pseudogenes, as discussed in (1.6.4). However, a significant decrease in the percentage of (eYFP+Oct4+)/eYFP+ cells in Oct4 KO tissue relative to WT tissue would suggest that Oct4 can be reactivated in SMC-P in the setting of cancer. Additionally, we could perform ISH-PLA on sections of human tumors to determine whether Oct4 is expressed in cells retaining the H3K4dime mark, indicating a SMC-derived cell. 2) Does Oct4 in SMC-P promote primary tumor growth, at least in part by promoting angiogenesis? Since tumor growth depends on angiogenesis, I would expect decreased tumor size in SMC-P Oct4 KO mice. However, tumor angiogenesis is more difficult to quantify due to its disorganized nature. Orthotopic tumor models also have unusually low numbers of perivascular cells,²⁴ probably due to a combination of the models themselves and

the fact that SMC-P investment is reduced in tumors.⁵⁴ 3) Does Oct4 in SMC-P promote PMN formation and metastasis, similar to the role of Klf4 in SMC-P in this setting?²⁴ Knockout of Oct4 and Klf4 in SMC-P yield quite different results, at least in the limited models tested, as previously discussed. Unlike Oct4, loss of Klf4 in SMC-P does not affect perfusion recovery following HLI (Hess and Haskins, unpublished). However, because of its role in promoting SMC-P migration and investment in the setting of atherosclerosis and angiogenesis, I would hypothesize that Oct4 in SMC-P would promote both PMN formation and metastasis due to increased migration of SMC-P away from blood vessels, allowing increased extravasation of tumors from the bloodstream into metastatic sites.¹⁵⁸ An alternative hypothesis is that Oct4 in SMC-P might promote SMC-P investment of primary tumor vasculature, leading to reduced tumor intravasation into the bloodstream.⁵⁶ Determining whether Oct4 function in SMC-P is adaptive or maladaptive in cancer pathogenesis could be performed using established orthotopic tumor models as outlined in Chapter 4, as well as more clinically relevant models outlined in greater detail below (5.4.2).

5.3 WHAT ARE THE CHANGES RESULTING FROM LOSS OF OCT4 IN THE VASCULATURE?

5.3.1 Oct4-dependent regulation of Slit-Robo signaling

Key unresolved questions remain regarding what downstream mechanisms mediate the effects of Oct4 in promoting angiogenesis and IL-1R in promoting tumor growth? In Chapter 3, we demonstrated that regulation of Slit3 is Oct4-dependent and this likely, at least in part, contributes to angiogenesis following injury (Figure 7). Slit-Robo signaling involves binding of three Slit ligands (Slit1-3) to four Robo receptors (Robo1-4). Numerous *in vitro* studies have shown that Slits modulate migration of multiple cell types, including EC and SMC-P.^{107,119,136} However, reports vary as to whether Slits promote or inhibit migration. There are a number of possible reasons for this discrepancy, such as the location of each cell in relation to the source of the Slit gradient and the

presence or absence of other cytokines that can modulate Slit-Robo signaling.¹⁰⁷ My studies investigating Slit-Robo were fraught with the same issues and limitations. Nevertheless, the totality of my data, plus the existing literature, on Slit-Robo signaling has led me to a working model of Oct4-dependent regulation of Slit-Robo mediated angiogenesis, which I outline below. There are a number of gaps in this model that could theoretically be filled using rigorous *in vivo* approaches, which I also outline below.

5.3.2 Proposed model of Slit-Robo signaling in the vasculature

At baseline, i.e. in the absence of an angiogenic stimulus, Slit-Robo signaling appears to maintain vessel quiescence. Because Oct4 plays no detectable role at baseline (**Figure 3-2**), my studies in Chapter 3 did not focus on Slit-Robo signaling at baseline. However, I have observed that Slit3 is expressed in eYFP+ cells at baseline in hindlimb muscle. Slit2 and Slit3 have been shown by others to be expressed in SMaA+ cells at baseline.¹⁵⁹ This group further demonstrated that global genetic deletion of Slit2 and Slit3 leads to increased vessel density, branching, and tortuosity in breast tissue.¹⁵⁹ Furthermore, Slit2 has been shown to counter-act VEGF signaling to maintain vessel quiescence at baseline.¹³⁹ Therefore, at baseline, Slit-Robo signaling appears to promote vessel stability and prevent angiogenesis. The lack of a baseline phenotype upon SMC-P Oct4 KO means that Slit-Robo signaling is either 1) not regulated by Oct4 at baseline, possibly because Oct4 is not expressed at baseline, or 2) it is regulated, at least in part, by Oct4 at baseline, but the phenotype does not manifest until after injury. This could be due to compensation by other Slit-Robo family members and/or pathways other than Slit-Robo. Although exclusively based on the literature, Slit2 and Slit3 production by SMC-P at baseline likely signal via Robo4 in EC to maintain association between EC and SMC-P.^{139,159} Because loss of Oct4 in SMC-P leads to no detectable phenotypic changes at baseline, studies to elucidate this signaling paradigm are not worth future investigation.

Following injury, Oct4 KO SMC-P produce less Slit3 compared to Oct4 WT SMC-P. Interestingly, RT-PCR data suggests that Slit2 levels are increased in Oct4 KO SMC-P relative to WT (data not shown). One could be compensating for a change in the other, most likely Slit2 being upregulated to compensate for decreased Slit3. This is speculative but is based on previous reports in the literature demonstrating extensive redundancy in the system.^{107,159} For instance, global deletion of Slit3 leads to no change in vessel density, whereas deletion of Slit3 plus only a single allele of Slit2 leads to a two-fold increase in vessel density in adult mammary glands.¹⁵⁹ Decreased Slit3 likely results in Oct4 KO SMC-P that are not able to appropriately migrate relative to WT SMC-P. This leads to impaired distance of eYFP⁺ cells from the limbus and may be partially responsible for the increased vascular leak and hemorrhaging observed in SMC-P Oct4 KO corneas (**Figure 3-4**). There are some secondary changes on nearby EC, including delayed migration (**Figure 3-5c**), likely due at least in part to reduced Slit3 levels.

5.3.3 Potential Slit3 loss-of-function approaches

One option to test the above model of Slit-Robo regulation of angiogenesis following injury would involve crossing our Myh11 CreER^{T2} Rosa STOP floxed eYFP mouse with a recently generated Slit3 floxed mouse.¹²⁴ Following tamoxifen injections, levels of Slit3, as well as Slit2 (and Slit1) in a number of SMC-rich tissues such as lung should be measured and compared between SMC-P Slit3 WT and Slit3 KO mice. Because Slits are secreted, ELISA would be the preferred method of detection, but Slit antibodies are particularly poor. Therefore, knockout might instead need to be validated at the RNA level using in situ hybridization.¹⁰⁷ Based on previous reports, I predict Slit2 levels would be upregulated in SMC-P Slit3 KO mice relative to WT.¹⁵⁹ Even if Slit2 levels are not increased as a result of SMC-P Slit3 KO, previous reports have demonstrated that deletion of a single Slit or single Robo results in no detectable changes whereas combined loss of two Slits or two Robos results in significant effects on vascular remodeling.^{107,159} Therefore, SMC-P Slit3 mice would likely need to be crossed to Slit2 floxed mice,¹⁰⁷ so that

following tamoxifen injection, Slit2 and Slit3 are simultaneously deleted exclusively in Myh11-expressing SMC-P. I am not aware of any reports of Slit1 expression in the vasculature, but it is still possible that Slit1 could at least partially compensate for loss of Slit2 and Slit3 in SMC-P.

Corneal burn and hindlimb ischemia studies could be performed in SMC-P Slit2 KO Slit3 KO mice, as performed in Chapter 3, in order to determine the contribution of SMC-P Slit2 and Slit3 signaling to angiogenesis following injury. Because Oct4 is a transcription factor controlling thousands of genes, this SMC-P Slit2 KO Slit3 KO mouse is highly unlikely to fully phenocopy the SMC-P Oct4 KO phenotype. Conversely, it is possible that Slit signaling in SMC-P is regulated by other upstream factors, in addition to Oct4, and as such, could manifest as a novel phenotype. Even if these SMC-P Slit2 KO Slit3 KO mice exactly phenocopied the SMC-P Oct4 KO mice, these studies would still not conclusively determine the complete role of Oct4 in the regulation of Slit-Robo signaling. Therefore, I believe these loss-of-function studies are only worthy of the time and effort required to complete them if interested in rigorously studying the role of SMC-P Slit2 and Slit3 to *in vivo* angiogenesis, independent of Oct4.

There are two other more complex loss-of-function approaches that are worthy of discussion. First, knockout of Slit3 could instead be achieved through Myh11 CreER^{T2}-driven homozygous knock-in of a fluorescent reporter other than eYFP, such as tdTomato, to the endogenous Slit3 locus. This would allow detection of Slit3 KO SMC-P *in vivo* and forgo the need for protein or RNA detection of Slit3. One method could involve insertion of a loxP Slit3 STOP loxP tdTomato transgene, so that tamoxifen activation of CreER^{T2} removes Slit3 and the STOP codon, generating SMC-P that lack Slit3 and are tdTomato+, allowing for *in vivo* tracking. However, it is possible the STOP codon would interfere with endogenous Slit3 production, in the absence of tamoxifen injections.

Second, our lab has recently generated a new Myh11DreER^{T2} ROSA roxed STOP loxed tdtomatoSTOP eGFP mouse. In this mouse, tamoxifen administration activates DreER^{T2}, which

recognizes rox sequences and therefore removes a stop codon allowing labeling of Myh11 expressing cells with tdtomato. This mouse could be crossed with an Oct4 Cre mouse, so that Myh11 expressing cells labeled with tdtomato after tamoxifen administration which go on to activate Oct4 will then become eGFP+. This mouse could then be crossed with any floxed mouse, including floxed Slit3. This would allow for Slit3 deletion in Myh11+ SMC-P, only once they activate Oct4 expression. This approach would be more specifically testing the role of SMC-P Oct4 in Slit-Robo mediated angiogenesis and would be useful in helping visualize Oct4+ SMC-P *in vivo*. However, this approach, as well as the previous approach, would be subject to the aforementioned caveats regarding Slit-Robo redundancy, including compensation by Slit2 and therefore might require additional crossing with a Slit2 floxed mouse. Additionally, each would require years to generate and validate the mice. Overall, I do not believe these studies are worth the time or effort of future pursuit.

5.3.4 Potential Slit3 gain-of-function approaches

Ascertaining the role of Oct4 in Slit-Robo mediated angiogenesis *in vivo* could also be achieved through several different gain-of-function approaches. Each of these approaches would require use of our SMC-P Oct4 mice, since this system is needed to generate the original phenotype and determine if the phenotype can be at least partially restored. The simplest approach would be to use the corneal micropocket model of CNV. This model works by making an incision in the center of the cornea, creating a small micropocket towards the lateral limbus, and implanting a pellet containing, in this case, Slit3. Using this model, Slit3 was previously shown to promote neovascularization.¹¹⁹ We could perform this model in SMC-P Oct4 KO mice, implant pellets containing either Slit3 or vehicle, and compare angiogenesis using intravital microscopy, as done in Chapter 3. Other potential gain-of-function approaches, including intravenous injection of Slit3 and use of a Slit3-loaded collagen sponge, were recently described in Xu et al, Nature Medicine, 2018.¹²⁴

Although theoretically possible, all of these potential gain-of-function approaches would be subject to off-target effects. Slit3 affects numerous cell types including monocytes¹²⁰ and nerve cells,¹⁴² both of which are highly prevalent in injured cornea and hindlimb muscle and also play critical roles in the angiogenic response.^{160,161} Additionally, exogenous administration of Slit3 would fail to appropriately re-establish SLIT3 gradients that are normally tightly regulated but are disrupted following loss of Oct4. As one example of this tight regulation, previous work has shown that SLIT3 gradients, like VEGF and PDGF-BB gradients, are highly dependent on the presence of HSPGs on the surface of cells and in the ECM. EC KO of NDST1, necessary for synthesis of HSPGs, decreases SLIT3 binding to EC Robo4, leading to impaired neovascularization.¹²² For these reasons, I would hypothesize that the above gain-of-function approaches would all lead to further dysregulation of angiogenesis, rather than partial restoration of angiogenesis. As such, these studies are not worth future investigation.

The most rigorous experiment to test whether the phenotype resulting from SMC-P loss of Oct4 can be restored by Slit3 involves the use of mice that are not currently available. First, we would need to develop transgenic mice that specifically overexpress Slit3 in Myh11-expressing SMC-P. Because these mice need to be compatible with our tamoxifen-inducible Cre system, the most plausible design would be to generate a CMV-STOPfloxed Slit3 mouse. These mice could then be crossed to our SMC-P Oct4 mice so that, upon tamoxifen injection, Cre-mediated recombination would occur at the Rosa locus, the Oct4 locus, and the Slit3 locus. This would allow for simultaneous lineage tagging of SMC-P, KO of Oct4, and constitutive Slit3 expression. Since the CMV-floxed STOP Slit3 transgene is driven by the constitutively active CMV promoter and should not be affected by loss of Oct4 since it does not contain the native Slit3 promoter, this approach should theoretically result in Slit3 overexpression specifically in SMC-P with Oct4 deleted. Generating and extensively validating these mice would require years of time. Even if the system initially induced Slit3 overexpression in SMC-P, Oct4 may only indirectly and partially

regulate Slit3, and other mechanisms may return Slit3 to near-normal levels. Additionally, levels of Slit1 and Slit2, and/or any of the Robo receptors, could be affected due to perturbation of the system. Because of these caveats, I do not feel these studies are worth further pursuit by the Owens Lab or others.

5.3.5 Summary: Slit3 loss and gain-of-function approaches

As outlined above, *in vivo* loss and gain-of-function approaches testing the role of Slit3 signaling in the Oct4 phenotype would require years of validation and experimentation and would, in almost all cases, still be inconclusive. The experiments outlined above focus almost exclusively on Slit3, but my *in vitro* data suggests that Slit2, as well as Robo1 and Robo2, are likely also regulated, at least in part, by Oct4. The cumulative phenotype that results from SMC-P Oct4 KO is likely due to perturbation of each of these genes, as well as many other genes including those identified in our previous RNA-Seq analyses. The Slit-Robo system, as evidenced by previous *in vivo* genetic knockout studies of Slit-Robo,^{107,159} has extensive redundancy, where knockout of a single member is compensated for by other members of the family. Taken together, further investigation of the Slit-Robo pathway as a mediator of Oct4-dependent angiogenesis is not worth future study.

5.3.6 Potential mechanisms of increased apoptosis following loss of Oct4

One potential avenue for future study is the finding that loss of Oct4 leads to increased TUNEL+eYFP+ cell apoptosis at day 1 post-burn. This was a late observation that I did not have time to pursue further experimentally, so I will briefly discuss possible explanations and future directions. Of note, this anti-apoptotic role for Oct4 appears to be transient, as it is not observed at days 2 and 5 post-burn (**Figure 3-11b-c**). This could be because Oct4 is most strongly activated between days 0-1 post-burn, leading to the most prominent effects. Interestingly, knockdown of

Oct4 in ESCs also leads to increased cell apoptosis,^{143,144} but these were both *in vitro* studies with single time points of analysis.

A highly intriguing idea is that the increased apoptosis in SMC-P Oct4 KO tissue is linked to defective Slit-Robo signaling. It was recently shown that the amyloid precursor protein (APP) can bind Slit ligands and that this interaction affects neuronal guidance.¹⁶² APP is also capable of inducing apoptosis in a cell-autonomous manner.¹⁶³ Therefore, it is conceivable that disrupted Slit-Robo signaling results in increased APP-mediated apoptosis. However, the temporal nature of the *in vivo* apoptosis phenotype makes this cascade of events less likely. Alternatively, studies in Oct4 knockdown ESCs have identified decreased survivin¹⁴³ and increased Trp53¹⁴⁴ as potential downstream mediators of increased cell death. Future initial experiments should include RT-PCR and Western blot using existing cDNA and protein generated from previous experiments to determine whether APP, survivin, and/or Trp53 transcripts and/or protein levels are significantly changed in Oct4 KO SMC relative to WT.

5.3.7 Identification of additional Oct4-dependent genes

To identify additional putative downstream Oct4 target genes that promote angiogenesis, we could flow sort eYFP+ cells from SMC-P Oct4 WT and KO tissue, perform RNA-Seq on sorted cells, and identify genes differentially expressed between SMC-P Oct4 WT and KO tissue. Ideally, analysis would be done on sorted eYFP+ cells from both injured hindlimb muscle and burned corneas to identify genes commonly up-regulated or commonly down-regulated in both hindlimb and cornea data sets. Because of presumed low yields of eYFP+ cells, single cell RNA-Seq (scRNA-seq) may need to be performed, instead of bulk RNA-Seq. scRNA-seq would also allow for identification of unique eYFP+ cell subsets. We could then validate the top candidate genes using qRT-PCR and determine whether there are similar directional changes at the protein level using Western blot. This would ideally be done in cultured pericytes, with or without CRISPR/cas9 KO of Oct4, as recently reported in cultured EC.¹⁵⁵ The top one or two validated candidates could

then be tested in gain-of-function experiments using the corneal micropocket model in SMC-P Oct4 KO mice implanted with pellets containing proteins of interest versus vehicle. However, these gain-of-function experiments would likely be subject to the same limitations as discussed in (5.3.4).

5.3.8 Potential role of Oct4 in EC

While the focus of this thesis is SMC-P, EC are also an essential component of blood vessels and can extensively modulate their phenotypic state.^{131,164} Therefore, they are also prime candidates for responding to injury and contributing to disease. Indeed, as Chapter 4 demonstrated, loss of a single gene critical in EC phenotypic modulation can significantly impair primary tumor growth. One broad question is whether mechanisms that regulate SMC-P phenotypic state, such as Oct4, also regulate EC phenotypic state and function. Of note, Oct4 was recently shown to be expressed in EC in aorta upon B-hydroxybutyrate injection, fasting,¹⁵⁵ or atherosclerosis (Cherepanova, unpublished observations). CRISPR/cas9 knockout of Oct4 in cultured EC leads to increased cell senescence.¹⁵⁵ Dr. Cherepanova is currently testing the role of Oct4 in EC in the setting of atherosclerosis and pulmonary hypertension. In theory, a functional role for Oct4 in EC could be tested for in any of the disease pathologies reported here or discussed above. The most potentially informative and personally interesting to me would be testing the role of EC Oct4 in tumor growth and metastasis. However, these potential future studies are only distantly related to this thesis and will not be discussed further.

5.4 WHAT ARE THE CHANGES RESULTING FROM LOSS OF IL-1R IN THE VASCULATURE?

5.4.1 IL-1R signaling in perivascular cells

While Chapter 3 showed that loss of Oct4 in perivascular cells leads to detrimental changes in the vasculature including decreased functional recovery, Chapter 4 showed that loss of IL-1R in

perivascular cells leads to no significant changes in cancer pathogenesis. Despite these negative results, there are a number of important points worth further discussion and/or experimentation. 1) Completed experiments were limited to B16 F10 and M3-9M cells for primary tumor growth and only M3-9M cells for metastasis. While those experiments showed no significant differences, there was a trending decrease in metastasis ($p=0.135$) in SMC-P IL-1R KO mice in the M3-9M orthotopic tumor model. However, there was no difference in survival, defined as humane decline or death, between genotypes following M3-9M tail vein injection (TVI). Since tumor cells are injected directly into systemic circulation, TVI studies better model later stages of metastasis including tumor extravasation from the bloodstream and colonization and growth in the lung. Therefore, together these results suggest that SMC-P IL-1R does not play a role in later stages of metastasis but may play a role in promoting early stages of metastasis, including intravasation of tumor cells into the circulation. To test this, we could collect blood daily via retro-orbital bleeds and run PCR on the blood for mCherry to determine whether the rate of appearance and number of tumor cells in the circulation differs between genotypes. However, this data may not be particularly meaningful, since only 0.01% of tumor cells that leave their primary site end up forming a distant metastasis, at least in humans.¹⁶⁵ This, coupled with the fact that survival curves are almost identical between genotypes, leads me to conclude that it is not worth pursuing any additional studies using orthotopic tumor models in Myh11 IL-1R mice.

5.4.2 Design of mouse models to better mimic CANTOS study design

However, models of primary lung tumor growth that better mimic the patient population studied in CANTOS, as described in (4.4), may yield different results. Immediate future efforts should focus on developing, validating, and optimizing these models. These models would likely involve induction of lung inflammation using bleomycin, LPS, and/or cigarette smoke extract (CSE) followed by low dose TVI of LLC, or another primary lung cancer line, in IL-1R WT and KO mice on an ApoE^{-/-} background. Bleomycin is a chemotherapeutic agent which induces lung

fibrosis through a variety of mechanisms including the formation of reactive oxygen species and production of pro-inflammatory cytokines such as IL-1 and IL-6.¹⁵² However, this pro-inflammatory state is short-lived and followed by a sustained pro-fibrotic state. LPS, in contrast, induces sustained lung inflammation and should not directly inhibit tumor growth.¹⁵³ However, since LPS can reduce SMC-P coverage of EC and increase vascular leakage, it should be administered prior to tumor seeding of the lung.¹⁶⁶ Cigarette smoke extract (CSE) induces upregulation of pro-inflammatory genes, including IL-1 β , and downregulation of SMC contractile genes.¹⁵⁴ It could be administered to mice intraperitoneally to induce systemic inflammatory changes consistent with chronic smoking.¹⁶⁷ Following tumor seeding of the inflamed lung, tamoxifen would be administered to lineage tag and knock out IL-1R, thus simulating late-stage intervention to inhibit IL-1 signaling. The full cohort would be harvested once tumors have fully developed in the lungs of WT mice, at which point tumor size would be measured with both IVIS and histology.

Other variables to consider in the development of these new models are the age and diet of the mice. Age of patients in the CANTOS study ranged from 54-71.⁷⁵ Cholesterol was well-controlled though, with a median cholesterol of 82.4 mg/dL (normal < 100), as over 93% were on lipid-lowering agents.¹⁴⁵ Studies in Chapter 4 were performed in mice on an ApoE^{-/-} background but were fed a normal chow diet. Because they lack the ApoE gene, these mice are still mildly hypercholesterolemic, despite consumption of a normal diet.¹⁶⁸ Potential modifications to better mimic the CANTOS patient cohort include using ApoE^{-/-} mice plus high fat western diet feeding then inducing lipid regression to near normal levels by switching to chow diet.¹⁶⁹ Additionally, we could initiate studies in aged mice (18-24 months), but logistical reasons including increased mortality rate make this less feasible.

Although no mouse model will be able to entirely recapitulate the CANTOS patient cohort, it is critical to utilize models that mimic it as closely as possible, since this was a strong biologic

effect in a phase III human clinical trial.⁷⁵ This means we need to test the effects of inhibition of IL-1R signaling on established primary lung tumor growth in a cohort with elevated inflammation in the lung, similar to the CANTOS cohort. Fortunately, our collaborators Dr. Rosandra Kaplan and Dr. Meera Murgai at the NCI have experience working with several aspects of the proposed models. Indeed, these experiments will most likely be performed by them at the NCI. Still, development of these models will require extensive experimentation to optimize each of these parameters.

5.4.3 Use of better models to test IL-1R signaling in EC and SMC-P

Because of results in Chapter 4, priority will be given to fully testing the role of Cdh5 IL-1R signaling in these more clinically relevant models. However, it would also be worthwhile to perform at least one experiment using an optimized model in a full cohort of SMC-P IL-1R WT and KO mice to determine whether SMC-P IL-1R signaling promotes primary lung tumor growth in the setting of atherosclerosis with elevated inflammation but well-managed cholesterol. It is entirely possible that elevated inflammation is a key variable that could affect outcome. Indeed, IL-1 β is induced and secreted in the setting of inflammation.⁷¹ Certainly, tumors and metastatic sites are themselves highly inflammatory environments, but increased inflammatory signaling, including in the lung, may impact how SMC-P respond in cancer pathogenesis.

Of course, we can always make additional adjustments and/or variations to this model. One highly likely adjustment is, in lieu of or in tandem with cell-specific genetic KO of IL-1R induced by tamoxifen administration, the systemic administration of a murine IL-1 β neutralizing antibody following seeding of the lung. Use of the murine IL-1 β neutralizing antibody requires approval from the pharmaceutical company Novartis. In the event that we are not granted permission to use it in these studies, we could instead use Anakinra, a recombinant form of IL-1Ra, the naturally occurring antagonist of the IL-1R. Either of these approaches would allow us to test the effects of global inhibition of IL-1 signaling. These studies would likely first be performed in Cdh5 IL-1R

WT mice, since our data to this point indicates EC IL-1R signaling is critical for tumor growth. Because of the Cdh5 lineage tracing, these studies would allow us to determine phenotypic changes on EC resulting from global IL-1 inhibition. One caveat is that the murine neutralizing antibody from Novartis, as well as canakinumab, specifically target and neutralize IL-1 β , but not IL-1 α . Anakinra, in contrast, binds to IL-1R and therefore inhibits both IL-1 α and IL-1 β mediated signaling. Genetic knockout of IL-1R, like that used in Chapter 4, also does not distinguish between the effects of IL-1 α versus IL-1 β . IL-1 α is present under homeostatic conditions and not normally secreted, but it has also been linked to cancer pathogenesis.⁷¹ Only if absolutely necessary, combinations of these loss-of-function approaches could allow us to distinguish between effects of IL-1 α versus IL-1 β .

5.4.4 IL-1R signaling in EC

In Chapter 4, we demonstrated that IL-1R signaling in EC promotes primary tumor growth, as evidenced by decreased tumor volume in B16 F10 and M3-9M primary tumors in Cdh5 IL-1R KO mice (**Figure 4-1**). The first future priority, as outlined above, would be to develop better models to mimic CANTOS and then test the role of Cdh5 IL-1R signaling in these models. Although unlikely, it is possible these newly developed models will determine there is no significant effect on tumor growth following EC IL-1R KO. In this event, we should compare microvessel density (MVD) within existing B16 F10 and M3-9M primary tumors of Cdh5 IL-1R WT and KO mice by staining for eYFP to determine whether MVD is decreased in Cdh5 IL-1R KO tumors. Possible mechanisms for decreased primary tumor growth include decreased angiogenesis, decreased recruitment of tumor cells and/or BMDCs, and/or decreased EPC maturation, which could all be reflected in decreased MVD. Cdh5+ cell contribution to MVD by staining for lineage tagged eYFP+ EC cannot distinguish between angiogenesis and vasculogenesis. Indeed, bone marrow-derived EPCs can also express VE-cadherin, and neutralization of this population reduces tumor vascularization.¹⁷⁰ Therefore, determining to what

extent BMDCs express VE-cadherin, are labeled with eYFP during tamoxifen administration, and therefore may ultimately contribute to eYFP⁺ capillaries in B16 F10 and M3-9M tumors, would require complex *in vivo* approaches, such as the use of bone marrow transfer (BMT) experiments. For the effort involved, these experiments would not be worthwhile. *In vitro* studies using isolated EC from Cdh5 IL1R WT and Cdh5 IL1R KO mice would also do little to advance the field. Therefore, additional mechanistic studies beyond quantification of MVD should not be performed in orthotopic tumor models.

Instead, if Cdh5 IL-1R KO leads to decreased MVD in B16 F10 and/or M3-9M primary tumors, it would be worth testing whether EC IL-1R promotes angiogenesis in established *in vivo* angiogenesis models, including corneal burn and HLI. There is a strong correlation between IL-1 signaling and inflammation-associated angiogenesis. For example, IL-1 β induces corneal angiogenesis in the corneal micropocket model.¹⁷¹ Global knockout of IL-1 β leads to impaired perfusion recovery and decreased capillary density in the HLI model.⁷⁹ Corneal burn and HLI studies comparing Cdh5 IL1R WT and KO mice would determine whether these effects are, at least in part, mediated by IL-1 signaling in EC.

On the other hand, if experiments using newly developed models of primary lung tumor growth determine that Cdh5 IL-1R signaling promotes tumor growth, in line with our orthotopic tumor model data, I would perform additional studies to help explain this phenotype. This would include characterizing phenotypic changes of EC within lung tissue of Cdh5 IL-1R WT and KO mice. This would be done by performing immunostaining of lung tissue for various previously used and validated markers including eYFP, KI67 (proliferation), TUNEL (apoptosis), ACTA2 and LGALS3 (markers of EndoMT), as well as quantification of MVD. I hypothesize that loss of IL-1R in EC would result in decreased EC proliferation, increased apoptosis, decreased EndoMT, and decreased MVD.

Of note, microvessel density correlates with increased metastasis and decreased patient survival in nearly all malignancies.¹⁶⁵ We previously observed no significant difference in metastasis in Cdh5 IL-1R mice, at least in the one cell line tested (M3-9M). There are certain primary lung cancer lines that reportedly metastasize to other tissues, which we could use to determine whether EC IL-1R signaling affects metastasis in primary lung tumor models. This is a critical question, since over 90% of cancer mortality is caused by metastasis.¹⁴⁹ If Cdh5 IL-1R signaling does play a role in metastasis, one possible mechanism is through IL-1 β induced upregulation of EC adhesion molecules,^{79,172} which are required for extravasation of tumor cells and BMDCs from the bloodstream. It is of course possible that effects of IL-1R signaling on metastasis are not mediated, or only modestly mediated, by EC or SMC-P. Instead, effects may be largely due to IL-1R signaling in tumor cells and/or BMDCs. Studies using promoter specific Cre transgenes such as LysM or Cx3cr1, coupled with IL-1R KO, could help determine this. Our lab has generated each of these mouse lines, and in the event that IL-1R KO in EC or SMC-P fail to produce a strong biological effect, these studies may be worth future pursuit by our lab or others.

5.5 HOW STUDIES MIGHT INFORM FUTURE THERAPEUTIC STRATEGIES

Studies in Chapters 3 and 4 were mostly performed in preclinical animal models, all of which fail to recapitulate the intricacies and complexity of human disease. Nevertheless, there are a number of important themes and concepts that emerge when considering how these studies might together inform the design and implementation of future therapies.

5.5.1 Angiogenic therapies beyond VEGF

Numerous therapies to modulate vessel growth have been undertaken, but here I focus primarily on the modulation of VEGF signaling, since multiple approaches have been used in a variety of disease settings. In the setting of PAD, despite promising preclinical results, clinical trial results have been largely underwhelming.⁴¹ This is evidenced by a phase II clinical trial which

found that intramuscular administration of VEGF to patients with IC led to no significant improvements in peak walking time or ABI but in fact led to increased peripheral edema, particularly at the higher dose.¹¹² In the setting of retinal diseases such as wet age-related macular degeneration (ARMD), anti-VEGF therapies have had more success. In particular, use of VEGF antibodies such as ranibizumab have led to significant improvement in vision in multiple clinical trials.¹⁷³ For treatment of CNV, VEGF inhibitory strategies have shown promise in pre-clinical models, but large-scale clinical trials are still needed to determine translatability.¹⁷⁴ In the setting of cancer, efforts to promote vascular normalization through inhibition of VEGF signaling have included use of VEGF neutralizing antibodies such as bevacizumab (Avastin), VEGF traps such as aflibercept, or inhibitors of VEGFR-2 function. Despite exciting pre-clinical data, clinical trials involving inhibition of VEGF signaling have been largely disappointing in solid tumors. Chemotherapy plus VEGF inhibition using bevacizumab, as opposed to chemotherapy alone, initially increased disease-free survival but this effect was lost after three years.²⁹ The take-away from use of VEGF inhibitory strategies in each of these disease contexts is that, despite initial promise, new strategies targeting additional angiogenic pathways are greatly needed. Experiments outlined above would start to determine whether Oct4 and/or IL-1R signaling might be potential future targets.

5.5.2 Vascular normalization

In addition to inhibition of angiogenic pathways such as VEGF, the concept of vascular normalization also includes the idea of promoting increased SMC-P investment of leaky, dilated tumor vasculature.⁵⁶ Since tumor vasculature is characteristically leaky, leading to elevated interstitial pressure and heterogeneous blood flow, promoting increased SMC-P investment might also improve vessel oxygenation and drug delivery to tumors. In support of this idea, global conditional knockout of the perivascular cell marker Rgs5 in mice resulted in increased vascular normalization, including decreased vessel diameter, increased oxygenation, and decreased vessel

permeability.¹⁷⁵ Additional murine studies promoting SMC-P investment and/or impairing SMC-P phenotypic switching, through strategies such as inhibition of the PDGF-BB/PDGFRB pathway or knockout of Klf4, result in decreased metastasis.^{24,176,177} These studies argue that specific targeting of SMC-P to halt primary tumor growth as well as metastasis are promising avenues of future research. Therefore, characterization of the role of SMC-P Oct4 in tumor progression and metastasis, as previously discussed (5.2.5), will be highly informative. If SMC-P Oct4 function in tumor pathogenesis proves to be either critically adaptive or maladaptive, activation or inhibition of downstream Oct4 signaling could be further investigated as a means to modulate SMC-P investment of tumor vasculature in both primary tumors and at metastatic sites.

5.5.3 Therapeutic angiogenesis to target both EC and SMC-P

This idea of targeting SMC-P, in addition to EC, is not limited to the setting of cancer but can be extended to any process dependent on proper vessel function, including angiogenesis. Indeed, as studies in Chapters 3 and 4 demonstrate, SMC-P Oct4 is rate-limiting in angiogenesis in the settings of HLI and CNV. Promoting Oct4 downstream signaling in the setting of PAD could aid in preventing the vascular edema associated with previous clinical trials using VEGF alone.⁴¹ Conversely, inhibition of downstream Oct4 signaling could be used in tandem with EC growth inhibitors to also inhibit migration and growth of SMC-P, in the setting of CNV. Clearly, a better understanding of downstream Oct4 signaling networks are needed to make this even a distant possibility. As a transcription factor, Oct4 may be a poor candidate for therapeutic intervention. Furthermore, targeting a stem cell pluripotency factor, particularly through activation, could have dire consequences, including promoting tumor and/or teratoma formation. However, it is interesting to note that a phase I study was recently completed using an activator of Klf4. Somewhat counter-intuitively, it showed promising results in patients with advanced solid tumors.¹⁷⁸ It will be interesting to follow progress of larger-scale trials, especially in light of recent findings demonstrating Klf4 signaling in SMC-P promotes metastatic growth.²⁴ Unfortunately, studies in

Chapter 3 were unable to fully characterize Oct4 downstream targets. Slit3 was proposed as a potential downstream effector but much more work is needed to more fully characterize its role in pre-clinical models of angiogenesis. Interestingly, Slit-Robo signaling positively correlates with cancer progression.¹³⁸ Therefore, more complete characterization of Slit-Robo angiogenic signaling may have translatability to cancer as well.

Even so, as evidenced by clinical trials involving VEGF modulation, as well as numerous other therapeutic approaches not discussed, preclinical models do not always translate to humans. However, neutralization of a single protein, IL-1 β , in the CANTOS phase III clinical trial resulted in a 70% reduction in lung cancer incidence and fatality.⁷⁵ All-cause mortality was not different between antibody and placebo groups because decreased cancer mortality was offset by an increase in the number of fatal infections due to canakinumab-treated patients being in an immunocompromised state.⁷⁵ Therefore, global inhibition of IL-1 β will not be a viable option moving forward and is additional impetus for performing studies to determine cell-specific effects of IL-1R signaling, as outlined above (**5.4.3**). Additionally, as evidenced by clinical trials with VEGF, single agent inhibition in the setting of cancer and other diseases often leads to rebound angiogenesis following neutralization. A number of mechanisms have been proposed for this effect including intrinsic adaptation of tumor cells to respond to other growth factors in the tumor microenvironment, adaptation of tumor stromal cells to secrete additional growth factors beyond VEGF, and increased secretion of VEGF by cells other than EC, including by VEGFR1+ BMCs.⁷¹ Combinational strategies that target multiple methods of growth are direly needed. Based on studies in Chapter 4, inhibition of IL-1 signaling in EC may represent an additional strategy to decrease tumor growth, possibly through decreasing tumor angiogenesis.

However, with the exception of lung and liver cancer, primary tumors rarely cause death.¹⁶⁵ Although our studies found no role for IL-1R signaling in EC or SMC-P in cancer metastasis, they were limited to only two cell types and limited by the models used, as previously discussed.

Previous murine studies have shown that global inhibition of IL-1 signaling leads to decreased tumor metastasis.⁷¹ IL-1 signaling is associated with increased tumor MVD, and tumor MVD correlates with increased metastatic potential and decreased survival in nearly all forms of malignancy.¹⁶⁵ Taken together, the strong link between IL-1 signaling and cancer pathogenesis, strengthened by studies in Chapter 4 demonstrating loss of IL-1R in EC results in decreased primary tumor growth, makes IL-1 signaling a promising target for future studies.

5.5.4 Summary and integration to inform future therapies

As discussed, far more work is needed to determine the precise contribution of Oct4 and IL-1R signaling in vascular cells, including both EC and SMC-P, in the setting of angiogenesis and cancer. This will initially be through the use of future pre-clinical models that more closely mimic human disease as well as future studies to better characterize downstream signaling. The hope is that these future studies will help inform future therapeutic strategies. Although far from reality, combined manipulation of both Oct4 and IL-1R signaling could theoretically be used to modulate the vascular response and improve disease outcome. In the setting of PAD or other ischemic occlusive diseases such as MI and stroke, I hypothesize that this could occur through combined activation of SMC-P Oct4 signaling and EC IL-1R signaling to promote stable, non-leaky vasculature. In the setting of CNV of various causes, I hypothesize that this could occur through combined inhibition of SMC-P Oct4 and EC IL-1R signaling to impair both EC and SMC-P functions critical for angiogenesis. In the setting of cancer, I hypothesize that this could occur through inhibition of EC IL-1R signaling, possibly combined with inhibition of downstream SMC-P Oct4 signaling, to promote normalization of the tumor vasculature. Extensive work is needed to test each of these hypotheses and ultimately determine whether they represent possible therapeutic approaches in the future.

5.5.5 Final Outlook

It is important to remember that therapeutic advances to treating any disease, including diseases of the vasculature, require countless incremental advantages over the span of many decades. For instance, inhibition of tumor angiogenesis as a potential therapy for cancer was originally proposed by Dr. Judah Folkman in 1971.⁵² Work by Dr. Jeffrey Isner and colleagues in the 1990s showed that therapeutic angiogenesis for treating PAD was a promising treatment option moving forward.¹⁷⁹ Despite major advances in our understanding of the pathogenesis of these diseases, cardiovascular disease and cancer remain the leading causes of death in the US.¹⁵⁰ The totality of work in this thesis represents one more incremental step towards a better understanding of the biology behind how blood vessels remodel and contribute to disease pathogenesis. I hope that one day results provided herein can prove useful, however microscopic that use may be, in the design of therapies that make an incremental dent in the totality of human suffering. My primary motivation to pursue biomedical research as part of an MD/PhD program has been, still is, and hopefully will always be, to aid in the collective effort of alleviating the incredible amount of human suffering in this world. I eagerly await the next phase of my journey and hope that my time in medical school and residency will fuel my desire to bring a tiny ray of light to the darkness of human disease.

6 REFERENCES

1. Alexander MR, Owens GK. Epigenetic control of smooth muscle cell differentiation and phenotypic switching in vascular development and disease. *Annu Rev Physiol*. 2012;74:13-40. doi:10.1146/annurev-physiol-012110-142315.
2. Owens GK. Regulation of differentiation of vascular smooth muscle cells. *Physiol Rev*. 1995;75(3):487-517.
3. Armulik A, Genové G, Betsholtz C. Pericytes: developmental, physiological, and pathological perspectives, problems, and promises. *Dev Cell*. 2011;21(2):193-215. doi:10.1016/j.devcel.2011.07.001.
4. Gan Q, Yoshida T, Li J, Owens GK. Smooth muscle cells and myofibroblasts use distinct transcriptional mechanisms for smooth muscle alpha-actin expression. *Circ Res*. 2007;101(9):883-892. doi:10.1161/CIRCRESAHA.107.154831.
5. Hall CN, Reynell C, Gesslein B, et al. Capillary pericytes regulate cerebral blood flow in health and disease. *Nature*. 2014;508:55. <https://doi.org/10.1038/nature13165>.
6. Hill RA, Tong L, Yuan P, Murikinati S, Gupta S, Grutzendler J. Regional Blood Flow in the Normal and Ischemic Brain Is Controlled by Arteriolar Smooth Muscle Cell Contractility and Not by Capillary Pericytes. *Neuron*. 2015;87(1):95-110. doi:10.1016/j.neuron.2015.06.001.
7. Clowes AW, Schwartz SM. Significance of Quiescent Smooth Muscle Migration in the

- Injured Rat Carotid Artery. *Circ Res*. 1985;56(1):139-145.
8. Bentzon JF, Sondergaard CS, Kassem M, Falk E. Smooth muscle cells healing atherosclerotic plaque disruptions are of local, not blood, origin in apolipoprotein E knockout mice. *Circulation*. 2007;116(18):2053-2061.
doi:10.1161/CIRCULATIONAHA.107.722355.
 9. Dandré F, Owens GK. Platelet-derived growth factor-BB and Ets-1 transcription factor negatively regulate transcription of multiple smooth muscle cell differentiation marker genes. *Am J Physiol Circ Physiol*. 2004;286(6):H2042-H2051.
doi:10.1152/ajpheart.00625.2003.
 10. Pidkovka NA, Cherepanova OA, Yoshida T, et al. Oxidized phospholipids induce phenotypic switching of vascular smooth muscle cells in vivo and in vitro. *Circ Res*. 2007;101(8):792-801. doi:10.1161/CIRCRESAHA.107.152736.
 11. Alexander MR, Murgai M, Moehle CW, Owens GK. Interleukin-1 β modulates smooth muscle cell phenotype to a distinct inflammatory state relative to PDGF-DD via NF-kB-dependent mechanisms. *Physiol Genomics*. 2012;44(7):417-429.
doi:10.1152/physiolgenomics.00160.2011.
 12. Hendrix J, Wamhoff B, McDonald O, Sinha S, Yoshida T, Owens G. 5' CArG degeneracy in smooth muscle α -actin is required for injury-induced gene suppression in vivo. *JCI*. 2005;115(2):418-427. doi:10.1172/JCI200522648.418.
 13. Wamhoff BR, Hoofnagle MH, Burns A, Sinha S, McDonald OG, Owens GK. A G/C element mediates repression of the SM22 α promoter within phenotypically modulated smooth muscle cells in experimental atherosclerosis. *Circ Res*. 2004;95(10):981-988.
doi:10.1161/01.RES.0000147961.09840.fb.

14. Gomez D, Shankman LS, Nguyen AT, Owens GK. Detection of histone modifications at specific gene loci in single cells in histological sections. *Nat Methods*. 2013;10(2):171-177. doi:10.1038/nmeth.2332.
15. Shankman LS, Gomez D, Cherepanova O, et al. KLF4-dependent phenotypic modulation of smooth muscle cells has a key role in atherosclerotic plaque pathogenesis. *Nat Med*. 2015;21(6):628-637. doi:10.1038/nm.3866.
16. Durgin BG, Cherepanova OA, Gomez D, et al. Smooth muscle cell-specific deletion of *Coll5a1* unexpectedly leads to impaired development of advanced atherosclerotic lesions. *Am J Physiol - Hear Circ Physiol*. 2017;312(5):H943-H958. doi:10.1152/ajpheart.00029.2017.
17. Gomez D, Baylis RA, Durgin BG, et al. Interleukin-1 β has atheroprotective effects in advanced atherosclerotic lesions of mice. *Nat Med*. 2018;24(9):1418-1429. doi:10.1038/s41591-018-0124-5.
18. Crisan M, Yap S, Casteilla L, et al. A Perivascular Origin for Mesenchymal Stem Cells in Multiple Human Organs. *Cell Stem Cell*. 2008;3(3):301-313. doi:10.1016/j.stem.2008.07.003.
19. Guimaraes-Camboa N, In C, Cattaneo P, et al. Pericytes of Multiple Organs Do Not Behave as Article Pericytes of Multiple Organs Do Not Behave as Mesenchymal Stem Cells In Vivo. 2017:1-15. doi:10.1016/j.stem.2016.12.006.
20. Birbrair A, Zhang T, Wang Z-M, et al. Type-2 pericytes participate in normal and tumoral angiogenesis. *AJP Cell Physiol*. 2014;307(1):C25-C38. doi:10.1152/ajpcell.00084.2014.
21. Teichert M, Milde L, Holm A, et al. Pericyte-expressed Tie2 controls angiogenesis and vessel maturation. *Nat Commun*. 2017;8:1-12. doi:10.1038/ncomms16106.

22. Eilken HM, Diéguez-Hurtado R, Schmidt I, et al. Pericytes regulate VEGF-induced endothelial sprouting through VEGFR1. *Nat Commun.* 2017;8(1). doi:10.1038/s41467-017-01738-3.
23. Dellavalle a, Maroli G, Covarello D, et al. Pericytes resident in postnatal skeletal muscle differentiate into muscle fibres and generate satellite cells. *Nat Commun.* 2011;2:411-499. doi:10.1038/ncomms1508.
24. Murgai M, Ju W, Eason M, et al. KLF4-dependent perivascular cell plasticity mediates pre-metastatic niche formation and metastasis. *Nat Med.* 2017;23(10):1176-1190. doi:10.1038/nm.4400.
25. Asahara T, Murohara T, Sullivan A, et al. Isolation of Putative Progenitor Endothelial Cells for Angiogenesis. *Science (80-)*. 1997;275(5302):964-966. doi:10.1126/science.275.5302.964.
26. Scholz D, Ziegelhoeffer T, Helisch A, et al. Contribution of arteriogenesis and angiogenesis to postocclusive hindlimb perfusion in mice. *J Mol Cell Cardiol.* 2002;34(7):775-787. doi:10.1006/jmcc.2002.2013.
27. Cai W, Schaper W. Mechanisms of arteriogenesis. *Acta Biochim Biophys Sin (Shanghai)*. 2008;40(8):681-692. doi:10.1111/j.1745-7270.2008.00436.x.
28. Potente M, Gerhardt H, Carmeliet P. Basic and Therapeutic Aspects of Angiogenesis. *Cell.* 2011;146(6):873-887. doi:10.1016/j.cell.2011.08.039.
29. Carmeliet P, Jain RK. Molecular Mechanisms and and clinical applications of angiogenesis. *Nature.* 2011;473(7347):298-307. doi:10.1038/nature10144.
30. Stratman AN, Malotte KM, Mahan RD, Davis MJ, Davis GE. Pericyte recruitment during vasculogenic tube assembly stimulates endothelial basement membrane matrix formation.

- Blood*. 2009;114(24):5091-5101. doi:10.1182/blood-2009-05-222364.
31. Levéen P, Pekny M, Gebre-Medhin S, Swolin B, Larsson E, Betsholtz C. Mice deficient for PDGF B show renal, cardiovascular, and hematological abnormalities. *Genes Dev*. 1994;8(16):1875-1887. doi:10.1101/gad.8.16.1875.
 32. Soriano P. Abnormal kidney development and hematological disorders in PDGF β -receptor mutant mice. *Genes Dev*. 1994;8(16):1888-1896. doi:10.1101/gad.8.16.1888.
 33. Enge M, Bjarnegård M, Gerhardt H, et al. Endothelium-specific platelet-derived growth factor-B ablation mimics diabetic retinopathy. *EMBO J*. 2002;21(16):4307-4316. doi:10.1093/emboj/cdf418.
 34. Bjarnegård M, Enge M, Norlin J, et al. Endothelium-specific ablation of PDGFB leads to pericyte loss and glomerular, cardiac and placental abnormalities. *Development*. 2004;131(8):1847-1857. doi:10.1242/dev.01080.
 35. Lindblom P, Gerhardt H, Liebner S, et al. Endothelial PDGF-B retention is required for proper investment of pericytes in the microvessel wall. *Genes Dev*. 2003;17(15):1835-1840. doi:10.1101/gad.266803.
 36. Abramsson A, Kurup S, Busse M, et al. Defective N-sulfation of heparan sulfate proteoglycans limits PDGF-BB binding and pericyte recruitment in vascular development. 2007;21:316-331. doi:10.1101/gad.398207.
 37. Gaengel K, Genové G, Armulik A, Betsholtz C. Endothelial-mural cell signaling in vascular development and angiogenesis. *Arterioscler Thromb Vasc Biol*. 2009;29(5):630-638. doi:10.1161/ATVBAHA.107.161521.
 38. Robbins JL, Jones WS, Duscha BD, et al. Relationship between leg muscle capillary density and peak hyperemic blood flow with endurance capacity in peripheral artery

- disease. *J Appl Physiol*. 2011;111(1):81-86. doi:10.1152/jappphysiol.00141.2011.
39. Duscha BD, Robbins JL, Jones WS, et al. Angiogenesis in skeletal muscle precede improvements in peak oxygen uptake in peripheral artery disease patients. *Arterioscler Thromb Vasc Biol*. 2011;31(11):2742-2748. doi:10.1161/ATVBAHA.111.230441.
40. Annex BH. Therapeutic angiogenesis for critical limb ischaemia. *Nat Rev Cardiol*. 2013;10(7):387-396. doi:10.1038/nrcardio.2013.70.
41. Iyer SR, Annex BH. Therapeutic Angiogenesis for Peripheral Artery Disease: Lessons Learned in Translational Science. *JACC Basic to Transl Sci*. 2017;2(5):503-512. doi:10.1016/j.jacbts.2017.07.012.
42. Couffinhal T, Silver M, Zheng LP, Kearney M, Witzenbichler B, Isner JM. Mouse model of angiogenesis. *Am J Pathol*. 1998;152(6):1667-1679.
43. Dokun AO, Keum S, Hazarika S, et al. A quantitative trait locus (LSq-1) on mouse chromosome 7 is linked to the absence of tissue loss after surgical hindlimb ischemia. *Circulation*. 2008;117(9):1207-1215. doi:10.1161/CIRCULATIONAHA.107.736447.
44. Lederman RJ, Mendelsohn FO, Anderson RD, et al. Therapeutic angiogenesis with recombinant fibroblast growth factor-2 for intermittent claudication (the TRAFFIC study): A randomised trial. *Lancet*. 2002;359(9323):2053-2058. doi:10.1016/S0140-6736(02)08937-7.
45. Nikol S, Baumgartner I, Van Belle E, et al. Therapeutic angiogenesis with intramuscular NV1FGF improves amputation-free survival in patients with critical limb ischemia. *Mol Ther*. 2008;16(5):972-978. doi:10.1038/mt.2008.33.
46. Belch J, Hiatt WR, Baumgartner I, et al. Effect of fibroblast growth factor NV1FGF on amputation and death: A randomised placebo-controlled trial of gene therapy in critical

- limb ischaemia. *Lancet*. 2011;377(9781):1929-1937. doi:10.1016/S0140-6736(11)60394-2.
47. Pascolini D, Mariotti SP. Global estimates of visual impairment: 2010. *Br J Ophthalmol*. 2012;96(5):614-618. doi:10.1136/bjophthalmol-2011-300539.
48. Anderson C, Zhou Q, Wang S. An Alkali-burn Injury Model of Corneal Neovascularization in the Mouse. *J Vis Exp*. 2014;(86):1-6. doi:10.3791/51159.
49. Ambati BK, Nozaki M, Singh N, et al. Corneal avascularity is due to soluble VEGF receptor-1. *Nature*. 2006;443(7114):993-997. doi:10.1038/nature05249.
50. Cursiefen C, Chen L, Borges LP, et al. VEGF-A stimulates lymphangiogenesis and hemangiogenesis in inflammatory neovascularization via macrophage recruitment. *J Clin Invest*. 2004;113(7):1040-1050. doi:10.1172/JCI20465.
51. Kelly-Goss MR, Ning B, Bruce AC, et al. Dynamic, heterogeneous endothelial Tie2 expression and capillary blood flow during microvascular remodeling. *Sci Rep*. 2017;7(1):9049. doi:10.1038/s41598-017-08982-z.
52. Folkman J. Tumor angiogenesis: Therapeutic implications. *N Engl J Med*. 1971;285(21):1182-1186. doi:10.1056/NEJM198603063141003.
53. Loges S, Mazzone M, Hohensinner P, Carmeliet P. Silencing or Fueling Metastasis with VEGF Inhibitors: Antiangiogenesis Revisited. *Cancer Cell*. 2009;15(3):167-170. doi:10.1016/j.ccr.2009.02.007.
54. Morikawa S, Baluk P, Kaidoh T, Haskell A, Jain RK, McDonald DM. Abnormalities in pericytes on blood vessels and endothelial sprouts in tumors. *Am J Pathol*. 2002;160(3):985-1000. doi:10.1016/S0002-9440(10)64920-6.
55. Ramaswamy S, Ross KN, Lander ES, Golub TR. A molecular signature of metastasis in

- primary solid tumors. *Nat Genet.* 2003;33(1):49-54. doi:10.1038/ng1060.
56. Goel S, Wong AHK, Jain RK. Vascular normalization as a therapeutic strategy for malignant and nonmalignant disease. *Cold Spring Harb Perspect Med.* 2012;2(3). doi:10.1101/cshperspect.a006486.
57. Valdez CN, Arboleda-Velasquez JF, Amarnani DS, Kim LA, D'Amore PA. Retinal microangiopathy in a mouse model of inducible mural cell loss. *Am J Pathol.* 2014;184(10):2618-2626. doi:10.1016/j.ajpath.2014.06.011.
58. Eilken HM, Diéguez-Hurtado R, Schmidt I, et al. Pericytes regulate VEGF-induced endothelial sprouting through VEGFR1. *Nat Commun.* 2017;8(1):1574. doi:10.1038/s41467-017-01738-3.
59. Cherepanova OA, Gomez D, Shankman LS, et al. Activation of the pluripotency factor OCT4 in smooth muscle cells is atheroprotective. *Nat Med.* 2016;22(6):657-665. doi:10.1038/nm.4109.
60. Wang X, Dai J. Concise review: Isoforms of OCT4 contribute to the confusing diversity in stem cell biology. *Stem Cells.* 2010;28(5):885-893. doi:10.1002/stem.419.
61. Nichols J, Zevnik B, Anastassiadis K, et al. Formation of pluripotent stem cells in the mammalian embryo depends on the POU transcription factor Oct4. *Cell.* 1998;95(3):379-391. doi:10.1016/S0092-8674(00)81769-9.
62. Zeineddine D, Hammoud AA, Mortada M, Boeuf H. The Oct4 protein: more than a magic stemness marker. *Am J Stem Cells.* 2014;3(2):74-82. doi:25232507.
63. Shi G, Jin Y. Role of Oct4 in maintaining and regaining stem cell pluripotency. *Stem Cell Res Ther.* 2010;1(5):39. doi:10.1186/scrt39.
64. Feldman N, Gerson A, Fang J, et al. G9a-mediated irreversible epigenetic inactivation of

- Oct-3/4 during early embryogenesis. *Nat Cell Biol.* 2006;8(2):188-194.
doi:10.1038/ncb1353.
65. Takahashi K, Yamanaka S. Induction of pluripotent stem cells from mouse embryonic and adult fibroblast cultures by defined factors. *Cell.* 2006;126(4):663-676.
doi:10.1016/j.cell.2006.07.024.
66. Gao Y, Chen J, Li K, et al. Replacement of Oct4 by Tet1 during iPSC induction reveals an important role of DNA methylation and hydroxymethylation in reprogramming. *Cell Stem Cell.* 2013;12(4):453-469. doi:10.1016/j.stem.2013.02.005.
67. Lengner CJ, Camargo FD, Hochedlinger K, et al. Oct4 expression is not required for mouse somatic stem cell self-renewal. *Cell Stem Cell.* 2007;1(4):403-415.
doi:10.1016/j.stem.2007.07.020.
68. Farashahi Yazd E, Rafiee MR, Soleimani M, Tavallaei M, Salmani MK, Mowla SJ. OCT4B1, a novel spliced variant of OCT4, generates a stable truncated protein with a potential role in stress response. *Cancer Lett.* 2011;309(2):170-175.
doi:10.1016/j.canlet.2011.05.027.
69. Jez M, Ambady S, Kashpur O, et al. Expression and differentiation between OCT4A and its pseudogenes in human ESCs and differentiated adult somatic cells. *PLoS One.* 2014;9(2). doi:10.1371/journal.pone.0089546.
70. Kehler J, Tolkunova E, Koschorz B, et al. Oct4 is required for primordial germ cell survival. *EMBO Rep.* 2004;5(11):1078-1083. doi:10.1038/sj.embor.7400279.
71. Voronov E, Carmi Y, Apte RN. The role IL-1 in tumor-mediated angiogenesis. *Front Physiol.* 2014;5:1-11. doi:10.3389/fphys.2014.00114.
72. Elaraj DM, Weinreich DM, Varghese S, et al. The role of interleukin 1 in growth and

- metastasis of human cancer xenografts. *Clin Cancer Res.* 2006;12(4):1088-1096.
doi:10.1158/1078-0432.CCR-05-1603.
73. Voronov E, Shouval DS, Krelin Y, et al. IL-1 is required for tumor invasiveness and angiogenesis. *Proc Natl Acad Sci U S A.* 2003;100(5):2645-2650.
doi:10.1073/pnas.0437939100.
74. Holen I, Lefley D V, Francis SE, et al. IL-1 drives breast cancer growth and bone metastasis in vivo. *Oncotarget.* 2016;7(46). doi:10.18632/oncotarget.12289.
75. Ridker PM, MacFadyen JG, Thuren T, et al. Effect of interleukin-1 β inhibition with canakinumab on incident lung cancer in patients with atherosclerosis: exploratory results from a randomised, double-blind, placebo-controlled trial. *Lancet.* 2017;390(10105):1833-1842. doi:10.1016/S0140-6736(17)32247-X.
76. Carmi Y, Dotan S, Rider P, et al. The Role of IL-1 in the Early Tumor Cell-Induced Angiogenic Response. *J Immunol.* 2013;190(7):3500-3509.
doi:10.4049/jimmunol.1202769.
77. Kaplan RN, Riba RD, Zacharoulis S, et al. VEGFR1-positive haematopoietic bone marrow progenitors initiate the pre-metastatic niche. *Nature.* 2005;438(7069):820-827.
doi:10.1038/nature04186.
78. Jagielska J, Kapopara PR, Salguero G, et al. Interleukin-1 β assembles a proangiogenic signaling module consisting of caveolin-1, Tumor necrosis factor receptor-associated factor 6, p38-mitogen-activated protein kinase (MAPK), and mapk-activated protein kinase 2 in endothelial cells. *Arterioscler Thromb Vasc Biol.* 2012;32(5):1280-1288.
doi:10.1161/ATVBAHA.111.243477.
79. Amano K, Okigaki M, Adachi Y, et al. Mechanism for IL-1 β -mediated neovascularization

- unmasked by IL-1 β knock-out mice. *J Mol Cell Cardiol.* 2004;36(4):469-480.
doi:10.1016/j.yjmcc.2004.01.006.
80. Carmi Y, Voronov E, Dotan S, et al. The Role of Macrophage-Derived IL-1 in Induction and Maintenance of Angiogenesis. *J Immunol.* 2009;183(7):4705-4714.
doi:10.4049/jimmunol.0901511.
81. Eun SY, Ko YS, Park SW, Chang KC, Kim HJ. IL-1 β enhances vascular smooth muscle cell proliferation and migration via P2Y2receptor-mediated RAGE expression and HMGB1 release. *Vascul Pharmacol.* 2015;72:108-117. doi:10.1016/j.vph.2015.04.013.
82. Wirth A, Benyó Z, Lukasova M, et al. G12-G13–LARG–mediated signaling in vascular smooth muscle is required for salt-induced hypertension. *Nat Med.* 2008;14(1):64-68.
doi:10.1038/nm1666.
83. Kisucka J, Butterfield CE, Duda DG, et al. Platelets and platelet adhesion support angiogenesis while preventing excessive hemorrhage. *Proc Natl Acad Sci U S A.* 2006;103(4):855-860. doi:10.1073/pnas.0510412103.
84. Hazarika S, Farber CR, Dokun a. O, et al. MicroRNA-93 Controls Perfusion Recovery After Hindlimb Ischemia by Modulating Expression of Multiple Genes in the Cell Cycle Pathway. *Circulation.* 2013;127(17):1818-1828.
doi:10.1161/CIRCULATIONAHA.112.000860.
85. Ho Sui SJ, Mortimer JR, Arenillas DJ, et al. oPOSSUM: Identification of over-represented transcription factor binding sites in co-expressed genes. *Nucleic Acids Res.* 2005;33(10):3154-3164. doi:10.1093/nar/gki624.
86. Sui Ho SJ, Fulton DL, Arenillas DJ, Kwon AT, Wasserman WW. OPOSSUM: Integrated tools for analysis of regulatory motif over-representation. *Nucleic Acids Res.*

- 2007;35(SUPPL.2):245-252. doi:10.1093/nar/gkm427.
87. Kwon AT, Arenillas DJ, Hunt RW, Wasserman WW. oPOSSUM-3: Advanced Analysis of Regulatory Motif Over-Representation Across Genes or ChIP-Seq Datasets. *Genes/Genomes/Genetics*. 2012;2(9):987-1002. doi:10.1534/g3.112.003202.
 88. Lengner CJ, Camargo FD, Hochedlinger K, et al. Oct4 Expression Is Not Required for Mouse Somatic Stem Cell Self-Renewal. *Cell Stem Cell*. 2007;1(4):403-415. doi:10.1016/j.stem.2007.07.020.
 89. Kumar SM, Liu S, Lu H, et al. Acquired cancer stem cell phenotypes through Oct4-mediated dedifferentiation. *Oncogene*. 2012;31(47):4898-4911. doi:10.1038/onc.2011.656.
 90. Armulik A, Genové G, Betsholtz C. Pericytes: Developmental, Physiological, and Pathological Perspectives, Problems, and Promises. *Dev Cell*. 2011;21(2):193-215. doi:10.1016/j.devcel.2011.07.001.
 91. Hellström M, Kalén M, Lindahl P, Abramsson A, Betsholtz C. Role of PDGF-B and PDGFR-beta in recruitment of vascular smooth muscle cells and pericytes during embryonic blood vessel formation in the mouse. *Development*. 1999;126(14):3047-3055. <http://www.ncbi.nlm.nih.gov/pubmed/10375497>.
 92. Armulik A, Abramsson A, Betsholtz C. Endothelial/pericyte interactions. *Circ Res*. 2005;97(6):512-523. doi:10.1161/01.RES.0000182903.16652.d7.
 93. Bergers G, Song S. The role of pericytes in blood-vessel formation and maintenance. *Neuro Oncol*. 2005;7(4):452-464. doi:10.1215/S1152851705000232.
 94. Stapor PC, Sweat RS, Dashti DC, Betancourt AM, Murfee WL. Pericyte dynamics during angiogenesis: New insights from new identities. *J Vasc Res*. 2014;51(3):163-174.

doi:10.1159/000362276.

95. Suri C, Jones PF, Patan S, et al. Requisite role of angiopoietin-1, a ligand for the TIE2 receptor, during embryonic angiogenesis. *Cell*. 1996;87(7):1171-1180.
doi:10.1016/S0092-8674(00)81813-9.
96. Seki T, Yun J, Oh SP. Arterial endothelium-specific activin receptor-like kinase 1 expression suggests its role in arterialization and vascular remodeling. *Circ Res*. 2003;93(7):682-689. doi:10.1161/01.RES.0000095246.40391.3B.
97. Larsson J, Goumans MJ, Sjöstrand LJ, et al. Abnormal angiogenesis but intact hematopoietic potential in TGF- β type I receptor-deficient mice. *EMBO J*. 2001;20(7):1663-1673. doi:10.1093/emboj/20.7.1663.
98. Domenga V, Fardoux P, Lacombe P, et al. Notch3 is required for arterial identity and maturation of vascular smooth muscle cells. *Genes Dev*. 2004;18(22):2730-2735.
doi:10.1101/gad.308904.
99. Mizugishi K, Yamashita T, Olivera A, Miller GF, Spiegel S, Proia RL. Essential Role for Sphingosine Kinases in Neural and Vascular Development. *Mol Cell Biol*. 2005;25(24):11113-11121. doi:10.1128/MCB.25.24.11113.
100. Lindahl P, Johanson B, Leveen P, Betsholtz C. Pericyte Loss and Microaneurysm Formation in PDGF-B-Deficient Mice. *Science*. 1997;277(5323):242-245.
doi:10.1126/science.277.5323.242.
101. Armulik A, Genové G, Mäe M, et al. Pericytes regulate the blood-brain barrier. *Nature*. 2010;468(7323):557-561. doi:10.1038/nature09522.
102. Hellström M, Gerhardt H, Kalén M, et al. Lack of pericytes leads to endothelial hyperplasia and abnormal vascular morphogenesis. *J Cell Biol*. 2001;152(3):543-553.

- doi:10.1083/jcb.153.3.543.
103. Limbourg FP, Takeshita K, Radtke F, Roderick T, Chin MT, Liao JK. Essential Role of Endothelial Notch1 in Angiogenesis. *Circulation*. 2005;111(14):1826-1832. doi:10.1161/01.CIR.0000160870.93058.DD.
104. High FA, Lu MM, Pear WS, Loomes KM, Kaestner KH, Epstein JA. Endothelial expression of the Notch ligand Jagged1 is required for vascular smooth muscle development. *Proc Natl Acad Sci U S A*. 2008;105(6):1955-1959. doi:10.1073/pnas.0709663105.
105. Shen T-LT-L, Park AY-J, Alcaraz A, et al. Conditional knockout of focal adhesion kinase in endothelial cells reveals its role in angiogenesis and vascular development in late embryogenesis. *J Cell Biol*. 2005;169(6):941-952. doi:10.1083/jcb.200411155.
106. Franco C, Blanc J, Parlakian A, et al. SRF selectively controls tip cell invasive behavior in angiogenesis. *Development*. 2013;140(11):2321-2333. doi:10.1242/dev.091074.
107. Rama N, Dubrac A, Mathivet T, et al. Slit2 signaling through Robo1 and Robo2 is required for retinal neovascularization. *Nat Med*. 2015;21(5):483-491. doi:10.1038/nm.3849.
108. Foo SS, Turner CJ, Adams S, et al. Ephrin-B2 controls cell motility and adhesion during blood-vessel-wall assembly. *Cell*. 2006;124(1):161-173. doi:10.1016/j.cell.2005.10.034.
109. Chen J, Luo Y, Hui H, et al. CD146 coordinates brain endothelial cell-pericyte communication for blood-brain barrier development. *Proc Natl Acad Sci U S A*. 2017;E7622-E7631. <http://www.ncbi.nlm.nih.gov/pubmed/28827364>.
110. Weir HK, Anderson RN, Coleman King SM, et al. Heart Disease and Cancer Deaths — Trends and Projections in the United States, 1969–2020. *Prev Chronic Dis*.

- 2016;13:160211. doi:10.5888/pcd13.160211.
111. Henry T, Annex B, McKendall G, et al. The VIVA Trial: Vascular Endothelial Growth Factor in Ischemia for Vascular Angiogenesis. *Circulation*. 2003;107(10):1359-1365. doi:10.1161/01.CIR.0000061911.47710.8A.
112. Rajagopalan S, Mohler ER, Lederman RJ, et al. Regional angiogenesis with vascular endothelial growth factor in peripheral arterial disease: a phase II randomized, double-blind, controlled study of adenoviral delivery of vascular endothelial growth factor 121 in patients with disabling intermittent cl. *Circulation*. 2003;108(16):1933-1938. doi:10.1161/01.CIR.0000093398.16124.29.
113. Annex BH, Simons M. Growth factor-induced therapeutic angiogenesis in the heart : protein therapy. *Cardiovasc Res*. 2005;65(3):649-655. doi:10.1016/j.cardiores.2004.09.004.
114. Cao R, Ebba B, Pawliuk R, et al. Angiogenic synergism, vascular stability and improvement of hind-limb ischemia by a combination of PDGF-BB and FGF-2. *Nat Med*. 2003;9(5):604-613. doi:10.1038/nm.
115. Gomez D, Shankman L, Nguyen A, Owens GK. Detection of histone modifications. 2013;10(2):171-177. doi:10.1038/nmeth.2332.
116. Hazarika S, Farber CR, Dokun AO, et al. MicroRNA-93 controls perfusion recovery after hindlimb ischemia by modulating expression of multiple genes in the cell cycle pathway. *Circulation*. 2013;127(17):1818-1828. doi:10.1161/CIRCULATIONAHA.112.000860.
117. Meisner JK, Annex BH, Price RJ. Despite normal arteriogenic and angiogenic responses, hind limb perfusion recovery and necrotic and fibroadipose tissue clearance are impaired in matrix metalloproteinase 9-deficient mice. *J Vasc Surg*. 2014.

doi:10.1016/j.jvs.2014.01.038.

118. Heuslein JL, Meisner JK, Li X, et al. Mechanisms of Amplified Arteriogenesis in Collateral Artery Segments Exposed to Reversed Flow Direction. *Arterioscler Thromb Vasc Biol.* 2015;35(11):2354-2365. doi:10.1161/ATVBAHA.115.305775.
119. Zhang B, Dietrich UM, Geng JG, Bicknell R, Esko JD, Wang L. Repulsive axon guidance molecule Slit3 is a novel angiogenic factor. *Blood.* 2009;114(19):4300-4309. doi:10.1182/blood-2008-12-193326.
120. Geutskens SB, Hordijk PL, van Hennik PB. The chemorepellent Slit3 promotes monocyte migration. *J Immunol.* 2010;185(12):7691-7698. doi:10.4049/jimmunol.0903898.
121. Ypsilanti AR, Zagar Y, Chédotal A. Moving away from the midline : new developments for Slit and Robo. 2010;1952:1939-1952. doi:10.1242/dev.044511.
122. Zhang B, Xiao W, Qiu H, et al. Heparan sulfate deficiency disrupts developmental angiogenesis and causes congenital diaphragmatic hernia. *J Clin Invest.* 2014;124(1):209-221. doi:10.1172/JCI71090.
123. Paul JD, Coulombe KKL, Toth PT, et al. SLIT3-ROBO4 activation promotes vascular network formation in human engineered tissue and angiogenesis in vivo. *J Mol Cell Cardiol.* 2013;64:124-131. doi:10.1016/j.yjmcc.2013.09.005.
124. Xu R, Yallowitz A, Qin A, et al. Targeting skeletal endothelium to ameliorate bone loss. 2018. doi:10.1038/s41591-018-0020-z.
125. Haskins RM, Nguyen AT, Alencar GF, et al. Klf4 has an unexpected protective role in perivascular cells within the microvasculature. *Am J Physiol Circ Physiol.* 2018:ajpheart.00084.2018. doi:10.1152/ajpheart.00084.2018.
126. Wei Z, Yang Y, Zhang P, et al. Klf4 interacts directly with Oct4 and Sox2 to promote

- reprogramming. *Stem Cells*. 2009;27(12):2969-2978. doi:10.1002/stem.231.
127. Long JZ, Svensson KJ, Tsai L, et al. A smooth muscle-like origin for beige adipocytes. *Cell Metab*. 2014;19(5):810-820. doi:10.1016/j.cmet.2014.03.025.
128. Sangwung P, Zhou G, Nayak L, et al. KLF2 and KLF4 control endothelial identity and vascular integrity. *JCI Insight*. 2017;2(4):e91700. doi:10.1172/jci.insight.91700.
129. Zhou G, Hamik A, Nayak L, et al. Endothelial Kruppel-like factor 4 protects against atherothrombosis in mice. *J Clin Invest*. 2012;122(12):4727-4731. doi:10.1172/JCI66056.
130. van der Harst P, Verweij Ni. Identification of 64 Novel Genetic Loci Provides an Expanded View on the Genetic Architecture of Coronary Artery Disease. *Circ Res*. 2018;122(3):433-443. doi:10.17632/2zdd47c94h.1.
131. Chen P, Qin L, Barnes C, Charisse K, Yi T, Zhang X. FGF regulates TGF- β signaling and endothelial-to-mesenchymal transition via control of let-7 miRNA expression. 2012;2(6):1684-1696. doi:10.1016/j.celrep.2012.10.021.FGF.
132. Passman JN, Dong XR, Wu S-P, et al. A sonic hedgehog signaling domain in the arterial adventitia supports resident Sca1+ smooth muscle progenitor cells. *Proc Natl Acad Sci*. 2008;105(27):9349-9354. doi:10.1073/pnas.0711382105.
133. Manavski Y, Lucas T, Glaser SF, et al. Clonal Expansion of Endothelial Cells Contributes to Ischemia-Induced Neovascularization. *Circ Res*. 2018;122:670-677. doi:10.1161/CIRCRESAHA.117.312310.
134. Jacobsen K, Carramolino L, Bentzon JF, et al. Diverse cellular architecture of atherosclerotic plaque derives from clonal expansion of a few medial SMCs. *JCI Insight*. 2017;2(19):1-13.
135. Loh Y-H, Wu Q, Chew J-L, et al. The Oct4 and Nanog transcription network regulates

- pluripotency in mouse embryonic stem cells. *Nat Genet.* 2006;38(4):431-440.
doi:10.1038/ng1760.
136. Liu D, Hou J, Hu X, et al. Neuronal chemorepellent Slit2 inhibits vascular smooth muscle cell migration by suppressing small GTPase Rac1 activation. *Circ Res.* 2006;98(4):480-489. doi:10.1161/01.RES.0000205764.85931.4b.
137. Guijarro-Muñoz I, Cuesta AM, Alvarez-Cienfuegos A, Geng JG, Alvarez-Vallina L, Sanz L. The axonal repellent Slit2 inhibits pericyte migration: Potential implications in angiogenesis. *Exp Cell Res.* 2012;318(4):371-378. doi:10.1016/j.yexcr.2011.12.005.
138. Wang B, Xiao Y, Ding BB, et al. Induction of tumor angiogenesis by Slit-Robo signaling and inhibition of cancer growth by blocking Robo activity. *Cancer Cell.* 2003;4(1):19-29. doi:10.1016/S1535-6108(03)00164-8.
139. Jones C, London NR, Chen H, et al. Robo4 stabilizes the vascular network by inhibiting pathologic angiogenesis and endothelial hyperpermeability. *Nat Med.* 2008;14(4):448-453. doi:10.1038/nm1742.
140. Li G-J, Yang Y, Yang G-K, et al. Slit2 suppresses endothelial cell proliferation and migration by inhibiting the VEGF-Notch signaling pathway. *Mol Med Rep.* 2017;15:1981-1988. doi:10.3892/mmr.2017.6240.
141. Tanno T, Fujiwara A, Sakaguchi K, Tanaka K, Takenaka S, Tsuyama S. Slit3 regulates cell motility through Rac/Cdc42 activation in lipopolysaccharide-stimulated macrophages. *FEBS Lett.* 2007;581(5):1022-1026. doi:10.1016/j.febslet.2007.02.001.
142. Schwend T, Lwigale P, Conrad G. Nerve Repulsion by the Lens and Cornea during Cornea Innervation is Dependent on Robo-Slit Signaling and Diminishes with Neuron Age. *Dev Biol.* 2012;363(1):115-127. doi:10.1016/j.ydbio.2011.12.039.

143. Guo Y, Mantel C, Hromas R, Broxmeyer H. Oct 4 is Critical for Survival/Antiapoptosis of Murine Embryonic Stem Cells Subjected to Stress. Effects Associated with STAT3/Survivin. *Stem Cells*. 2008;26(1):1-15. doi:10.1634/stemcells.2007-0401.
144. Chen T, Du J, Lu G. Cell growth arrest and apoptosis induced by Oct4 or Nanog knockdown in mouse embryonic stem cells : a possible role of Trp53. *Mol Biol Rep*. 2012;39(2):1855-1861. doi:10.1007/s11033-011-0928-6.
145. Ridker PM, Everett BM, Thuren T, et al. Antiinflammatory Therapy with Canakinumab for Atherosclerotic Disease. *N Engl J Med*. 2017:NEJMoa1707914. doi:10.1056/NEJMoa1707914.
146. Bhat IA, Naykoo NA, Qasim I, et al. Association of interleukin 1 beta (IL-1 β) polymorphism with mRNA expression and risk of non small cell lung cancer. *Meta Gene*. 2014;2(1):123-133. doi:10.1016/j.mgene.2013.12.002.
147. Zienolddiny S, Ryberg D, Maggini V, Skaug V, Canzian F, Haugen A. Polymorphisms of the interleukin-1 β gene are associated with increased risk of non-small cell lung cancer. *Int J Cancer*. 2004;109(3):353-356. doi:10.1002/ijc.11695.
148. Bergers G, Benjamin LE. Tumorigenesis and the angiogenic switch. *Nat Rev Cancer*. 2003;3(6):401-410. doi:10.1038/nrc1093.
149. Grivennikov SI, Greten FR, Karin M. Immunity, Inflammation, and Cancer. *Cell*. 2010;140(6):883-899. doi:10.1016/j.cell.2010.01.025.
150. Heron M. National Vital Statistics Reports Volume 67, Number 5 July 26, 2018, Deaths: Final Data for 2016. *Natl Vital Stat Reports*. 2018;67(6):1-15.
151. Thacker SG, Berthier CC, Mattinzoli D, Rastaldi MP, Kretzler M, Kaplan MJ. The Detrimental Effects of IFN- on Vasculogenesis in Lupus Are Mediated by Repression of

- IL-1 Pathways: Potential Role in Atherogenesis and Renal Vascular Rarefaction. *J Immunol.* 2010;185(7):4457-4469. doi:10.4049/jimmunol.1001782.
152. Moeller A, Ask K, Warburton D, Gauldie J, Kolb M. The bleomycin animal model: a useful tool to investigate treatment options for idiopathic pulmonary fibrosis? *Int J Biochem Cell Biol.* 2008;40(3):362-382. doi:10.1038/jid.2014.371.
153. De Souza Xavier Costa N, Ribeiro G, Dos Santos Alemany AA, et al. Early and late pulmonary effects of nebulized LPS in mice: An acute lung injury model. *PLoS One.* 2017;12(9):1-16. doi:10.1371/journal.pone.0185474.
154. Starke RM, Thompson JW, Ali MS, et al. Cigarette smoke initiates oxidative stress-induced cellular phenotypic modulation leading to cerebral aneurysm pathogenesis. *Arterioscler Thromb Vasc Biol.* 2018;38(3):610-621. doi:10.1161/ATVBAHA.117.310478.
155. Han Y, Bedarida T, Ding Y, et al. β -Hydroxybutyrate Prevents Vascular Senescence through hnRNP A1-Mediated Upregulation of Oct4. *Mol Cell.* 2018:1064-1078. doi:10.1016/j.molcel.2018.07.036.
156. Madsen CS, Regan CP, Hungerford JE, White SL, Manabe I, Owens GK. Smooth Muscle Specific Expression of the Smooth Muscle Myosin Heavy Chain Gene in Transgenic Mice Requires 5'-Flanking and First Intronic DNA Sequence. *Circ Res.* 1998;82(8):908-917. doi:10.1161/01.RES.82.8.908.
157. Pitulescu ME, Schmidt I, Benedito R, Adams RH. Inducible gene targeting in the neonatal vasculature and analysis of retinal angiogenesis in mice. *Nat Protoc.* 2010;5(9):1518-1534. doi:10.1038/nprot.2010.113.
158. Peinado H, Zhang H, Matei IR, et al. Pre-metastatic niches: Organ-specific homes for

- metastases. *Nat Rev Cancer*. 2017;17(5):302-317. doi:10.1038/nrc.2017.6.
159. Marlow R, Binnewies M, Sorensen LK, et al. Vascular Robo4 restricts proangiogenic VEGF signaling in breast. *Proc Natl Acad Sci U S A*. 2010;107(23):10520-10525. doi:10.1073/pnas.1001896107.
160. Okabe K, Kobayashi S, Yamada T, et al. Neurons limit angiogenesis by titrating VEGF in retina. *Cell*. 2014;159(3):584-596. doi:10.1016/j.cell.2014.09.025.
161. Hsu CW, Poché RA, Saik JE, et al. Improved angiogenesis in response to localized delivery of macrophage-recruiting molecules. *PLoS One*. 2015;10(7):1-27. doi:10.1371/journal.pone.0131643.
162. Wang B, Li H, Mutlu SA, et al. The Amyloid Precursor Protein Is a Conserved Receptor for Slit to Mediate Axon Guidance. *Eneuro*. 2017;4(3):1-19. doi:10.1523/ENEURO.0185-17.2017.
163. Cheng N, Jiao S, Gumaste A, Bai L, Belluscio L. APP Overexpression Causes A β -Independent Neuronal Death through Intrinsic Apoptosis Pathway. *eNeuro*. 2016;3(4):1-12. doi:10.1523/ENEURO.0150-16.2016.
164. Piera-Velazquez S, Li Z, Jimenez SA. Role of endothelial-mesenchymal transition (EndoMT) in the pathogenesis of fibrotic disorders. *Am J Pathol*. 2011;179(3):1074-1080. doi:10.1016/j.ajpath.2011.06.001.
165. Bielenberg DR, Zetter BR, Program VB. The Contribution of Angiogenesis to the Process of Metastasis. 2016;21(4):267-273. doi:10.1097/PPO.0000000000000138.
166. Zeng H, He X, Tuo QH, Liao DF, Zhang GQ, Chen JX. LPS causes pericyte loss and microvascular dysfunction via disruption of Sirt3/angiopoietins/Tie-2 and HIF-2 α /Notch3 pathways. *Sci Rep*. 2016;6:1-13. doi:10.1038/srep20931.

167. Tabata C, Tabata R, Takahashi Y, Nakamura K, Nakano T. International Immunopharmacology Thalidomide prevents cigarette smoke extract-induced lung damage in mice. *Int Immunopharmacol*. 2015;25(2):511-517. doi:10.1016/j.intimp.2015.02.036.
168. Getz GS, Reardon CA. Do the Apoe^{-/-}-and Ldlr^{-/-}-mice yield the same insight on atherogenesis? *Arterioscler Thromb Vasc Biol*. 2016;36(9):1734-1741. doi:10.1161/ATVBAHA.116.306874.
169. Peled M, Nishi H, Weinstock A, et al. A wild-type mouse-based model for the regression of inflammation in atherosclerosis. *PLoS One*. 2017;12(3):1-12. doi:10.1371/journal.pone.0173975.
170. Nolan DJ, Ciarrocchi A, Mellick AS, et al. Bone marrow-derived endothelial progenitor cells are a major determinant of nascent tumor neovascularization. *Genes Dev*. 2007;21(12):1546-1558. doi:10.1101/gad.436307.
171. Nakao S, Kuwano M, Ono M, et al. Infiltration of COX-2-expressing macrophages is a prerequisite for IL-1 β -induced neovascularization and tumor growth. 2005;115(11):2979-2991. doi:10.1172/JCI23298.antitumor.
172. Narita T, Kawakami-Kimura N, Kasai Y, et al. Induction of E-selectin expression on vascular endothelium by digestive system cancer cells. *J Gastroenterol*. 1996;31(2):299-301. doi:10.1007/BF02389535.
173. Ferrara N. Vascular endothelial growth factor and age-related macular degeneration: from basic science to therapy. *Nat Med*. 2010;16(10):1107-1111. doi:10.1038/nm1010-1107.
174. Chang J-H, Garg NK, Lunde E, Han K-Y, Jain S, Aszar DT. Corneal Neovascularization: An Anti-VEGF Therapy Review. *Surv Ophthalmol*. 2013;57(5):415-429.

doi:10.1016/j.survophthal.2012.01.007.Corneal.

175. Hamzah J, Jugold M, Kiessling F, et al. Vascular normalization in Rgs5-deficient tumours promotes immune destruction. *Nature*. 2008;453(7193):410-414.
doi:10.1038/nature06868.
176. Hosaka K, Yang Y, Seki T, et al. Pericyte–fibroblast transition promotes tumor growth and metastasis. *Proc Natl Acad Sci*. 2016;113(38):E5618-E5627.
doi:10.1073/pnas.1608384113.
177. Keskin D, Kim J, Cooke VG, et al. Targeting Vascular Pericytes in Hypoxic Tumors Increases Lung Metastasis via Angiopoietin-2. *Cell Rep*. 2015;10(7):1066-1081.
doi:10.1016/j.celrep.2015.01.035.
178. Cercek A, Wheler J, Murray PE, Zhou S, Saltz L. Phase 1 study of APTO-253 HCl, an inducer of KLF4, in patients with advanced or metastatic solid tumors. *Invest New Drugs*. 2015;33(5):1086-1092. doi:10.1007/s10637-015-0273-z.
179. Isner JM, Pieczek A, Schainfeld R, et al. Clinical evidence of angiogenesis after arterial gene transfer of phVEGF165 in patient with ischaemic limb. *Lancet*. 1996;348(9024):370-374. doi:10.1016/S0140-6736(96)03361-2.